Opportunistic Spectrum Access
Designing Link and Transport Layer

Opportunistic Spectrum Access
Designing Link and Transport Layer

PROEFSCHRIFT

ter verkrijging van de graad van doctor
aan de Technische Universiteit Delft,
op gezag van de Rector Magnificus Prof. dr. ir. J.T. Fokkema,
voorzitter van het College voor Promoties,
in het openbaar te verdedigen op vrijdag 24 april 2009 om 10.00 uur
door

Przemysław PAWEŁCZAK

magister inżynier van Politechnika Wrocławska, Polen
geboren te Tomaszów Lubelski, Polen.

Dit proefschrift is goedgekeurd door de promotor:

Prof. dr. ir. I.G.M.M. Niemegeers

Samenstelling promotiecommissie:

Rector Magnificus	voorzitter
Prof. dr. ir. I.G.M.M. Niemegeers	Technische Universiteit Delft, promotor
Prof. dr. ir. S.M. Heemsta de Groot	Technische Universiteit Delft
Prof. dr. J.R. Long	Technische Universiteit Delft
Prof. dr. ir. B. Nauta	Universiteit Twente
Prof. dr. N. Balakrishnan	Indian Institute of Science
Prof. dr hab. inż. A. Wolisz	Technische Universität Berlin and University of California Berkeley

This research has been supported by the AAF project in the framework of the Freeband programme sponsored by the Dutch Ministry of Economic Affairs. Work presented in this thesis has been performed at the Wireless and Mobile Communications Group of Delft University of Technology.

ISBN 978-90-79746-05-7

Printed in the Netherlands by Wöhrmann Print Service

Front cover: Yayoi Kusama, Retrospective at Museum Boijmans Van Beuningen, 24 June 2008
Back cover: Photo assistance by Daniel Lewandowski

Typeset by the author with the LaTeX Documentation System.
Author email: przemyslaw.pawelczak@ieee.org

To the memory of Józef Drzewosz (1926–2001)

Acknowledgements

Nie mówimy ani słowa, bo tego się nie da powiedzieć słowami

This thesis would not be possible without the help as well as physical and remote presence of many people. I would like to thank Prof. Ignas Niemegeers, my promotor, for inviting me to come to Delft, constant support and helping me to learn many things about the surrounding world. My gratitude goes to my two supervisors: Dr Ramin Hekmat, and especially to Dr Rangarao Venkatesha Prasad — for having the same academic passion, constant support, and helping me when it was really needed. वेन्कटेश धन्यवादः. I would also like to thank the Freeband AAF project for funding my research and the team of its researchers for a fruitful cooperation: Ir. Fokke Hoeksema, Dr. Andre Kokkeler and Ir. Marnix Heskamp, all from University of Twente; Ir. Ibrahim Budiarjo and Dr. Homayoun Nikookar, both from TU Delft; Ir. Hugo de Graaf and Ir. Jan Stemerdink from TI-WMC and Ir. Mauritius de Graaf from Thales Netherlands.

I would like to thank my parents, Urszula and Jerzy Pawełczak, for a careful shaping of my character and investing so much time and energy into making me what I am. *Kochani Mamo i Tato* — thank you for injecting the passion for knowledge, showing me the world of possibilities and for being my true soul mates and friends. It is simply impossible to express how grateful I am to have you!

Also, this dissertation would not exist if I had not met the following people on my life path. I would like to thank mgr inż. Adrian Bohdanowicz from Nokia Siemens Networks for helping me making a first step towards TU Delft. I am indebted to Prof. Andrzej Jajszczyk from AGH University of Science and Technology, Kraków who made me realize what I want to achieve. My words of thankfulness go to people from the Connectivity Lab of the University of California, Berkeley and in particular to Dr Hoi-Sheung Wilson So and Dr Sofie Pollin, now with IMEC Belgium, for numerous discussions and common research interests, and to Prof. Ahmad Bahai for helping me to fund my stay at the UC

Berkeley.

I also had a great support for decision on pursuing my academic carrier from various people at my *alma mater* – Wrocław University of Technology. In particular I would like to thank Prof. Wojciech Kordecki from the Institute of Mathematics, Prof. Krzysztof Abramski from the Laser and Fibre Electronics Group and especially mgr inż. Tomasz Rogowski, now affiliated with Scuola Superiore Sant'Anna of Pisa.

Without certain people, life on the 19th floor of the EWI department would be just incomprehensible. In particular, I would like to thank Ir. Alex Slingerland for helping me understand the complexity of the Dutch language, and for never refusing when I asked for help. Also, Chapter 5 of this thesis is based on the work we did together. Alex, *hartelijk bedankt*! I would also like to thank Dr Gerard Janssen for help in the initial stage of my research, and Dr Jos Weber for sharing with me his views and opinions, for all his advice, and the support at the last stage of my PhD. Dr Martin Jacobsson and Dr Antohny Lo served as a great source of life ideas and Ir. Cheng Guo, with whom I had the great pleasure of sharing office space with, shown me the beauty and richness of Chinese culture.

Words of acknowledgment also go to my master students at TU Delft: Ir. Rahman Doost and Ir. Frank E. Visser — Chapter 2 of this thesis would be incomplete without their contribution. Also this thesis would not be possible without the help of our beloved secretaries – Laura Bauman, Wendy Murtinu-van Schagen and Marjon Verkaik-Vonk. My words of acknowledgment go also to the former and current members of the WMC and NAS groups at TU Delft, and especially to Xueli An, Giovanni Bellusci, Anteneh Ayalew Beshir, Bao Linh Dang, Santpal Singh Dhillon, Bingjie Fu, Javier Martín Hernández, Almerima Jamaković, Milena Janić, Nauman Farooq Kiyani, Robert Kooij, Tom Kleiberg, Jing Wang and Jinglong Zhou.

I am indebted to people from IEEE SCC41 project and in particular James Hoffmayer and Bernard Eydt for helping me to comprehend the complicated structures of the IEEE standardization process. I would also like to thank Dr Wolter Lemstra and Ir. Vic Hayes from TPM Department of TU Delft.

Wielkie dziękuję goes to all polish friends that I met in the Netherlands, and in particular to Partycja and Krzysztof Gradowscy, Agnieszka and Daniel Lewandowscy and Lidia Burzała. Yet another *wielkie dziękuję* goes to all the members of Polish Student Association in the Netherlands. I would also like to thank my friends in Poland, who have not forgotten about me yet, i.e, Seweryn Krawiecki, Marcin Suszkiewicz and Jerzy Tenerowicz.

Finally I would like to thank Izabela Grudzińska for everything she did for me and for the wonder of love she has brought into my life. Iza, always remember — *there is a light that never goes out.* This thesis is also dedicated to you.

Przemysław Pawełczak
Delft, April 2009

Thesis Summary

Opportunistic Spectrum Access: Designing Link and Transport Layer

Due to the rapid growth of wireless services the radio spectrum needs to be efficiently utilized to fulfill the quality of service requirements of the end users. However, many independent observations show that radio frequency resources are often wasted. That is, while channels where WiFi and Bluetooth operate are crowded, other radio frequencies, like those assigned to analogue cellular telephony or TV bands stay silent. Our own limited observations of Dutch 400 MHz channel occupancy, presented in the Appendix of this thesis, indicate less than 10% spectrum utilization. Thus if secondary wireless networks were able to exploit those voids in radio spectrum, its overall utilization would dramatically increase and the pace of wireless networks proliferation would be kept. Therefore this idea, called Opportunistic Spectrum Access (OSA), has attracted lots of recent attention of numerous research labs and universities.

There are many open problems related to OSA, mostly associated with physical layer. However, of high importance is to understand and explore network-related properties of OSA. Therefore the aim of this thesis was to progress further networking research on OSA. Particularly, in the context of Link and Transport layer of the Open Systems Interconnection reference model, the presented results give certain insights into the design and performance of Medium Access Protocols (MAC) and Transport Control Protocols (TCP) for OSA networks.

We introduce the reader to the topic in Chapter 1, where we discuss the open issues and research questions that are associated with the OSA protocol design. In particular we have found that better a OSA MAC protocol needs to be developed, which would be flexible enough to support high throughput for secondary users and induce minimum interference to the licensees. Also the interaction between physical layer, MAC and transport protocols in OSA networks needs to be better

understood.

Our first results are given in Chapter 2 where we present the contributions on the physical layer analysis for OSA, which serve as the basis for the protocol analysis in the subsequent chapters. We discuss unique properties of the OSA physical layer that affect the operation of higher layers of the protocol stack. These are: i) the licensed user activity detection process and ii) the randomness in channel occupancy by the licensee. It has been shown that the best way to mitigate the destructive propagation effects in the detection process is to distribute spectrum sensing amongst all nodes in the OSA network. We have proposed cooperative log-likelihood combining as a good sensing scheme, which outperforms other existing methods like hard decision combining. As a result of this analysis a protocol has been proposed that serves as a substrate for spectrum sensing information dissemination. In the context of channel variation statistics we have also explored the networking properties of this protocol, i.e., how frequently an OSA network needs to observe the licensed channel such that the maximum observation time can be achieved with the minimum energy consumption.

In Chapter 3 a general analysis of OSA network performance is presented. We explore the blocking probabilities in such networks, using Markov chain analysis, taking into account the physical layer features explored in Chapter 2. Two general channel access strategies for OSA networks with non-uniform licensed user channel utilization have been defined: i) random and ii) leased-used channel access. We have concluded that leased-used channel access strategy improves OSA network throughput significantly, when utilization imbalance between individual licensed user channels is apparent. With this information in mind we have designed a simple OSA MAC protocol, based on modified ALOHA, that exploits the knowledge of channel utilization and operates within the interference constraints given by the radio regulator.

As a follow-up to the proposed OSA MAC in Chapter 3, different implementations of multichannel MAC protocols for OSA networks have been performed in Chapter 4. It has been concluded that hopping MACs perform better than ones with a dedicated control channel in terms of obtained throughput, as well as in terms of interference induced to licensed users. Also, we have proposed a new class of MAC protocols in OSA context, called Multiple Rendezvous MAC, that outperforms all other multichannel MACs existing in the literature, given different performance metrics like delay, throughput or interference induced to the licensee.

Having the foundation of the MAC design for the Data Link layer, we have performed the analysis of OSA network Transport layer focusing on TCP. One of the conclusions to be drawn from this analysis is that the length of the non-activity time of the channel licensed user has more negative impact on the OSA channel utilization by the TCP than the licensed user activity time. Also, we have observed that with the existing spectrum situation all currently available TCP designs with Selective Acknowledgments implemented, should have no problem with grabbing as much available licensed user bandwidth as needed. These results are presented in Chapter 5.

Finally the results of this thesis are summarized in Chapter 6. Also, some open research questions related to the topic of OSA protocol design and performance are presented there.

Przemysław Pawełczak

Samenvatting

Opportunistische Spectrumtoegang: Ontwerp van de Link- en de Transportlaag

Vanwege de snelle groei van draadloze diensten dient het radiospectrum efficiënt te worden benut om te voldoen aan de eisen van de eindgebruikers met betrekking tot de kwaliteit van de service. Maar veel onafhankelijke waarnemingen tonen aan dat radiofrequenties vaak verspild worden. Terwijl de kanalen waar WiFi en Bluetooth opereren vol zijn, worden andere radiofrequenties, zoals die toegewezen aan analoge cellulaire telefonie of TV kanalen, vrijwel niet benut. Onze eigen beperkte observaties van de bezetting van het Nederlandse 400 MHz kanaal, die in het aanhangsel van dit proefschrift geplaatst zijn, tonen minder dan 10% gebruik van het spectrum. Dus als secundaire draadloze netwerken de leemten in het radiospectrum konden benutten, zou het algehele gebruik drastisch toenemen en het tempo waarmee draadloze netwerken zich prolifereren worden gehandhaafd. Daarom heeft dit idee, genaamd Opportunistic Spectrum Access (OSA) [Opportunistische Spectrumtoegang], recentelijk veel aandacht van talloze onderzoekslaboratoria en universiteiten gekregen.

Er zijn veel open problemen met betrekking tot OSA, meestal geassocieerd met de fysieke laag. Het begrijpen en verkennen van netwerk gerelateerde eigenschappen van OSA is echter van groot belang. Het doel van dit proefschrift was om onderzoek op het gebied van OSA netwerken te bevorderen. Vooral in het kader van de Link- en Transportlaag van het Open Systems Interconnection referentiemodel, geven de gepresenteerde resultaten inzicht in de prestaties van Medium Access Protocol (MAC) en Transport Control Protocol (TCP) voor OSA netwerken.

We introduceren het onderwerp aan de lezer in hoofdstuk 1, waar we de open kwesties en vragen uiteenzetten geassocieerd met het OSA protocol ontwerp. In het bijzonder hebben we vastgesteld dat een beter OSA MAC protocol moet worden ontwikkeld, dat flexibel genoeg is voor de ondersteuning van een hoge doorvoersnelheid voor secundaire gebruikers en minimale interferentie induceert bij de licentiehouders. Ook de interactie tussen de fysieke laag, MAC en transport protocollen in OSA netwerken moet beter worden begrepen.

Onze eerste resultaten zijn te vinden in hoofdstuk 2 waar we de bijdragen aan de fysieke laag analyse voor OSA presenteren, die als basis dienen voor de protocol analyse in de volgende hoofdstukken. We bespreken de unieke eigenschappen van de OSA fysieke laag die invloed hebben op de werking van de hogere lagen van de protocol stack. Deze zijn: i) detectie van activiteit van een gelicentieerde gebruiker en ii) de willekeurigheid in kanaalbezetting door de licentiehouder. Het is aangetoond dat de beste manier om de destructieve effecten van het detectieproces in te perken is het verkennen van het spectrum te verdelen over alle knooppunten in het OSA netwerk. Wij hebben cooperative log-likelihood combining voorgesteld als een goed verkenningsschema, dat beter presteert dan andere bestaande methoden zoals hard decision combining. Als resultaat van deze analyse is een protocol voorgesteld dat dient als een substraat voor de verspreiding van informatie uit de spectrumverkenning. In het kader van kanaalvariatiestatistieken hebben we ook de eigenschappen van het netwerkprotocol onderzocht, dat wil zeggen, hoe vaak een OSA netwerk het licentiekanaal moet observeren, zodat een maximale observatietijd kan worden bereikt met een minimum aan energieverbruik.

In hoofdstuk 3 wordt een algemene analyse van de netwerkprestaties van OSA gepresenteerd. We onderzoeken de blokkeringskansen in deze netwerken, met behulp van een Markov-keten analyse, rekening houdend met de kenmerken van de fysieke laag onderzocht in hoofdstuk 2. Twee algemene kanaaltoegangstrategieën voor OSA netwerken met een niet-uniform licentie-kanaalgebruik zijn gedefinieerd: i) de willekeurige en ii) leased-used kanaaltoegang. We hebben geconcludeerd dat de leased-used kanaal strategie de doorvoersnelheid van het OSA netwerk aanzienlijk verbetert, indien het gebruik van licentiekanalen waarneembaar onevenwichtig is. Met deze informatie in het achterhoofd hebben we een eenvoudig OSA MAC protocol ontworpen, gebaseerd op gemodificeerd ALOHA, dat gebruik maakt van de kennis van het kanaalgebruik en opereert binnen de interferentiebeperkingen die zijn opgelegd door de radio-toezichthouder.

Als vervolg van de voorgestelde OSA MAC in hoofdstuk 3, zijn diverse implementaties van multikanaals MAC protocollen voor OSA netwerken uitgevoerd in hoofdstuk 4. Er wordt geconcludeerd dat hopping MACs beter presteren dan degenen met een special controlekanaal in termen van de verkregen doorvoer, alsmede op het vlak van interferentie toegebracht aan gelicentieerde gebruikers. Ook hebben we een nieuwe klasse van MAC-protocollen voorgesteld in de OSA context, genaamd Multiple Rendezvous MAC, die beter presteert dan alle andere multikanaals MACs in de bestaande literatuur, gegeven verschillende prestatiemetrieken zoals vertraging, doorvoer of interferentie toegebracht aan de licentiehouder.

Met gebruik van de basis van het MAC ontwerp voor de Linklaag, wordt een prestatieanalyse van de OSA netwerk Transportlaag uitgevoerd met de nadruk op TCP. Een van de conclusies die wordt getrokken uit deze analyse is dat de tijd dat de kanaal primaire gebruiker niet actief is, meer negatieve invloed uitoefent op het OSA kanaalgebruik door het TCP dan de tijd dat de kanaal primaire gebruiker wel actief is. Ook hebben we geconstateerd dat met de bestaande situatie in het radiospectrum, alle momenteel beschikbare TCP ontwerpen, waarin Selective Acknowledgments zijn geimplementeerd, geen probleem zouden vormen wanneer de voor de gelicentieerde gebruiker benodigde bandbreedte wordt benut. Deze resultaten worden gepresenteerd in hoofdstuk 5.

Tot slot zijn de resultaten van dit proefschrift samengevat in hoofdstuk 6. Tevens wordt er een aantal open vragen gepresenteerd met betrekking tot OSA protocolontwerp en -prestaties.

Przemysław Pawełczak

Contents

Chapter 1

Introduction

to słowa
tak mówią
to myśli

Siekiera, "To słowa," from the album "Nowa Aleksandria," Tonpress KAW, 1986

Wireless communication has been constantly evolving from the moment humans communicated for the first time using radio waves. Thanks to the technological development wireless devices surround us wherever we go and whatever we do. However there is a problem. Currently though there are so many networks around us with only a handful of radio channels available for the new networks and services. Exploiting the fact that most of the radio spectrum assigned is used inefficiently, future networks would be able to communicate using the technique called Opportunistic Spectrum Access (OSA). This thesis will describe how.

Particularly, from the perspective of Link and Transport layer of the classical Open Systems Interconnection (OSI) basic reference model, this thesis investigates the aspects of OSA networks. Results presented here give certain insights into the performance of OSA, as well as into the design and performance of Medium Access Protocols (MAC) and Transport Control Protocols (TCP) for OSA networks.

This chapter introduces the notion of OSA as well as all its accompanying topics, presenting the background for the results obtained in the subsequent chapters. First we start by introducing the idea of OSA in Section 1.1. All the concepts related to OSA, especially the ones that interrelate to the future spectrum management, that will be used throughout this thesis are described in Section 1.2. Then, in Section 1.3 we list problems and open research questions related to OSA. Positioning this research and the motivation for the work in this thesis and an overview are given in Sections 1.4 and 1.5, respectively. Finally, a summary of the main results from this thesis is given in Section 1.6. Chapter is concluded in

Section 1.7.

We emphasize here that this thesis was written with the assumption that the reader has been exposed to the basics of digital telecommunication principles and is familiar with classical performance analysis techniques.

1.1 Opportunistic Spectrum Access

Everything has its beginning — life, PhD thesis, as well as any technological development. It is then necessary to start this dissertation with a discussion on how everything started with OSA, what OSA can offer, and what are the research problems associated with OSA. We also feel strongly that it is necessary to look at this communication technique in a proper historical context.

1.1.1 Infinite Capacity, Infinite Possibilities

Martin Cooper – former corporate director of Research and Development for Motorola and considered by many as the father of the mobile phone – once stated that the number of wireless voice or data transmissions that can be transported over a given area in all of the useful radio spectrum doubles every two and a half years[1]. Thus at the time of writing this thesis the theoretical number of possible wireless connections at the spot where Guglielmo Marconi performed his first spark gap transmission[2] in 1895 raised from 1 to an astonishing 4.04×10^{13}.

But, for example, when one looks closely at the proliferation and utilization of Wi-Fi Access Points (APs) in crowded city areas, not much space is left for the Cooper's law to prove itself in the near future in these bands. To give a sharp example, one of the Ofcom (United Kingdom's communications market regulator) studies showed that the average number of APs that can be accommodated per square kilometer, such that reasonable Quality of Service (QoS) can be experienced by individuals, is ≈ 26, assuming that no other devices, e.g., Bluetooth and microwave ovens, radiate at a given frequency [1]. In contrast to that, rough estimates of Wi-Fi proliferation in central London, performed by British futurist Peter Cochrane, revealed a stunning number of 200 APs/km^2!

1.1.2 Cooper's Law: Theory versus Reality

Wireless Local Area Networks (WLANs) in 2.4 and 5 GHz bands are overpopulated since their capacity is too small for a far too higher number of interested parties. But even if WLAN network administrators would like to direct some of the traffic to different bands to reduce the congestion, they are forbidden to do

[1] Although we are not aware of any document to cite this observation, the Internet legend credits this law to Cooper.

[2] Which does not necessarily mean that he was the first one to demonstrate wireless communication using radio waves — Bengali Hindu, Jagadish Chandra Bose was the first, see IEEE History Center.

so since it would violate local spectrum licensing laws. Even more interesting, if we look closely at any recent spectrum utilization measurement (an example is given in Appendix A) we will notice a huge asymmetry in spectrum utilization. That is, while popular spectrum bands like WLAN are highly congested in certain geographical areas, majority of spectrum bands, although assigned to different systems, are practically silent. Under-utilization is specifically visible in the licensed bands, i.e., bands that one must acquire a license, potentially from a spectrum regulator before usage. Pagers, analogue television and telephony, although slowly disappearing from the annals of telecommunication history, still have a reserved place in spectrum charts, which no one except for these licensees can use.

Thus the problem lies not in Cooper's law but in an archaic spectrum licensing and management. Such static spectrum assignment, applied to radio frequencies for almost a century, led to *quasi-scarcity of the spectrum.* It would be thus practical to allow unlicensed users to exploit dynamically and opportunistically the licensed frequencies when they are free at a specific time and space (to minimize interference). Theoretically, such approach would increase overall frequency reuse and would boost the throughput for applications that opportunistically use the empty frequencies. This way of spectrum access will be called throughout this thesis as OSA (more formal definition will be given in Section 1.2.2). Therefore through OSA WLAN, users would benefit from a temporal channel change, while this would not cause interference to anyone, since there would be no one to interfere with!

There have been many successful attempts in the past to liberalize spectrum access this way. Before going further with the OSA overview let us briefly discuss the history of non-conservative approach to spectrum management.

1.1.3 A Brief History of Elastic Spectrum Management

Dynamic and opportunistic spectrum sharing is not a novel idea and is probably as old as radio communication itself. Looking at the history of radio regulation (especially in the United States) we can find many examples of attempts to liberalize spectrum market. Here, by liberalization we mean maintaining a set of radio channels and assigning them on demand basis. Such maintenance would be completely distributed (using specific radio layer management protocols) or supported by a spectrum regulator.

One of the first communication systems with shared radio resources, developed in early 1920s, was maritime communication, see Fig. 1.1). In this system 2.182 kHz band was used as emergency and control channel on which all ships listen whether someone wants to communicate by broadcasting working carrier identifier for further communication. After the World War II, around 1960, USA's Federal Communications Commission (FCC) allowed using shared channels in land mobile communication, where one trunking channel could be used by many parties. With hardware extensions, like tone-coded squelch or Listen Before Talk

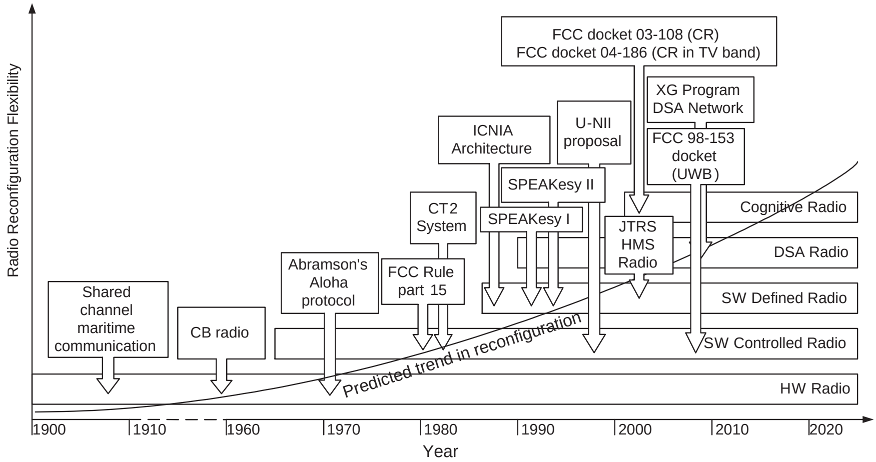

Figure 1.1: *History of dynamic spectrum access systems and their relation to the implementation platforms, with the view on the future; DSA: Dynamic Spectrum Access, HW: hardware, SW: Software (for the explanation of all terms and other abbreviations reader is referred to Section 1.1.3.)*

(LBT), and the fact that most transmitted messages were short, shared channel communication became very efficient. In the mid 1970s FCC allowed to share channels at 27 MHz band (so called Citizen Band (CB)) on a first come first served (FCFS) basis. The only restriction that users of CB bands had to adhere to was maximum transmitting power limits.

With the advent of wireless data communication more flexible ways of spectrum management were possible. Abramson's Aloha protocol, presented in 1970, was a solution to use radio channels for wireless data communication without any centralized coordinating entity. The ideas of random access were later extended to Packet Radio Networks. This, indirectly, gave a way to an FCC Rule part 15, which described the ways of coexistence of low power wireless devices in Industrial, Scientific and Medical (ISM) bands. Adopted in 1985, it initially described the methods for wireless devices using spread spectrum as a communication technique. Later FCC part 15 Rule was changed to allow any modulation technique that met required power limits, is wide enough and did not contain "strong spectral lines". Neither Etiquette nor LBT protocols were defined in FCC Rule. Its huge success was later legitimized by FCC's acceptance of Apple Corp. proposal in 1995, to allow everyone to use 5 GHz band (called Unlicensed-National Information Infrastructure (U-NII)) without any prior allowance. Currently, U-NII is used with success for wireless packet-based communication. British Cordless Telephone Second Generation (CT2) system standardized in the mid 1980s was another example of a successful distributed channel management technique. 40 MHz band divided in 40 channels was managed by a Base Station (BS) that could monitor the level of interference on all channels and choose one that possessed minimum interference.

In George Gilder's article "Auctioning the Airwaves" published in Forbes on April 11, 1994, the author envisioned the future in which "the wireless systems (...) will offer bandwidth on-demand and send packets wherever there is room". In parallel, Eli Noam from University of Columbia proposed in 1995 an "Open Spectrum Access" paradigm [2], in which interested parties would pay for bandwidth whenever there is demand. Although both proposals addressed no technical issues and were mainly aiming at packet data communication, it was a sign for radio regulators that real steps in liberalizing spectrum market were needed, i.e., it was a clear indication that it might be better to promote licensed parties that share their unutilized resources, instead of not controlling how the spectrum is utilized by the licensees.

Therefore, in 2002 FCC issued 98-153 Docket permitting many users to transmit on a single channel using low power communication based on Ultra Wide Band (UWB) communication. Recently released FCC Docket 03-122 revisited rule 15 allowing wireless data users to share channels with radar systems on LBT basis. Finally FCC realized that Cognitive Radio (CR) techniques are the future substrate that stimulate full growth of "open spectrum" (see FCC Docket 03-108 on CR techniques and FCC Docket 04-186 on CR in TV spectrum). Finally on the day of the historical 2008 US presidential election FCC released 08-260 Docket that formally allowed unlicensed transmission in the TV broadcast bands.

We note that some probes of radio channel liberalization were not so spectacular, mainly due to inflexible rules of operation enforced by the regulator. Examples of such systems were Radio Common Carrier (RCC) issued in mid 1970s, 800 MHz channel Air Ground Telephone Service (AGTS) from 1990s, Unlicensed Personal Communications Service (UPCS) and Large Scale Low-Earth Orbit Satellite System (called "Big" LEOS) with shared Code Division Multiple Access channels (early 1990s). First, RCC could operate only when multiple service providers decided how to share common channels that was not so financially attractive due to competition between all interested parties. Second, AGTS was not popular due to many rules of operation that FCC provided. Third, UPCS specification by FCC also included many restrictions to the operation of potential systems. Moreover it had to share channels with microwave point to point links, which are now ubiquitous, and often space separation was necessary between different UPCS devices. Finally, "Big" LEOS failure was due to financial problems of service providers because of licensing fees.

More information on the historical developments in dynamic spectrum management can be found in [3], where some of the systems are more elaborately explained. Brief illustration of the above discussion is given in Fig. 1.1, where we map discussed solutions onto different types of hardware platforms, which we describe in more detail in Section 1.2.1. Note that we can observe semi-exponential growth in radio reconfiguration flexibility. That is on the course of history hardware that supported wireless communication became more capable of doing complicated signal processing tasks, while software design that supported radio hardware became more important during the design process. Now, given the knowledge of the past on flexible spectrum management, we obviously need to look at the future.

1.1.4 A View of Wireless Network Futurists

In the late 1990's, in tune with what has been happening over the last 100 years in radio spectrum management, community of researchers, visionaries, futurists and the like started to think about combining flexible spectrum access concepts with intelligent radio hardware platforms and smart networks. In this framework, emerging paradigms of dynamic spectrum access were related to cognitive communications[3]. The computational abilities of current electronic devices as well as recent developments in computer science and artificial intelligence led researchers to start thinking of introducing the cognition into the wireless networks and devices. This functionality would allow wireless systems in general to become more flexible, inferring from the environment on the required actions and adapt the internal parameters to fulfil the needs of the user to the possible best. These cognitive devices would *per se* also allow harvesting the radio spectrum more optimally, allowing more users to communicate efficiently, without additional need for licensing. The ultimate dream is to use and reuse the available spectrum to the fullest.

The CR, as it is usually called in the literature, started to attract lots of attention gradually. Since the introduction of this concept formally in 1999 by Mitola [4] a massive amount of literature has been published on this topic. In nine years more than 35 conference and workshops that focused solely on CR have been organized and approximately 20 scientific journal special issues on CR have been published, see http://www.scc41.org/crinfo/. Looking at the popularity of papers published by Institute of Electrical and Electronics Engineers (IEEE) on CR since 2001, see Fig. 1.2a, and the results of our simple investigation based on Internet webpage crawling, see Fig. 1.2b, we can conclude that CR, Dynamic Spectrum Access (DSA) and OSA, which are inter-related with CR, have become increasingly popular.

Moreover, recent research papers outline the possibility of extending the principle of cognitivism to entire heterogeneous networks, thus a new concept called Cognitive Networks (CN) [5] has been making inroads as one of the future networking construct. The aim of CNs is to self-adapt to the changing requirements from users and applications in order to provide QoS and self-management capability. Such a networking paradigm is based on the availability of Software Adaptable Network elements, driven and configured by a *cognitive process*[4]. Growing

[3] The term *cognition* is a popular topic in psychological and social sciences that relates to information processing, understanding and making sense of the observations, and finally using it in future interactions with the environment.

[4] Cognitive process is a decision making engine whose decisions are based on the current

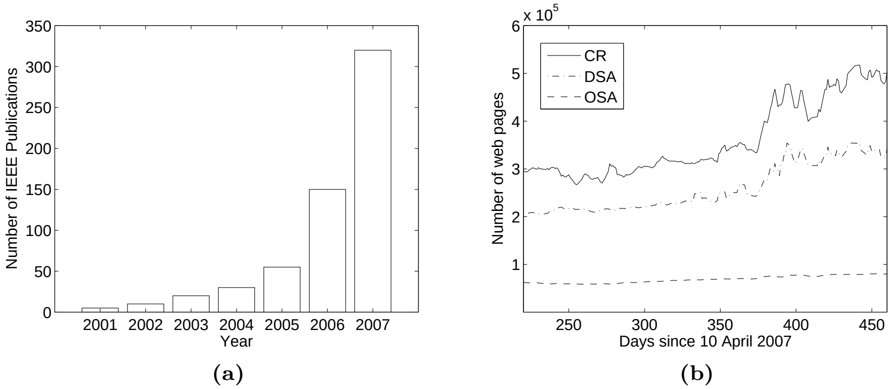

Figure 1.2: *Popularity of OSA and its related concepts: (a) number of articles related to Cognitive Radio published by IEEE (source: Dr. A. Swami, US Army Research Laboratory); and (b) statistics of the Google search engine responses for 'Cognitive Radio' (CR), 'Dynamic Spectrum Access' (DSA) and 'Opportunistic Spectrum Access' (OSA) phrases in terms of number of WWW pages found.*

interest on this research topic can be recognized by the commencement of an IEEE Communications Society Technical Committee on Cognitive Networks, see www.eecs.ucf.edu/tccn/.

1.1.5 Advantages and Applications of OSA

Since OSA and its related concepts are radio access techniques, they can be applied to any communication system or network that suffers from spectrum shortage. It becomes attractive since it does not need any specially designed modulation technique, coding, etc. OSA reuses spectrum which has been detected as vacant using the appropriate communication technology. Ad Hoc, sensor and cellular are the ones that will immensely benefit from additional spectrum capacity that OSA can offer. Operation specific networks can also benefit from the introduction of OSA. For example in this thesis a specific application of OSA into Emergency Communication Networks (ECNs) will be introduced and discussed in detail.

Further, attractiveness of OSA has been recognized by European Telecommunications Standards Institute (ETSI), and has been considered as one of the candidates for future radio interface of 4G networks. The potential for OSA has also been found by IEEE. Its newest standard specifying protocols for future Regional Access Networks (RANs), called IEEE 802.22, aims at design of a new radio interface that would work in the so called *white spaces*, i.e., places in radio

---

network conditions and involving adaptation and learning techniques.

spectrum vacated by analog television signal. Yet another initiative by the IEEE is a standard related to reconfigurable heterogeneous radio interfaces, called IEEE 1900.4.

A discerning reader will notice some inconsistency in terminologies related to OSA, e.g., what is the relation between CR, DSA and OSA. In the following section we will discuss each concept in detail, pointing to the essential differences between them.

1.2 Essential Concepts Related to OSA

Unfortunately, during the course of research on OSA, there has been a lot of ambiguity in naming certain concepts. We noticed that different modern approaches of spectrum management are commonly mistaken with CR. We will briefly elaborate on this issue in the subsequent paragraphs.

1.2.1 Ambiguity in CR Definitions

Historically, CR was first described by Mitola in [4; 6; 7] as a decision making layer in which "wireless personal digital assistants and the related networks were sufficiently computationally intelligent about radio resources, and related computer-to-computer communications, to detect user needs as a function of use context, and to provide radio resources and wireless services most appropriate to those needs." It was a vision of an intelligent wireless "black-box" with which user travels. Wherever the user goes CR device would adapt to new environment allowing the user to be always connected [4]. We need to note here that Mitola was not only the initiator of the CR notion, but also coined the term Software Defined Radio (SDR). He thought of CR as a natural extension of SDR, where software allowed to flexibly altering transmission and reception parameters, to all layers of communication stack. Also, he was the first one to think of including "intelligence *ergo* cognition to the whole radio setup.

Six years after Mitola's first article on CR, Haykin in his invited article to IEEE Journal on Selected Areas in Communications [8], recapitulated the idea of CR. He defined CR as "inclusive of SDR, [idea] to promote efficient use of spectrum by exploiting the existence of spectrum holes", or "intelligent wireless communication system (...) that adapt(s) to statistical variations in the input stimuli with two primary objectives in mind: highly reliable communication (...); [and] efficient utilization of radio spectrum." Thus he reduced CR to spectrum utilization-oriented concept. His whole article focused on signal processing techniques that in his view would be helpful in managing particularly the second goal, i.e., efficient utilization of radio spectrum. Not only he defined his own CR, but also altered the basic cognitive cycle proposed by Mitola [4]. This paper was the first major publication that gave totally different definition of CR, and at the same time caused confusions in terminology. Interestingly, according to Google Scholar, as

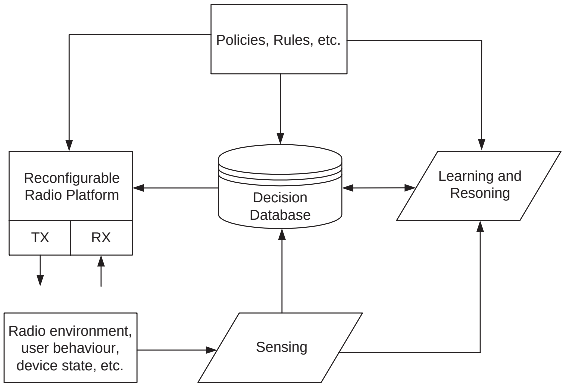

Figure 1.3: *Components of CR node, see also [9].*

of 30 September 2008, original Mitola's paper on CR [4] was cited 404 times, while Haykin's paper [8] was cited 669 times.

Yet another notion of CR can be found in Information Theory (IT) community, see for example [10]. Very broadly, in IT field CR is reduced to the analysis of capacity and throughput of Transmit/Receive Pair-1 (called Secondary Users[5]) with Transmit/Receive Pair-2 (called Primary Users) that interferes with Pair-1. In this context a notion of *cognitive channel* is presented, i.e., a channel in which secondary pair of nodes possesses some kind of side information on what actually the interferer is transmitting. It is clearly seen that cognition for IT community is far different from the concept of cognition introduced by Mitola.

Interestingly the SDR Forum explains CR as "a radio that has, in some sense, i) awareness of changes in its environment and ii) in response to these changes adapts its operating characteristics in some way to improve its performance or to minimize a loss in performance". In contrast to the above mentioned definitions, FCC describes CR as wireless node or network able to negotiate cooperatively with other users to enable more efficient utilization of radio resources, see FCC Docket 03-108 and 03-186 for more detailed description. CR would be able to identify portion of the unused spectrum and utilize it for communication purposes. Thus, the FCC approach is a simplified form of Mitola's vision where only radio spectrum conditions are considered while taking the decision about future transmission and reception.

In this thesis we take the position that the cognitive functionality may be spread across the layers of the communication architecture resulting in coordination amongst the layers for an efficient use of available spectrum. Fig. 1.3 explains the basic functional blocks of such a CR node, which we believe is the most complete one. Specifically, apart from a reconfigurable radio, a CR node has various

[5]See Section 1.2.2 for the definition of Primary and Secondary User in the spectrum management context.

Table 1.1: *Adaptable Radio Devices; DB: Database, HW: Hardware, ML: Machine Learning, SW: Software.*

Type of Radio	Platform	Reconfiguration	Intelligence
Hardware	HW	Minimal	None
Software	HW/SW	Automatic	Minimal
Adaptive	HW/SW	Automatic/Predefined	Minimal/None
Reconfigurable	HW/SW	Manual/Predefined	Minimal/None
Policy-based	HW/SW	DB/Automatic	Minimal/None
Cognitive	HW/SW	Full	Artificial/ML
Intelligent	HW/SW	Full	ML/Prediction

other components. The sensing and policies block (if available) are extensively used in deciding the availability of spectrum. These blocks also help to drive the learning and reasoning functions, where the decision database, along with the input from the sensing and policies block, drives learning. The end result is that the radio is configured based on input from different layers of the communication stack as well as from the environment inputs.

Yet another definitional ambiguity comes from the CR implementation. Categories and classes of different future adaptive radio devices are listed in Table 1.1. This simplistic comparison tries to show the differences between them, since some confusion still subsists in CR community on how to classify different devices and systems. Please note that in Fig. 1.1 different milestones in spectrum management flexibility have been mapped onto different hardware platforms. The more flexible the given system is, the more flexible the hardware platform becomes. Certain milestones that we have to note in developing software based radio platforms are SpeakEasy [11], Joint Tactical Radio System [12], DARPA XG Program radios [13] and Integrated communications, navigation, identification avionics (ICNIA) [14].

We have remarked earlier that other names are used in the literature to define CR systems, for instance, DSA, Spectrum Agile Radio or OSA, see Section 1.2.1. We feel that any intelligent spectrum management technique is a logical component of CR but it is not a synonym. We refer to IEEE P1900.1 standard [15] for further discussion.

1.2.2 Modern Spectrum Management Approaches

OSA belongs to a class of modern spectrum management techniques that are often vaguely defined [9; 16; 17]. To clear the ambiguity in terminology let us briefly introduce our classification given in Fig. 1.4.

We consider three essential models: *Exclusive Spectrum Management* (ESM), the *Spectrum Commons* (SC) sharing model, and *Hierarchical Spectrum Management* (HSM). The ESM model still gives exclusive channel use to each user or

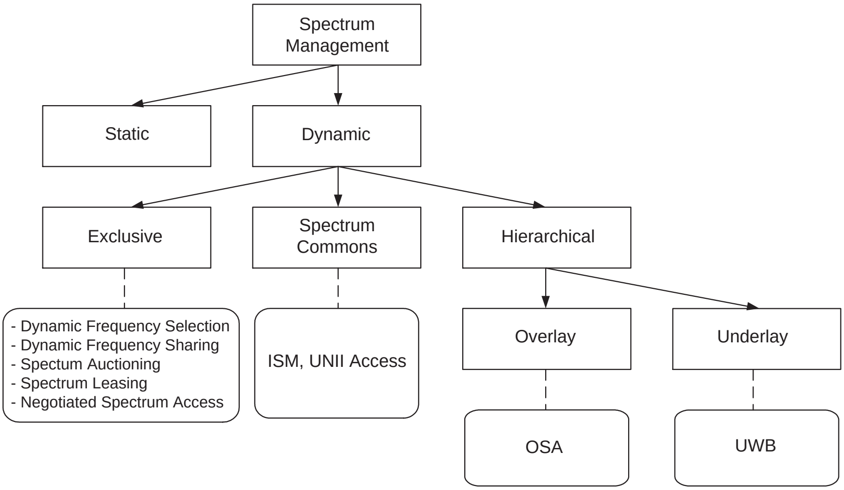

Figure 1.4: *Modern spectrum management: Classification with the application examples (see also [16; 17]).*

provider, but differs from a static assignment in the sense that the channels are allocated dynamically among possible licensees. The process of exclusive channel access is usually governed by radio regulation bodies. The differences between ESM approaches, specified in Fig. 1.4, depend on the economic model that varies from country to country. In the SC model, different users compete for the assigned frequencies on equal terms. The HSM model gives *Primary (Licensed) Users* (PUs) more rights to use the spectrum than other *Secondary (Unlicensed) Users* (SUs). We can distinguish two HSM approaches. In *Overlay* HSM, only one user/system can use a frequency band at particular space and time, and the SUs have to back off when a PU is present. However, when no PU is present, the SU can opportunistically use the frequency band, so this technique is also referred to as OSA. In *Underlay* HSM, a SU can transmit in an already occupied band if this transmission does not increase the interference to the PU above a given threshold. A further classification of Overlay HSM (not shown in Fig. 1.4) involves *Symmetric Coexistence* (when both SU and PU networks adapt) and *Asymmetric Coexistence* (when only the SU network adapts, obeying the PU requirements). In this thesis, we consider only the case where the PU does not adapt to the operation of the SUs. Clearly, OSA is the most flexible spectrum management technique. Furthermore, Asymmetric OSA allows achieving maximal spectrum use without significantly altering the current spectrum regulation market.

Given the discussion on OSA, its history and related definitions, we can proceed further with the introduction. This will help us to anchor the scope of this thesis. First we will present and discuss what the research problems associated with OSA.

1.3 Research Challenges

Instead of providing an exhaustive analysis of all research works available on OSA communications – due to the amount of published papers and the interdisciplinary nature of the topic (see for example [16] and the references therein) – we provide a contextual references to the established works, while expounding on the issues tackled here.

The purpose of this section is therefore to briefly describe issues which are yet open and currently debated in the framework of research on OSA and CR networks. We will focus on the issues that are solely characteristic to OSA, omitting where possible discussions on the problems that are common to usual wireless communication research. In the following sections we will enlist essential problems grouping them into Computation-, Architecture-, Physical Layer-, and Protocol-related categories.

1.3.1 Computation-related Problems

Decision Process

As CRs, Cognitive Networks (CNs) and Cognitive Radio Networks[6] (CRNs) are driven by a decision process, a relevant research issue related to *where* and *how* the decision should be taken, for instance on spectrum availability. The first question is directly related to whether the cognitive process should be implemented in a centralized or distributed fashion. This aspect is more critical for CNs, where intelligence is more likely to be distributed, but also CRs, as decision-making could be influenced by collaboration with other devices. The second issue is related to the choice of the decision algorithm. It represents a challenging topic. Although several optimization schemes based on learning are available in the literature, like neural networks, genetic algorithms, ant-colony optimization, etc., they need further analysis and customization to fulfil the system requirements.

Interaction with all Layers of Protocol Stack

While the aspect of inter-protocol interaction is, by definition, included in the concept of CN as a means to support user and requirements of applications, no relevant and comprehensive analysis is available to address the performance and, in general, the behaviour of applications and networks based on CR and CN technology.

[6] *Cognitive Radio Network* is a network capable of establishing links between its CR Nodes, and to adjust its connectivity to adapt to the changes in environment, topology, operating conditions, or user needs.

1.3.2 Architecture-related Problems

Implementation

While general block diagrams and functional blocks of CR are being identified, an open issue is represented by the hardware and software architectures to support CR and related designs. Indeed, in the case of a single CR device this problem is closely related to research on SDR. However, in a broader scenario including cooperation amongst several devices across different networks and higher levels of adaptation, architectural issues represent a complex challenge as they, not only, include mainly the definition of architectures for Software Adaptable Networks [5], but also compliance and inter-operability with, e.g., OSI or TCP/IP protocol stacks.

Equipment Test Procedures and Certification

Devices with potential CR capability bring new challenges also for the certification process. To prove that a CR device will always remain within the operational boundaries is more difficult compared to classical radios. Future hardware vendors must know the design methodologies and testing procedures to affirm that their devices shall not interfere with any PU of a given frequency channel. Many technical studies are involved such as hazard analysis, listing potential causes for out of compliance transmission, and description of previous behaviour-based certification efforts. In fact, its most important task is to standardize the dependability of a radio system vis-á-vis quantifying the level of trust one has.

1.3.3 Physical Layer-related Problems

Every OSA network or device needs to detect which parts of the spectrum are vacant. The spectrum sensing should be performed such that it will result in high confidence in spectrum occupancy decision. Also, the spectral sensing protocols must guarantee that even a malicious adversary cannot trick the secondary users into using a non-vacant channel and interfere with a PU. One of the primary goals of OSA networks is to identify spectrum holes and to make these available to applications, without requiring the PU to reprogram their hardware and functionality. In other words, it is essential for the SUs to detect the presence of a PU and evacuate immediately if there is a PU active in the band. However noise and propagation conditions make spectrum sensing a very difficult task.

1.3.4 Protocol-related Problems

Medium Access Control

Although IEEE 802.22 Working Group is already developing the MAC Protocol for Wireless Regional Access Networks utilizing concepts of OSA, other OSA MAC designs have not been made into standards. Particularly distributed MAC for ad hoc networks operating in the opportunistic spectrum access manner are not well covered. In the standardization domain IEEE 802.11 group covers some of the topics of intelligent spectrum management, e.g., IEEE 802.11k, but those are limited to the operations in the unlicensed bands.

Signaling

It represents a key research issue as both CRs and CRNs need to configure lower level parameters of the networking devices, and therefore the underlying infrastructure needs to provide software reconfiguration and programming, thus requiring SDR or Software Adaptable Network [5] technology. The requirement for programmable devices leads to two main challenges.

First, because of the limitations of the layering principle, in order to provide efficient operation, programmable devices should offer cross-layer interfaces suitable for adaptation and optimization. Specific signaling architectures are needed in order to enable internal or network-wide exchange of information between cognitive devices or among distributed devices constituting a single cognitive entity.

Second, while the debate on cross-layering has already gained maturity even with conflicting ideas [18], it is worthwhile to address signaling architecture as a relevant point to support cross-layer or in general optimized solutions. Indeed, several signaling architectures are available which can be classified on the basis of different types of interactions among protocols at different layers, or network-wide signaling [19].

Inter-operability

With the ability to switch between various bands of frequencies to achieve higher spectrum usage, the OSA devices will not be confined to one frequency band. Thus many technologies will be using multiple frequency bands. In such a scenario, the question is how to maximize the spectrum usage with these devices co-existing and co-operating or collaborating with each other. The different networks and the users should use the available free spectrum in an efficient and fair fashion.

Security

Most of the work has been concentrated on Denial-of-Service attacks that affect the design of authentication protocols. Although it is essential to build on these initial forays to develop secure protocols for spectrum access by the SUs, it is also important to consider other aspects of security like authorization. First, CRNs inherently assume that PUs and SUs are distinguishable. Authenticating PU and SU is especially important since they have unequal privileges. Although, this may be fairly straightforward for centralized architectures by making the SUs sign using a centralized authority, this is harder to achieve in a distributed secondary network where a centralized authority is not available. Second, in the context of CNs, there is a unique authorization requirement called conditional authorization.

It is conditional because the SUs are authorized to transmit in licensed bands only as long as they do not interfere with PU communications in that band. As it is difficult to pinpoint exactly which of the secondary users are responsible for harmful interference to the PU transmission, this type of authorization is hard to enforce and even more so in a distributed setting. Hence conditional authorization poses a unique challenge in OSA. So far several researchers have begun working on security implications for CRNs [20–22], however this area is still in its infancy.

1.4 Research Position and Motivation

Within the framework of wireless communication, different sub-topics can be identified, where one of them relates to organization of spectrum management. This can be synthesized later on into separate sub-research topics. OSA is indeed a spectrum management concept, as it has been explained earlier in Section 1.2. The question was, however, which sub-area of OSA needed to be explored. Knowing how many topics that attract the attention of the researchers in OSA context, see Section 1.3, it was difficult to decide what to focus on. We have decided to cover the topics that attracted least attention of the research community, which at the same time spanned all aspects solely related to OSA. After the first literature search in the beginning of 2005 it has been found that the most results were obtained for physical layer aspects of OSA, as well as for architectural and computational design of OSA which are interrelated to CR(N). There was void, however, with respect to the results on the protocols of the OSA. In particular, as we have pointed out in Section 1.1.5, all ad hoc networks will potentially benefit from the introduction of OSA to their radio access. How to organize communication within OSA network was indeed a research challenge.

It is obvious to note, after the above discussions, that the concept of OSA introduces new challenges to the notion of QoS-driven communication. Large fluctuations in the use of radio resources result in strongly varying throughput for OSA networks, and compulsory detection of PUs causes additional operational overhead. Therefore the introduction of OSA requires new approaches for the design of OSA MAC protocols. That is, protocols that manage common channel access. To protect QoS of the PU, SUs need to detect the presence of the PUs, which is prone to errors due to propagation conditions and noise. Whenever SU nodes make a wrong observation about the channel availability, their transmissions will harm the operation of the PU. Considering the QoS of the SU, it is clear that this QoS is largely determined by the channel utilization intensity and traffic pattern of the PUs.

The functionality of OSA MAC depends on the PU activity on individual OSA channels and is solely a function of physical layer. Also to know the impact of the channel availability on the MAC, fluctuating utilization of typical licensed channels need to be understood. Therefore the only way to solve the problem of proper MAC (or to be more general Data Link layer) design is to take a cross-layer approach. Another facet worth investigating, given our interest in protocols for OSA, was to see how low layer issues affect the operation of layers higher than Data Link. We were mostly interested in understanding how physical layer effects influences the operation of TCP in an OSA environment.

Summarizing, understanding the need for such a design in the OSA context, it is well motivated to split research presented in this thesis into separate layers of the classical OSI Basic Reference Model, i.e., research on MAC for OSA representing Data Link layer and research on TCP representing Transport layer.

It needs to be pointed out that research presented in this thesis was a result of collaboration within the Adaptive Ad Hoc Freeband (AAF) project, see http://aaf.freeband.nl. AAF is one of many spin-offs of Freeband consortium, promoting information and communication technology research in the Netherlands and sponsored by Dutch ministry of Economic Affairs. Apparently, when the AAF project took off in the middle of 2004, it was presumably the first European project solely related to research on CR (from a spectrum utilization perspective) and its applications to Emergency Communication.

1.5 Overview of the Thesis

This thesis reflects the results of research on Data Link and Transport layer of OSA networks. Its structure is divided into three major parts each one specific to a certain layer of the OSI Basic Reference Model.

Specifically, Chapter 2 (*OSA Spectrum Sensing Architecture*) is devoted solely to the design of optimal spectrum occupancy detectors. We start with an implementation example of OSA into ECNs. Later physical layer issues are analyzed with a strong focus on the protocol implementation, i.e., how to distribute sensing tasks amongst individual network nodes.

Foundations of physical layer given by Chapter 2 are later used to explore design issues of Data Link layer. In Chapter 3 (*General OSA Network Performance*) we derive blocking probabilities for OSA networks, particularly in the context of non-uniform PU channel utilization. Certain PU channel access strategies are proposed and analyzed. Based on the results of these analysis, in Chapter 4 (*OSA MAC Protocol Performance*) extensive performance analysis of all possible implementations of multichannel MAC protocols for OSA networks are given. Also, two new classes of multichannel MACs are proposed.

Given all the aspects of MAC design, in Chapter 5 (*Performance of TCP over OSA Links*), we explore issues related to TCP performance in the OSA context. First we analyze how different popular TCP designs perform on the OSA links, given different activity values of the PU. At the end we wrap-up the thesis by cross-layer design of TCP, i.e., we analyze what is the impact of PU detection quality on the performance of TCP.

Finally, Chapter 6 (*Conclusion*) summarizes major results obtained in the thesis and lists recommendations for future research on OSA.

1.6 Summary of Main Results

As one hairy and moustached German physicist once said: “If we knew what we were doing, it would not be called research, would it?” Well, we definitely did not know what we were doing, when we started the work as a *promovendus* at Delft University of Technology on 25 February 2005. Research on Data Link, and Transport layer, in particular, for OSA was at that time at its infancy. Luckily, after four years of wandering among endless corridors of science and engineering, there is handful of interesting conclusions that can be drawn from the research presented here. Some of them are listed below.

1. Cooperative PU detection analysis for OSA networks has been performed by building the foundation for analysis. It has been shown that the best way to mitigate the destructive propagation effects in PU detection process is to distribute spectrum sensing amongst all nodes in a network. As a result of this conclusion **a protocol has been proposed that serves as a substrate for spectrum sensing** information dissemination.

2. Two channel access strategies for OSA network with non-uniform PU channel utilization have been defined, i.e., random and least-used channel access. We have concluded that **least-used channel access strategy improves OSA network throughput significantly, when utilization imbalance between individual PU channels is apparent**.

3. Knowing the effects of least-used channel access strategy **we have proposed a new random access MAC for the OSA environment. Also, we have proposed coexistence metrics for OSA networks using interference limiting constraints defined at the link level**. The proposed MAC protocol has been analyzed from this perspective as well.

4. As a follow-up to the proposed OSA MAC design, different implementations of multichannel MAC protocols have been performed. It has been concluded that **hopping MACs perform better than ones with dedicated control channel**, both in terms of obtained throughput and in terms of interference induced to PU.

5. We have proposed a new class of MAC protocols in OSA context called **Multiple Rendezvous MAC, that outperforms all other multichannel MACs proposed in the literature**, given different performance metrics like delay, throughput or interference to PU.

6. Having the foundation of MAC design for the Data Link layer, we have performed the analysis of OSA network Transport layer specifically for TCP. One of the many conclusions to be drawn from these analyses is that **inactivity length of the PU has more negative impact on the TCP performance than activity time**. Also, we have observed that with the

existing spectrum situation all currently available **TCP designs with implementation of Selective Acknowledgments should have no problem with grabbing as much available PU bandwidth as needed**.

7. Finally, parallel to the research results obtained in this thesis, **we have co-authored a first IEEE Standard related to modern spectrum management**. The document abbreviated as IEEE 1900.1 [15] focuses on definitions related to DSA and presents concepts related to the topic. Issues related to OSA are also standardized there and views in this thesis conform to the views of the standard.

1.7 Chapter Summary

Starting from a historical perspective we motivated the need for more flexible spectrum usage. Essential definitions and concepts related to OSA have been introduced that are used later in this thesis. We have briefly outlined open research questions related to OSA. From that we have motivated and positioned our research work to focus on the issues not well explored in the OSA context. In the end we have briefly outlined our research results and contributions.

Chapter 2

OSA Spectrum Sensing Architecture

We sail through endless skies (...)
As we travel the universe

Black Sabbath, "Planet Caravan", from the album "Paranoid", Vertigo Records, 1970

In the previous chapter we introduced the notion of OSA, where we positioned the research on the design of networking protocols for such networks. As we have noted there, the most fundamental feature that distinguishes OSA-based wireless networks from classical ones is their need for PU detection. That is, OSA network should know at every instant about the activity and condition of every licensed wireless channel it has access to. Therefore we need to understand the physical layer issues that impact the performance of PU detection. Even more importantly, we need to understand and explore how to distribute the tasks related to spectrum sensing amongst multiple network components.

Our contributions in this chapter lie in the fact that we look at the PU detection problem not only from the theoretical performance point of view, but also from the protocol perspective. We emphasize that such a research path has been so far completely absent in the OSA literature.

We structure this chapter in the following way. First, as an example, we give a brief overview of design requirements for modern ECNs in Section 2.1. We stress the fact that the spectrum shortage is sharply visible in these types of networks and advocate the introduction of OSA. The logical structure of ECN introduced in this section will serve as a foundation for the design of distributed spectrum sensing protocol. Then in Section 2.2, we introduce the theory of PU detection process and propose new techniques for optimal measurement combining resulting in a better PU detection performance. Then in Section 2.3 we explore theoretically the performance of PU detection from the protocol perspective. We tried to answer the question on the conditions in which randomized measurement scheduling approaches fixed scheduling. Given the theory of PU detection we finally proposed a protocol that aims at supporting a cooperative detection process, which is described in Section 2.4. The description of implementation of PU detection is given in Section 2.5. Finally, the chapter is concluded in Section 2.6.

We stress that in this chapter we lay the foundation for the analyses of a MAC protocol and transport layer for OSA networks, which we will cover in the subsequent chapters.

2.1 Spectrum Sensing from the ECN Perspective

The proposed design of spectrum sensing protocol is anchored on the structure of the modern ECN. Contemporary ECNs suffer the most from the problem of spectrum shortage. The most natural and efficient way to solve this problem is by introducing OSA functionality into all ECN components. We now give a brief overview of the future ECN with a glimpse of the relevant and current state of the art in their development.

2.1.1 Uniqueness of ECN Design: Spectrum Management

Emergency ad hoc wireless networks must address much broader set of services than their civilian purpose counterparts, since many of the requirements for particular functionalities arise only during rescue operations. For example in the aftermath of a severe flood or earthquake when some parts of communication infrastructure have been damaged, emergency service workers must still communicate effectively. The set of requirements that are pivotal to ECN only were enlisted for example in [23]. These were, apart from reliability and robustness, self organization, scalability and power efficiency. From the services perspective, ECN nodes need to support data transfer, i.e., still picture forwarding between first responders and the command center, and real-time video and voice. However, in contrast to the conventional networks, ECNs need more stringent constraints in terms of delay, jitter, packet error, loss rate and bandwidth for each of these services.

Communication systems that are now available for rescue teams lack crucial characteristics which are very important when human lives are at stake. Most of these issues arise from the inappropriate spectrum management problems and spectrum scarcity phenomenon [24]. For example, TErrestrial Trunked RAdio (TETRA) standard-based ECNs, like nationwide C2000 infrastructure introduced in the Netherlands [25], hardly supports high data rate communication, mostly due to the incompatible channelization of each of the supported network. To give another example, since different emergency networks occupy different frequency bands, where each band is heavily congested during the rescue operation and exclusively available for specific group of users, cooperation between two emergency networks built on top of the same standard becomes impeded.

Many studies, so far, covered functional and service specifications of next generation ECNs to address the above mentioned problems. One of the first was MESA project [26] launched in 2000 by ETSI and Telecommunications Industry Association of the USA. Similar tasks were performed in the SAFECOM program [27] of the USA Department of Homeland Security, in which requirements for ECNs were stated taking into account more recent technology advancements than those done earlier by Public Safety Wireless Advisory Committee of the US government [28]. Wireless Deployable Network System (WIDENS) [29], a MESA official liaison, focused on the design of high data rate emergency networks able to cooperate with the existing infrastructure networks like TETRA. WIDENS network was composed of "terminoids" — wireless nodes with IP capabilities enhanced by SDR, where network structure was purely ad hoc. Each node utilized Multiple Input Multiple Output scheme for transmission and reception, however it still suffered from static frequency allocation. IP Firefighter project, also having its roots in MESA, focused on utilizing existing IP based wireless hardware for fire fighter brigades. It consisted of personal wireless nodes built on top of IEEE 802.11 standard. Each node transmitted information about the position of fireman together with other data to the control center. However reliability of the network was questionable since it was built on top of legacy WLAN equipment and the problem of fixed spectrum allocation was still lingering.

To alleviate the problem of spectrum shortage in contemporary ECNs, which has not been covered by any of the projects listed above, an OSA paradigm has been identified in [23] as a basis for physical and link layer design of emergency network. In the same article architecture for OSA-enabled ECN has been proposed. We shall elucidate on it briefly here.

2.1.2 Network Architecture of Future ECN

Future ECN architecture consists of *Incident Area Network* (IAN), *Jurisdiction Area Network* (JAN) and *External Area Network* (EAN) [27], see Fig. 2.1a. IAN serves as a network created for a specific incident in a small area and is temporary in nature. JAN serves as a backbone with which IAN can access general purpose networks as well as EAN. Finally EAN contains all infrastructure networks, including PSTN, Internet, etc. as well as IAN and JAN.

Usually, rescue workers are organized into groups for operational ease. Thus, equipments for communication carried by rescue personnel are also accordingly clustered into different groups. To follow this requirement we use Fig. 2.1b that gives an architecture for IANs, where devices are classified into communication node, group gateway and IAN gateway. Each group has a gateway, which is responsible for communication with other groups or IAN gateways. Devices which have more capabilities in terms of processing power, power supply, and storage capacity are selected as group gateways. IAN gateways mainly support commu-

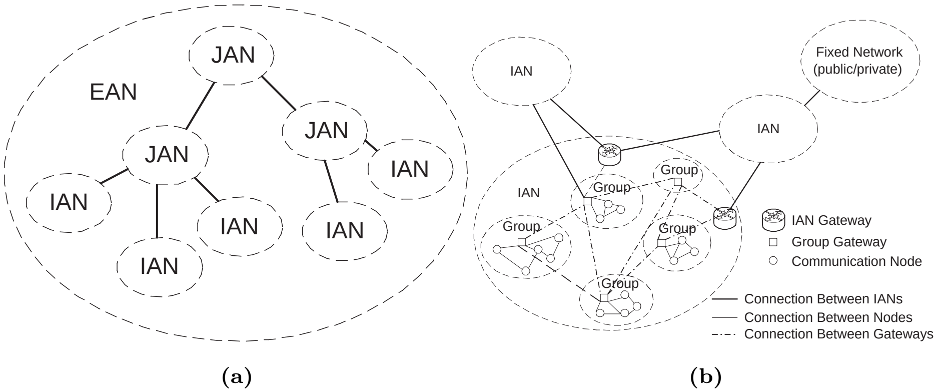

Figure 2.1: *Logical components of future ECN: (a) relations between elementary ECN components, and (b) structure of IAN.*

nication from or to IAN. They could be the same devices as group gateways, i.e., dedicated devices or control centers which have fixed connections to backbone networks.

As we have emphasized earlier ECNs need to be robust and self-managing, thus scavenging for free spectrum should be done autonomously by itself. In this context looking for new spectrum opportunity should be distributed amongst all elements of the emergency network. In the reminder of this chapter we will present a protocol that enables cooperative spectrum sensing for ECN. We note that reference to ECN is just an example. In the subsequent chapters we will generalize our discussion which is applicable to any OSA network. Before that we need to introduce theoretical foundations of the PU detection.

2.2 PU Detection Process Analysis

In this section we will recapitulate the classical theory of known signal detection in the presence of noise and fading. This will be later extended to a more general multiple node case. We will also propose novel cooperative detection techniques, utilizing measurement combining.

We can enlist two essential PU detection methods: i) feature and ii) energy based[1]. In the case of feature detection, PU detector has some pre-assigned knowledge about the detected signal, i.e., type of modulation, coding scheme, bandwidth, and power mask. During the observation process it looks for certain features in the observed signal and makes a decision about the availability of PU. This method is very effective when applied to signals transmitted with low power

[1]More detailed discussion on different approaches of PU detection can be found in [30].

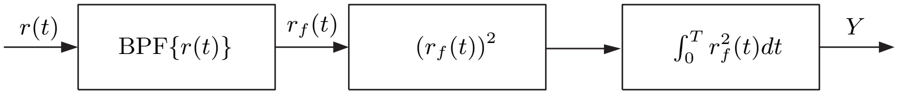

Figure 2.2: *Block diagram of the energy detector.*

and spread spectrum signals. However this detector must know what signals to look for beforehand.

In the case of the energy detection, detector collects the energy of a particular frequency channel for certain amount of time. When the collected energy exceeds the pre-assumed threshold, detector assumes PU to be present. This method is very simple to implement since it assumes no information about the detected channel (since any radio transmission needs energy to be transferred between source and destination). The drawback of the energy detection is that it cannot reliably detect the signals with low Signal to Noise Ratio (SNR).

In the ultimate scenario OSA network and future ECN in particular, cannot assume any predefined knowledge about the detected channels. Therefore energy detection, although having its limitations, has been chosen as a candidate for future analysis. We will also show how to solve the problem of energy detection in low SNR conditions.

2.2.1 Energy Detection: PU Signals in Fading Channel

In the following section we will derive the theory of unknown signal detection in the presence of noise and composite Rayleigh and Log-Norman shadow fading. As we have noted earlier we will focus only on the energy detection here.

Noise Only Case

A block diagram of the energy detector is given in Fig. 2.2. We assume detection of signals in the presence of additive white Gaussian noise (AWGN) with known parameters [31]. The received signal, which in our case represents the PU signal, $r(t)$ can be written as

$$r(t) = hs(t) + n(t), \tag{2.1}$$

where $s(t)$ is the detected signal waveform at time t, $n(t)$ is AWGN at time t and $h = 0$ under hypothesis H_0 (no PU signal present) and $h = 1$ under hypothesis H_1 (PU signal present). First, the received signal is filtered by an ideal band pass filter with impulse response $f(t)$ and bandwidth W to limit the noise power. The filtered signal $r_f(t) = f(t) * r(t)$ is squared and integrated over time s resulting in the decision statistic $Y = \int_0^T r_f^2(t)dt$, which is described by [32]

$$Y \sim \begin{cases} \chi_{2u}^2, & \text{under } H_0, \\ \chi_{2u}^2(2\gamma), & \text{under } H_1, \end{cases} \tag{2.2}$$

where χ_{2u}^2 is the chi-square distribution with $2u$ degrees of freedom, $\chi_{2u}^2(2\gamma)$ is a non-central chi-square distribution with $2u$ degrees of freedom and non-centrality parameter 2γ, $u = sW$ is the time-bandwidth product and $\gamma = \frac{E_s}{N_0}$ is the ratio of signal energy to noise spectral density. It is assumed that s and W are chosen such that u only takes integer values.

In a non-fading environment the probability of detection, p_d, and the probability of false alarm, p_f, for non-cooperative single node are given by [33; 34]

$$p_d = \Pr(Y > \theta | H_1) = Q_u(\sqrt{2\gamma}, \sqrt{\theta}), \tag{2.3}$$

$$p_f = \Pr(Y > \theta | H_0) = \frac{\Gamma(u, \theta/2)}{\Gamma(u)}, \tag{2.4}$$

where θ is the threshold of the energy detector, $\Gamma(.)$, and $\Gamma(.,.)$ are the complete and upper incomplete gamma function, respectively, and $Q_u(.,.)$ is the generalized Marcum Q-function. From (2.4) it is clear that the probability of false alarm p_f is independent of γ, since no signal is present under H_0.

When the receiver is in a fading channel, the received signal energy and SNR are location dependent. Therefore, the average probability of detection p_d is derived by averaging (2.3) over the fading statistics

$$p_d = \int_0^\infty Q_u(\sqrt{2\gamma}, \sqrt{\theta}) f_{\bar{\gamma}}(\gamma) d\gamma, \tag{2.5}$$

where $f_\gamma(\gamma)$ is the Probability Density Function (PDF) of the SNR due to fading. The probability of false alarm is the same for all locations, since it does not depend on the SNR.

Noise plus Composite Shadow and Rayleigh Fading

When a signal experiences a NLOS multipath channel, the signal amplitude follows a Rayleigh distribution, and γ is exponentially distributed as

$$f_{\bar{\gamma}}(\gamma) = \frac{1}{\bar{\gamma}} \exp\left(\frac{-\gamma}{\bar{\gamma}}\right) \tag{2.6}$$

where $\overline{\gamma}$ is the mean SNR value. A closed-form expression for p_d is obtained, by substituting $f_{\bar{\gamma}}(\gamma)$ in (2.5) resulting in

$$p_d = e^{-\frac{\theta}{2}} \left\{ \sum_{a=0}^{\lfloor u \rfloor - 2} \frac{\theta^a}{a! 2^a} + \left(\frac{1+\bar{\gamma}}{\bar{\gamma}} \right)^{\lfloor u \rfloor - 1} \left[e^{\frac{\theta \bar{\gamma}}{2+2\bar{\gamma}}} - \sum_{a=0}^{\lfloor u \rfloor - 2} \frac{(\theta \bar{\gamma})^a}{a!(2+2\bar{\gamma})^a} \right] \right\}, \tag{2.7}$$

which corrects the typographical error of [33, (16)].

However, it is likely that a channel will experience both shadowing and multipath fading. Empirical measurements show that on a log scale the attenuation due to shadowing follows a zero-mean Gaussian distribution [35], which is characterized by the standard deviation σ_{dB}, or dB-spread, which results in γ being log-normally distributed. The PDF of the composite log-normal shadowing plus Rayleigh fading channel is found by averaging the log-normal over the exponential distribution. In this case (2.6) can be written as

$$f_{\bar{\gamma}}(\gamma) = \int_0^\infty \frac{1}{x_s} e^{-\frac{\gamma}{x_s}} \frac{10}{\sigma_{dB}\sqrt{2\pi}\ln 10 x_s} e^{-\frac{(10\log 10(x_s)-\mu_{dB})^2}{2\sigma_{dB}^2}} dx_s. \qquad (2.8)$$

Here x_s is the log-normal random variable, γ in this case is the random variable after shadowing and multipath and μ_{dB} is the mean of the shadow fading. To the best of our knowledge there is no closed form expression for a log-normal plus Rayleigh distribution, and therefore the performance of local energy detection will be evaluated here using Monte Carlo method.

Detection in Composite Rayleigh Fading and Log-Normal Shadowing

The performance of the energy detector may be characterized by the complementary Receiver Operating Characteristic (ROC). The complementary ROC, which is a plot of the probability of missed detection $p_\xi = 1 - p_d$ versus the probability of false alarm p_f, is shown in Fig. 2.3a. These results indicate that the detection performance is heavily degraded by log-normal shadowing plus Rayleigh fading. For example, $p_f > 0.8$ for $p_\xi < 0.1$, which indirectly results in a low spectrum utilization. The ideal PU detector obtains low p_f (realistic value would be $p_f < 0.05$), while keeping p_d very high (again, realistic value would be $p_d > 0.95$).

One of the most promising solutions for mitigating this problem is by introduction of distributed and cooperative spectrum sensing amongst the multiple nodes in an OSA network.

2.2.2 Cooperative PU Detection based on Energy Observation

In order to improve the performance of spectrum sensing, the SUs can cooperate to detect the presence of the PU. Some initial discussion on cooperative detection in OSA setup can be found in, e.g., [36; 37].

The detection topology used for cooperative detection is a parallel network with a fusion centre as shown in Fig. 2.4a. This topology consists of $N \geq 2$ local detectors, all observing the same phenomenon. The local detectors transmit their measurement statistics to a fusion center, a dedicated node in the OSA network, which later makes a global decision on the status of PU (active or inactive). Let us briefly describe the system model used in analysis later.

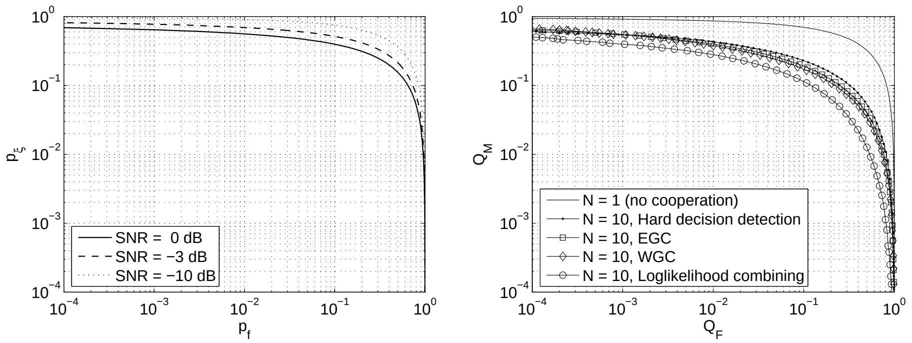

(a) **(b)**

Figure 2.3: *Complementary ROC curve: (a) under log-normal shadowing plus Rayleigh fading at different SNR values for $u = 10$ and $\sigma_{dB} = 6$ dB; and (b) for the iid composite fading channel for several cooperative techniques with $N = 10$, SNR=-8 dB and $u = 10$.*

System Model

A geographical overview of a OSA network sharing the spectrum with a PU is illustrated in Fig. 2.4b. Network, consisting of several SUs, is at a distance r from the Primary Transmitter (PT). Around the PT there is a region of decodability with a radius of r_{dec}, which we call as $\mathfrak{R}$. In the absence of interference and fading a PU receiver can only decode the signal if it is inside this region of decodability. The secondary users are clustered in a OSA network with a radius r_s. We see that all the SUs are within the region of decodability, so they can only use the spectrum when the PT does not transmit.

It is assumed that all the N SUs experience independent and identically distributed (iid) fading. The sensors are conditionally independent, which means that the SUs' measurements are independent, and for each SU the same hypothesis $\{H_0, H_1\}$ applies. We now introduce two new cooperative detection techniques: *weighted gain combining* (WGC) and *log-likelihood combining.*

Measurement Combining

In measurement combining, the fusion center weighs and combines the measurement values of the N local detectors. Based on a threshold test a global decision is generated. The test statistic Y_{WC} is the weighted sum of the N local measurements

$$Y_{WC} = \sum_{n=1}^{N} w_n Y_n, \tag{2.9}$$

where Y_n is the non-quantized output of the energy detectors and w_n is the weight for node n.

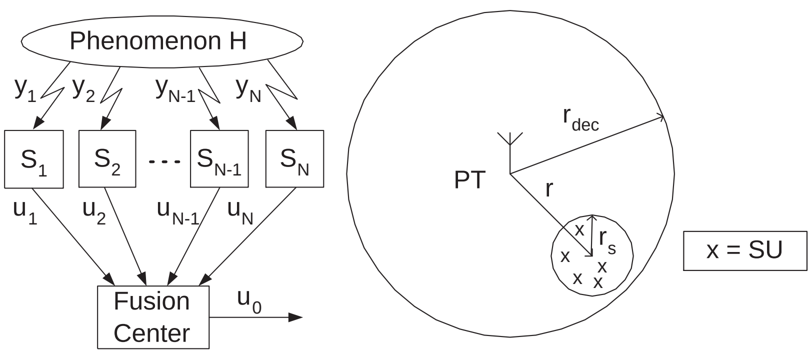

(a) (b)

Figure 2.4: *System model: (a) parallel cooperative detection topology with fusion center [38, Fig. 1], and (b) geographical overview of the OSA network in region $\mathfrak{A}$ operating on the PU network region $\mathfrak{R}$.*

Weighted Gain Combining In a channel experiencing shadowing, some nodes will have a better location dependent SNR than others. To gain from this SNR diversity, the fusion center can provide different weights to different nodes. For WGC, the proposed SNR dependent weights are given by

$$w_n = \frac{\overline{\gamma_n}}{\sum_{n=1}^{N} \overline{\gamma_n}}, \tag{2.10}$$

where the mean SNR $\overline{\gamma_n}$ measured over k_c SNR values of user n, is given by

$$\overline{\gamma_n} = \frac{1}{2k_c} \sum_{j=i-k_c}^{i} (Y_{n,j} - 2u), \tag{2.11}$$

and $Y_{n,j}$ is the non-quantized jth measurement of SU n. This results in a high weight for nodes with a high SNR and low weight for SU nodes with a low SNR. The weights are calculated by the fusion center, since it already received the SNR measurements from all the nodes. When information regarding the SNR of the nodes is not available during the start-up or after a long time without any signal, the weights are made uniform setting them to $w_n = \frac{1}{N}$. To make WGC adaptable, the fusion center only uses the last k_c measurements to compute the weights.

Equal Gain Combining A special case of measurement combining is *Equal Gain Combining* (EGC). In EGC the fusion center combines the measurements with equal weights, e.g., $w_n = 1$ for all n.

The global probability of detection Q_D and global probability of false alarm Q_F for both schemes for the AWGN channel are derived in [33]. However, for the log-normal shadow fading and log-normal plus Rayleigh fading channel, Q_D has to be derived numerically.

Log-likelihood Combining

The optimal solution to the distributed detection problem with conditionally independent sensors is obtained by applying a likelihood ratio test (LRT) at the fusion center [38]. The LRT performed at the fusion center is given by

$$\Lambda(\mathbf{Y}) = \frac{p\left(\mathbf{Y}|H_1\right)}{p\left(\mathbf{Y}|H_0\right)} \underset{H_0}{\overset{H_1}{\gtrless}} \theta. \tag{2.12}$$

Here, $\mathbf{Y} = (Y_1, Y_2, \ldots, Y_N)$ is the vector of SU energy detector outputs. To employ the LRT, it is assumed that the conditional PDFs $\Pr\left(Y|H_0\right)$ and $\Pr\left(Y|H_1\right)$ are known. In reality this is not the case because the SNR is not known *a priori*. To employ the LRT, an estimate of the SNR can be used to derive the PDFs.

We can see that the LRT of the fusion center is the same as a threshold test, and therefore we can use (2.12) to construct the test statistic Y at the fusion center. Due to the assumption of independence statistics (2.12) can be written as

$$Y_{LLC} = \prod_{n=1}^{N} \frac{p(Y_n|H_1)}{p(Y_n|H_0)} = \sum_{n=1}^{N} \log\left[\frac{p(Y_n|H_1)}{p(Y_n|H_0)}\right]. \tag{2.13}$$

In this form, the LRT can be seen as a sum of weights from the local detectors, each given by the local ratio of the likelihood of H_1 and the likelihood of H_0.

Hard Decision Combining

For comparison, we recall the classical cooperative measurement technique: *hard decision combining* [36]. Here, the local detectors have their own decision rule and make a decision based on their own measurements, which takes the value 0 or 1. Previous studies on cooperative detection for OSA with hard decision detection [39; 40] use energy detection with a fixed threshold identical for all sensors. This cooperative scheme is suboptimal [41], however, the local and global decision rules are simple and easy to implement.

The fusion center decides H_1 if any of the N local decisions decides H_1. This fusion rule is a threshold rule and is also known as OR-rule or 1-out-of-N rule [41]. In this case the global probability of detection $Q_D = 1 - \left(1 - p_d\right)^N$ and global probability of false alarm $Q_F = 1 - \left(1 - p_f\right)^N$, where p_d and p_f are given by (2.3) and (2.4), respectively.

2.2.3 Numerical Results

For most cooperative techniques, closed form solutions for Q_D and Q_F do not exist. Therefore, the performance of the techniques presented in the previous sections are determined from simulations based on the system model as given in Section 2.2.2 and using the Monte Carlo method. Except for the simulations showing the influence of the distance, the maximum distance between SUs is

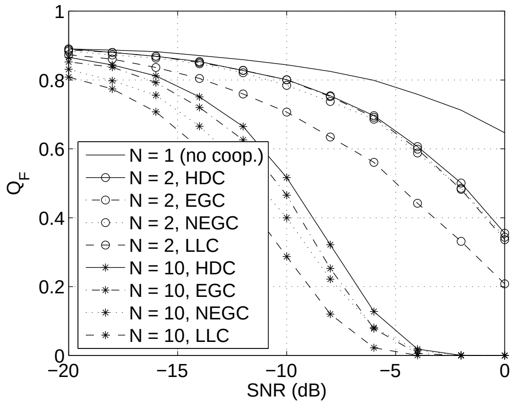

Figure 2.5: *Probability of false alarm vs SNR under iid log-normal shadowing plus Rayleigh fading for different cooperative techniques and number of sensors,* $Q_D = 0.9$.

assumed to be much smaller than the distance to the PT, i.e., $r_s \ll r$. In this case, the differences in the distance dependent path loss between the SUs are relatively small and can be neglected. Unless stated otherwise, the following system parameters are used: the measurement bandwidth of the SU is $W = 100\,\text{kHz}$, the integration time $s = 0.1\,\text{ms}$, thus $u = 10$, the number of nodes $N = 10$, and the standard deviation of the shadow fading is $\sigma_{dB} = 6\,\text{dB}$.

An overview of the performance of cooperative techniques is given in Fig. 2.3b. The average SNR of the nodes over the whole network is $\overline{\gamma} = -8\,\text{dB}$. The results indicate that there is an increase in performance for all the cooperative techniques when compared to the single node performance. For $Q_M = 1 - Q_D < 0.1$ the Q_F is reduced from 0.8 for the single node detection to 0.1 for 10-node log-likelihood detection. We also see that the more information is available for the global decision, larger is the performance improvement.

The global probability of false alarm Q_F versus SNR under iid log-normal shadowing plus Rayleigh fading for different cooperative detection techniques and different number of sensors is given in Fig. 2.5. The local and global decision thresholds are chosen such that $Q_D = 0.9$. The results show an improvement in Q_F when cooperative detection is used, and log-likelihood combining shows the best performance at all SNRs. In particular for log-likelihood combining with $N = 10$ and $\overline{\gamma} = -10\,\text{dB}$, Q_F is substantially lower compared to hard decision combining and EGC. This improvement will lead indirectly to higher spectrum efficiency.

The probability of false alarm Q_F versus the number of nodes N under iid log-normal shadowing plus Rayleigh fading is plotted in Fig. 2.6a for $Q_D = 0.9$. The results show an increase in performance with increasing number of nodes. For low SNR case the increase in performance is less compared to that of higher

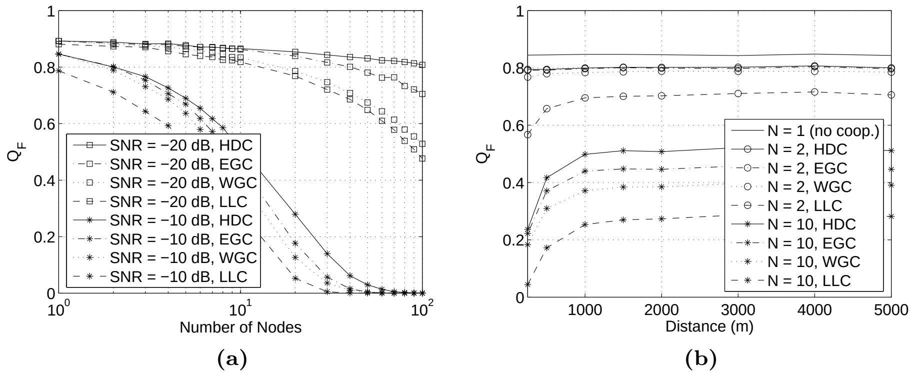

Figure 2.6: *Probability of false alarm with fixed probability of detection, $Q_D = 0.9$, for different cooperative techniques under iid log-normal shadowing plus Rayleigh fading versus: (a) the number of nodes and SNR; and (b) distance from the primary transmitter and number of sensors (for all distances the average SNR at the center of the OSA network is -10 dB).*

SNR. It can also be observed that for low SNR, log-likelihood combining and WGC perform much better than hard decision combining or EGC.

For a system where the maximum distance between SUs is bigger than the distance to the PT, the variation of the SUs' distance dependent path loss can be significant. For an OSA network with a radius of $r_s = 250\,\mathrm{m}$ at a distance $r = 1000\,\mathrm{m}$ from the PT, the difference in SNR can be approximately 9 dB when the path-loss exponent $\delta = 4$.

Fig. 2.6b shows Q_F versus distance under iid log-normal shadowing plus Rayleigh fading for different cooperative techniques and number of sensors for $Q_D = 0.9$. The average SNR at the center of the OSA network is then -10 dB. These results show a smaller Q_F at a short distance from the PT, since the SNR variation becomes larger with larger distances, which results in improved detection performance. For $r_s = 250\,\mathrm{m}$, the influence of the distance dependent path loss becomes negligible for $r > 3\,\mathrm{km}$. In general, we can consider a large distance network when $\frac{r_s}{r} < \frac{1}{12}$.

The local mean SNR $\overline{\gamma_n}$ can be estimated from the last k measurements using (2.11). The effect of the number of samples to determine $\overline{\gamma_n}$ on the complementary ROC curves for log-likelihood combining under iid log-normal shadowing plus Rayleigh fading is shown in Fig. 2.7. The mean SNR of the OSA network is -5 dB, and due to shadowing each local sensor experiences a different $\overline{\gamma_n}$. We have assumed that the log-normal shadowing does not change between the k measurements, but the Rayleigh fading is assumed independent for the k_c measurements. These results indicate that the performance of log-likelihood detection

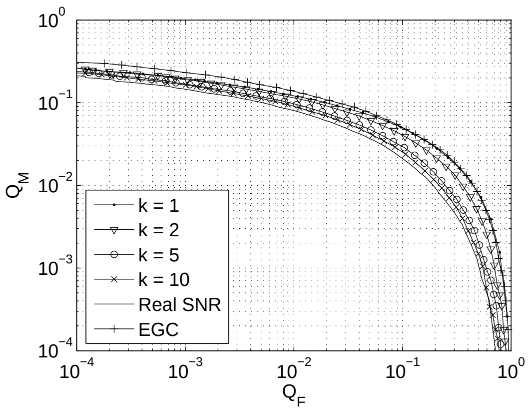

Figure 2.7: *Complementary ROC curves of log-likelihood combining under iid log-normal shadowing plus Rayleigh fading for different number of SNR estimation steps k, with $N = 10$, $u = 10$. ROC curve of EGC is plotted for comparison.*

with $k_c = 1$ is approximately the same as the performance of EGC. It also shows that the performance improves with each additional measurement. For $k \geq 10$ the performance is close to the performance of log-likelihood combining with perfectly known local mean SNR.

2.3 Protocol Aspects of PU Detection

Knowing the physical layer issues of spectrum sensing, now our task is to investigate the protocol issues of the cooperative spectrum sensing. Let us introduce the following extension to the existing system model from Section 2.2.

2.3.1 System Model

We assume that the OSA network cooperatively detects the absence of PUs in the set $\mathbb{M}$ of M radio channels, by means of energy detection. We again emphasize that we neglect other signal detection techniques, i.e., those based on the feature detection, or where interaction between OSA and the PU is allowed, i.e., by means of spectrum etiquette.

The OSA consists of a set $\mathbb{N}$ of N nodes, each having the capability of sensing PU channels. Specifically let us assume that we have a sufficient number of nodes in the OSA network, such that each channel $m \in \mathbb{M}$ is scanned by a set of g_m groups $\mathbb{G}_m = \{\mathbb{G}_{m,1}, \ldots, \mathbb{G}_{m,g_m}\}$ of nodes, where $\mathbb{G}_{m,i} \subset \mathbb{N}$, $|\mathbb{G}_{m,i}| = k_m$, and $\mathbb{G}_{m,i} \cap \mathbb{G}_{m,j} = \emptyset$. Each group $\mathbb{G}_{m,i}$ scans channel m for an observation time of s, after which a period of no scanning, t_{is}, occurs. We assume that PU do not change its state in s, i.e., PU was either absent or present during whole s. We also assume that OSA network can distinguish whether channel m was used by PU or OSA network itself, so the nodes that do not take part in the scanning can communicate on channel m during the period s. During the inter scanning time, t_{is}, nodes contact the *Detection Entity* (DE), in other words OSA nodes through a dedicated non-PU *control channel*[2], share their knowledge about the scanned frequency bands. DE can be treated as a dedicated OSA node responsible for collection and analysis of scanned data obtained by scanning nodes. Interval t_{is} is also used to exchange data on selected PU channels between OSA nodes. We denote $t_c = t_{is} + s$ as one *scanning cycle* performed by $\mathbb{G}_{m,i}$.

OSA nodes can incorporate two simple cooperative scanning schemes, that aim at observing PUs of each channel $m \in \mathbb{M}$ as long as possible, without excessive power consumption at each OSA node [42].

1. In *Scheduled* scanning, the group $\mathbb{G}_{m,i}$ starts its scanning cycle immediately after the group $\mathbb{G}_{m,i-1}$, and after scanning cycle of group $\mathbb{G}_{m,g_m}$ group $\mathbb{G}_{m,1}$ starts.

2. In *Random* scanning, each group switches between scanning cycles randomly, such that time until group $\mathbb{G}_{m,i}$ takes part in the scanning process again, and its scanning duration, are exponentially distributed with parameters $\lambda_{s,m,i}$ and $\mu_{s,m,i}$, respectively.

In both schemes assignment of particular groups and their members during each scanning cycle can be performed either by DE or by individual OSA nodes. We note that both schemes require synchronization of all scanning OSA nodes.

In our network model the mean energy value observed during s from each of k_m nodes in one scanning group is sent to the DE. DE then makes a decision about the presence of the PU, based on the set of energy values obtained from other nodes in the scanning group. It is done by comparing the sum of energy values with a given threshold, as in Section 2.2.1, and respond back to the OSA, through control channel, about availability of the PU channels. This is in contrast to the case when DE itself would make a decision based on its own measurement. For simplicity of analysis we neglect propagation delays, transmission errors and multi access issues, which are discussed more detail in [43].

Since nodes are moving, each time they have a different instantaneous SNR, denoted as γ, and for saving power, after each s, a different set of k_m nodes are chosen to scan channel m in $\mathbb{G}_{m,i}$. The OSA nodes are distributed over a region $\mathfrak{R}$, see Fig. 2.4b, such that they are placed within the operational area of each PU[3]. The PU signal detected by each OSA node is attenuated and suffers from log-normal shadow fading with a mean value of 0 dB and standard deviation σ_{dB}

[2] Discussion on different control channel designs is given in Chapter 4.

[3] We will generalize to model the case where in $\mathfrak{R}$ multiple PUs (*ergo* PTs) are available.

dB. Thus the PDF of the SNR of the detected signal from PU m is given by

$$f_m(\gamma, r_{n,m}) = \frac{10/\ln 10}{\sqrt{2\pi}\sigma_{dB}\gamma} \exp\left(-\frac{(10\log_{10}\gamma - \mu_\gamma(r_{n,m}))^2}{2\sigma_{dB}^2}\right), \tag{2.14}$$

where $\mu_\gamma(r_{n,m}) = P_{t,m} - 10\delta\log_{10}(r_{n,m}/r_{0,m})$ is the expected path loss in dB observed by node n, at a distance $r_{n,m}$ from the PU m. Here $r_{0,m}$ is the reference range in the far field of the PU antenna, where the transmitted power $P_{t,m}$ is attenuated over a distance with the path loss exponent δ.

We assume that the OSA network knows the duty cycle of the PUs in $\mathbb{M}$, such that the period of PU absence and presence on the observed channel are exponentially distributed with parameters $\lambda_{p,m}$ and $\mu_{p,m}$, respectively, see Table A.3 in Appendix app:measure and [44] for examples. This knowledge can be gained, prior to OSA network deployment, from external spectrum regulators, who measure occupancy of PU channels, or by OSA network itself estimating the channel occupancy parameters after each scanning cycle.

2.3.2 Obtaining Optimal Number of Scanning Nodes

For the sake of simplicity we assume that the scanning nodes are uniformly distributed within $\mathfrak{R}$, ranging from r_1 to r_2 from the center of $\mathfrak{R}$, thus the PDF of the distance distribution from the PU m, is $p_m(r) = \frac{1}{r_2 - r_1}$. In our model, during each scanning cycle different set of k_m nodes in scanning group $\mathbb{G}_{m,i}$ are chosen. Thus we can have a different representative SNR from each node, depending on its position. Therefore

$$\begin{aligned} \mathrm{E}[\mu_\gamma(r_{n,m})] &= P_{t,m} - 10\delta \int_{r_1}^{r_2} \frac{\log_{10}\left(\frac{r_{n,m}}{r_{0,m}}\right)}{r_2 - r_1} dr_{n,m} \\ &= P_{t,m} - 10\delta \left(\frac{\ln\left(r_2^{r_d} r_{0,m}^{-r_d} - r_d\right)}{r_d \ln(10)}\right), \end{aligned} \tag{2.15}$$

where $r_d = r_2 - r_1$. We assume that OSA network is farther away from PU such that σ_{dB} does not change appreciably, and therefore we can write (2.14) independent of position of nodes leading to $f_m(\gamma, r_{n,m})$ with $\mu_\gamma(r_{n,m})$ given by (2.15). Later we use the notation $f_m(\gamma)$ for the same.

Now to obtain the desired probability of detection of the PU on channel m by the DE, based on scanning results from k_m OSA nodes, in the presence of log-normal shadowing we first need to find $f_m(\gamma_\Sigma)$ – PDF of instantaneous SNR $\gamma_\Sigma = \sum_{i=1}^{k_m} \gamma_i$ detected by each of the k_m nodes – which the DE combines to detect the presence of PU. Since there is no closed form expression for the PDF of the sum of log-normally distributed variables, one of the methods is to approximate such PDF as another log-normal distribution and find its parameters by means of numerical integration [45]. Then probability of detection of PU at channel m is (just like in (2.5))

$$p_{d,m} = \int_0^\infty Q_{k_m u/2}(\sqrt{\gamma_\Sigma}, \sqrt{\theta_m}) f_m(\gamma_\Sigma) d\gamma_\Sigma \tag{2.16}$$

yielding the probability of detection of the PU by k_m OSA network nodes. To the best of our knowledge there is no known closed form expression for $P_{d,m}$ when the fading distribution of γ_Σ is log-normal. Thus one has to evaluate (2.16) numerically. Please note that in case of Rayleigh fading, where we have derived already a closed form expression for probability of detection in Section 2.3, probability of false alarm if k_m nodes are scanning is computed using (2.4) as

$$p_{f,m} = \frac{\Gamma(k_m u, \theta_m/2)}{\Gamma(k_m u)}. \tag{2.17}$$

Before computing an optimal number k_m, let us first derive the probability of channel m being in busy state. Solving the two state Markov chain

$$\mathbf{Q}_m = \begin{bmatrix} -\lambda_{p,m} & \lambda_{p,m} \\ \mu_{p,m} & -\mu_{p,m} \end{bmatrix}, \tag{2.18}$$

we get the steady state probability of channel m being in the busy state as $p_{b,m} = \frac{\lambda_{p,m}}{\lambda_{p,m}+\mu_{p,m}}$. Thus to find the number of scanning nodes resulting in the required Quality of Detection (QoD) defined as

$$\text{QoD} \triangleq 1 - p_{b,m}(1 - p_{d,m}) - (1 - p_{b,m})p_{f,m}, \tag{2.19}$$

we only need to solve (2.17) over k_m for $p_{f,m}$ evaluated from (2.19), possibly with the help of numerical integration.

2.3.3 Scheduling of PU Observations within OSA Network

Finally, we need to compare the observation intervals of both the scanning schemes: Scheduled and Random. To make it simple we assume that s is the total channel observation time in one scanning cycle of one scanning group. In the Scheduled scheme the normalized channel observation for one node in the set $\mathbb{G}_m$ during scanning interval of length t_c equals to

$$O_s = \frac{1 - t_{is}/t_c}{g_m}. \tag{2.20}$$

We now need to find O_r, the expected channel observation time of one node in scanning group utilizing Random scheme. With the assumption of an exponential on-off behavior of the Random scheme we can construct a sampled time continuous Markov chain that allows us to compute the steady state probabilities $\Pr[B_{\mathbb{G}_{m,i}} =$

1], i.e., group $\mathbb{G}_{m,i}$ is scanning channel m. The infinitesimal generator matrix $\mathbf{Q}_{S,g_m}$ for the Random scanning scheme of channel m with g_m sets of scanning nodes is defined in a compact form as

$$\mathbf{Q}_{S,g_m} = (\mathbf{Q}_{s,g_m} - \mathbf{\Lambda}_{s,g_m})\, t_c, \tag{2.21}$$

where

$$\mathbf{\Lambda}_{s,g_m} = diag\left(\sum_{i=1}^{2^{g_m}} Q_{s,g_m}[1,i], \ldots, \sum_{i=1}^{2^{g_m}} Q_{s,g_m}[g_m,i]\right), \tag{2.22}$$

$$\mathbf{Q}_{s,i} = \begin{bmatrix} \mathbf{Q}_{s,i-1} & \mathbf{D}_i(\lambda_{s,i}) \\ \mathbf{D}_i(\mu_{s,i}) & \mathbf{Q}_{s,i-1} \end{bmatrix}, \tag{2.23}$$

$$\mathbf{Q}_{s,1} = \begin{bmatrix} 0 & \lambda_{s,1} \\ \mu_{s,1} & 0 \end{bmatrix}, \tag{2.24}$$

and $\mathbf{D}_i(x)$ is $i \times i$ matrix with element x at the diagonal and 0 elsewhere. Solving the Markov chain $\mathbf{Q}_{S,g_m}$ will yield a steady state probability vector

$$\mathbf{B}_{\mathbb{G}_m} = \left[\frac{\lambda_{s,m,1}}{\lambda_{s,m,1} + \mu_{s,m,1}}, \frac{\lambda_{s,m,2}}{\lambda_{s,m,2} + \mu_{s,m,2}}, \ldots, \frac{\lambda_{s,m,g_m}}{\lambda_{s,m,g_m} + \mu_{s,m,g_m}}\right]. \tag{2.25}$$

Since each group is scanning independently a PU channel, we can use the inclusion-exclusion formula for evaluating probability $p_\Sigma \triangleq \Pr\left[\bigcup_{i=1}^{g_m} B_{\mathbb{G}_{m,i}} = 1\right]$ that at least one of the g_m groups of OSA nodes was observing the channel m as

$$p_\Sigma = 1 - \prod_{i=1}^{g_m} \Pr[B_{\mathbb{G}_{m,i}} = 0]. \tag{2.26}$$

Since each set $\mathbb{G}_{m,i}$ should consume the same amount of power during scanning, i.e., $\lambda_{s,m,i} = \lambda_{s,m}$, $\mu_{s,m,i} = \mu_{s,m}$ which yields $\Pr[B_{\mathbb{G}_{m,1}} = 1] = \ldots = \Pr[B_{\mathbb{G}_{m,g_m}} = 1] \triangleq \Pr[B_{\mathbb{G}_m} = 1]$ we can express (2.26) as

$$\begin{aligned} p_\Sigma &= \sum_{i=1}^{g_m} (-1)^{i-1} \binom{g_m}{i} \Pr[B_{\mathbb{G}_m} = 1]^i \\ &= 1 - \Pr[B_{\mathbb{G}_m} = 0]^{g_m}. \end{aligned} \tag{2.27}$$

Therefore solving (2.27) for $p_\Sigma = 1 - t_{is}/t_c$, such that one scanning group with Random scanning scheme would scan the channel m for the same fraction of time as that of Scheduled scheme over $O_r = \Pr[B_{\mathbb{G}_m} = 1]$, yields

$$O_r = 1 - \sqrt[g_m]{t_{is}/t_c}. \tag{2.28}$$

Finally defining function $Z(g_m) = O_r - O_s$ we can compare two proposed channel observation algorithms. We see that difference between the Random and the Scheduled schemes, expressed in terms of normalized average observation time,

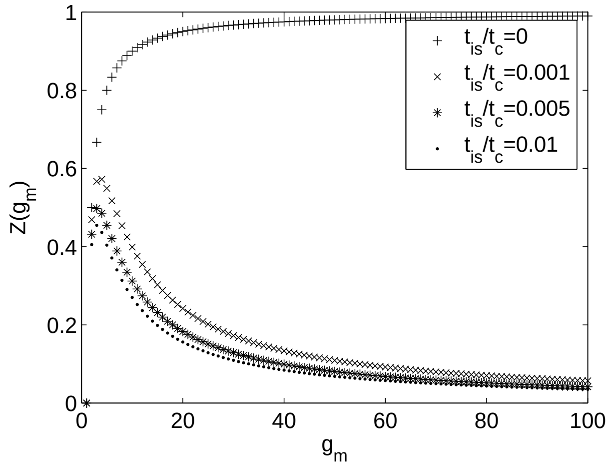

Figure 2.8: *Plot of* $Z(g_m)$ *for* $t_{is}/t_c = \{0, 0.001, 0.005, 0.01\}$.

converges to zero for large g_m, with $t_{is} > 0$. The function $Z(g_m)$ has one extreme point at

$$g_{m_{ext}} = \left\lceil \frac{\ln(t_{is}/t_c)}{\ln(t_{is}/t_c - 1) - \ln(\ln\{t_{is}/t_c\})} \right\rceil. \tag{2.29}$$

Therefore, each OSA node is observing on an average the same fraction of time given by O_s and O_r for large g_m. Moreover with larger t_{is} both algorithms converge faster. Plot of $Z(g_m)$ for different t_{is}/t_c is given in Fig. 2.8.

2.4 Protocol Design

Now, it is somehow imperative to connect the theory obtained for distributed PU detection with the architecture of ECN proposed in the beginning of this chapter. Therefore given the information above we can now design a protocol supporting the spectrum detection data exchange within OSA network.

2.4.1 Prerequisites

In our sensing architecture an ECN is divided into three tiers, see Fig. 2.1a, with the core layer of IAN, which we can treat as one cluster. Each cluster is managed and represented by a Cluster Head (CH), where in the ECN context this will be commander of IAN. Nodes from each cluster scan the spectrum at the same time and then send data to CH (which implements all the functions and tasks of a DE. As explained in Section 2.3) they execute the tasks in the slots of a frame assigned to them. All CHs will exchange spectrum measurements with other CHs,

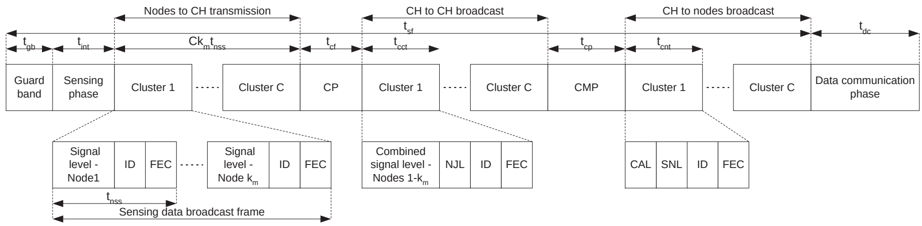

Figure 2.9: *Frame structure of the proposed spectrum data exchange protocol; CAL - Channel Availability List, CP - Contention Phase, CH - Cluster Head, CMP - Cluster Management Phase, FEC - Forward Error Correction, NLJ - Newly Joined List, SNL - Scheduled Nodes List.*

and make decisions about the presence of PU on each scanned channel. Later, each CH will respond back to its OSA nodes leading to a network-wide decision on the availability of each PU channel. Please note that we have assume that a PU does not change state during observation and an OSA network can distinguish whether channel $m \in \mathbb{M}$ was used by PU or by OSA network itself.

Each node is equipped with two separate radio front-ends: one responsible for data communication within an OSA, and the other for spectrum sensing[4], see for example [46] for a similar approach. All OSA nodes except for CH have limited energy to consume. Therefore, the protocol has to assign sensing cycles such that it will not force one subset $\mathbb{N}$ to scan excessively, thereby balancing the load. Thus in each sensing frame different subsets $\mathbb{G}_{m,i} \subset \mathbb{N}$ gather energy samples. During sensing phase nodes of OSA stay silent, so that energy detector will not misinterpret communication between OSA nodes as the PU activity. The number of sensing nodes in a group (cluster) k_m is limited by the maximal number of slots in the protocol reserved for nodes-to-CH communication. Nodes in the operational area of OSA are aggregated into L clusters, where each cluster is managed by a CH. Moreover one of the CHs will have temporal management functionality for all CHs. After scanning, each sensing node communicates to its respective CH to inform about the measured signal energy level. In the next phase all CHs exchange their measurements, thus all CHs can make the same decision about the presence of the PU based on the set of Lk_c energy values as given in Section 2.2.2[5]. Finally all CHs respond back to their nodes about the availability of the channels. We also assume that OSA is synchronized, such that not only sensing, but whole communication between CH and nodes is performed using TDMA.

Our protocol aims at network-wide knowledge of the presence of the PU on

[4]Discussion on the hardware complexity of spectrum sensing implementation will be given in Chapter 4.

[5]We note that selection of cooperative sensing technique is purely transparent to the protocol proposed here.

each of M channels, thus there is neither negotiation between CHs about which channels are free, nor forcing nodes to change their decision about spectrum occupancy, contrary to the approach proposed in, e.g., [44]. We note that communication between nodes, CH and between different CHs are performed on a dedicated control channel which is not affected by the operation of any PU[6]. The following discussion aims at spectrum sensing protocol only, i.e., protocol for robust detection of spectral opportunities. We therefore do not focus on the analysis of protocol for data communication of OSAN, for which a distinct block is reserved in the network super-frame. This will be covered in-depth in Chapter 4.

2.4.2 Structure of the Protocol

Exchange of sensing data is done in the following phases. First a guard band is allowed for clock synchronization between OSA nodes. Then the nodes selected by each CH in the previous frame senses the set of frequencies for s units of time. After the sensing period each node has a reserved slot in the frame of t_{nss} length to report to the CH about the observed energy level. Reports are sent in such a way that when a node reports to its CH all other nodes in that cluster and other clusters remain silent waiting for their turn. To guard against the errors during transmission each measured data is secured by Forward Error Correction (FEC) scheme. Total length of this part of the frame equals to $Lk_m t_{sss}$. We note that sometimes each cluster can have a smaller number of nodes than k_m. Therefore in cluster management phase (CMP) one of CHs will decide how to divide slots for all L clusters.

CH-to-CH communication phase is preceded by contention phase (CP), during which nodes moving from one cluster to another register to a new cluster, e.g., sensing domain. A node decides to join a particular cluster based on the signal strength received from each CH. In the next phase CHs send combined energy samples to other CHs. We assume that all CHs are within one hop reach of each other unlike normal OSA nodes with sensing capability, where they can only reach CH with the best signal strength. Combining energy can be done by each CH in the periods between successive transmissions of nodes from other clusters and CP, thus we do not need to reserve additional slot for processing. Result of the computation together with the Newly Joined List (NJL) of nodes is broadcasted to other CHs. This part of the frame is also protected from errors by FEC. Total size of the CH-to-CH frame is equal to t_{cct}. We note that transmission takes place in slots to minimize the probability of losing data due to collision. We note that, since each CH receives information from other CHs it can combine measurements applying the same criteria and thus results in a consistent Channel Availability List (CAL) at all the CHs. Moreover, using the NJL, each CH can update its node member list by removing all nodes that have been reported to have been joined by other CHs. In case of temporal node outage or if signals from a node

[6] As noted earlier, the implementation of different dedicated control channels will be discussed extensively in Chapter 4.

are not received by CH – as soon as the node re-appears – the node would join a new CH. In these cases, the number of sensed data would be less and it must be taken care of. However, this will not affect the PU detection explained earlier.

In the next phase, one of the CHs elected in the previous frame as OSA Manager (OMNG), decides how to divide sensing slots among all clusters. The unequal assignment of slots exists only when each cluster has $N_i < k_m$ nodes. Thus in this case OMNG assigns additional slots to cluster that has at least $2k_m - N_i$ nodes. Together with this information OMNG assigns and then transmits the IDs of all the nodes that will transmit in the next sensing frame. Each node is chosen with a probability $1/N$. Additionally, OMNG schedules who is going to be the next OMNG in OSA network. This scheduling can be performed randomly and usually will not change frequently. While all CHs receive information from OMNG they automatically resend to their nodes within the frame containing CAL and SNL. Total time of this transmission is equal to t_{cnt} and it is also secured by FEC. At the end of the sensing protocol frame, data communication on distinct channels listed by CAL is performed. The complete frame structure is depicted in Fig. 2.9.

Now, given the description of the protocol we will discuss one of the core issues related to it. That is, we need to understand how the mobility of the nodes impacts the sensing scheduling in the proposed protocol.

2.4.3 Impact of Nodes Mobility on PU Detection Quality

Since the nodes move in the OSA operational zone, a constant change in availability of nodes in the cluster may make sensing and decision process a difficult chore. Thus we focus on obtaining the level of node density in each cluster, such that the probability of scheduling a sensing task to a node which no longer exists in the cluster is minimized. We present initial performance analysis of the protocol and analyze the effect of mobility on the contention for joining a cluster when the nodes move.

We assume that nodes have to register first to a CH to take part in the sensing process. However due to the multiple access phenomenon during CP, some nodes will not be able to register successfully. The following analyses are performed under the assumption that the probability of not receiving the information from a sensor due to transmission errors is negligible. We first derive the arrival rate $\kappa(t)$ of nodes contending for the cluster during time t.

Assume uniformly distributed nodes over a circular area $\mathfrak{A} \subset \mathfrak{R}$ of radius r_s, which we consider in this chapter, see Fig. 2.4b. At time t_0 all nodes are within $\mathfrak{A}$. We assume that at the time $t = t_0 + \Delta t$, where $\Delta t > 0$ each node has travelled with speed v a distance $r_c = vt$ along a straight line in a random direction. Then the proportion of nodes that have moved outside the service area $\Omega = 1 - \frac{A}{\pi r_s^2}$, where

$$A = 2r^2 \cos^{-1}\left(\frac{r_c}{2r_s}\right) - \frac{1}{2} r_c \sqrt{4r^2 - r_c^2} \tag{2.30}$$

is the overlap area between two areas $\mathfrak{R}$ with a distance r_c between their centers. This observation is based on the fact that for a circular service area the number of nodes moved outside the area when they chose random directions is the same as when they all choose to move in the same direction. With a circular service area, in all the experiments when each node chooses a random direction to move, we may expect the same number of nodes to fall outside the service area. Therefore, there is no reason to assume that this number would be any different when this direction is the same for all nodes.

We then obtain

$$\Omega = 1 - \frac{2}{\pi}\left[\cos^{-1}\left(\frac{r_c}{2r_s}\right) - \frac{r_c}{2r_s}\sqrt{1-\left(\frac{r_c}{2r_s}\right)^2}\right]. \tag{2.31}$$

When OSA nodes are moving randomly in each cluster having the size $N_L = N/L$, arrival rate $\kappa(t)$ can be finally found using (2.31) as

$$\kappa(t) = N_L \Omega. \tag{2.32}$$

Let us now analyze the following two cases:

1. Only nodes that arrive during inter contention phase $t_{icf} = t_{dc} + t_{sf} - t_{cf}$ can contend for the channel;

2. Any arrival can contend for the channel, even those nodes that changed their position during CP, i.e., during $t_{tot} = t_{dc} + t_{sf}$.

These cases clearly depend on the relation between t_{tot} and t_{cf}. Specifically if $t_{icf} \gg t_{cf}$ then, indeed, number of new arrivals during CP can be assumed to be negligible. This also implies that, on the average, fixed number of packets will contend for the channel at the beginning of each CP. In case $t_{icf} \lessapprox t_{cf}$ arrival traffic will be the sum of fixed aggregated stream of packets from t_{icf} and arrival of new registration packets in each slot of CP.

We analyze both cases using Slotted Aloha multiaccess protocol [47]. We note that Slotted Aloha assumption implies that all registration packets containing node ID have equal size. We also assume boundless OSA network operation area $\mathfrak{R}$. Given this foundation we assume that the average number of nodes within a cluster is always the same and equal to N_L.

Case 1 ($t_{icf} \gg t_{cf}$)

Analysis of multiaccess protocols can be divided into two based on whether the receiver, i.e., CH, has the ability to capture one packet in case of a collision. Let t_{sl} be the number of available slots during CP. In the capture case the best strategy is to force all buffered registration packets during t_{icf} to immediately contend for a slot. This assumption might be unrealistic from the physical point of view however we can treat this result as an upper bound on the performance of our proposed protocol. Thus the average number of nodes that unsuccessfully contend for registration is

$$W_{1c} = \begin{cases} \kappa(t_{icf}) - t_{cf}/t_{sl}, & \kappa(t_{icf}) > t_{cf}/t_{sl}, \\ 0, & \kappa(t_{icf}) < t_{cf}/t_{sl}. \end{cases} \tag{2.33}$$

Without the CH's ability to capturing, when nodes would immediately contend for the channel, all of them will experience collision. To resolve this problem the simple strategy employed is to randomly delay each buffered packet and transmit it with a probability $p_{dl} = 1/\lceil\kappa(t_{icf})\rceil$. Whenever nodes experience collision, each colliding packet will again be transmitted with probability p_{dl} until the first success. Therefore, the probability of successful transmission when $\kappa(t_{icf})$ nodes are contending for the access is

$$p_{s,\lceil\kappa(t_{icf})\rceil} = \lceil\kappa(t_{icf})\rceil p_{dl}(1-p_{dl})^{\lceil\kappa(t_{icf})\rceil-1}. \tag{2.34}$$

The reason for fixing $p_d = 1/\kappa(t_{icf})$ follows from the fact that (2.34) approaches maximum exactly with this value of p_{dl}. Thus the expected number of unsuccessfully transmitted register packets is

$$W_{1n} = \begin{cases} p_{s,\Sigma} - t_{cf}/t_{sl}, & p_{s,\Sigma} > t_{cf}/t_{sl}, \\ 0, & p_{s,\Sigma} < t_{cf}/t_{sl}, \end{cases} \tag{2.35}$$

where $p_{s,\Sigma} = \sum_{i=1}^{\lceil\kappa(t_{icf})\rceil} p_{s,i}^{-1}$.

We note that if all contending nodes would be able to receive information whether there was a successful transmission in a slot or not, then each remaining node could increase $p_{dl} = 1/(\lceil\lambda(t_{icf}\rceil - s_p)$, where s_p is the number of successful transmissions in CP so far, that is equivalent to the number of slots in this CP.

Case 2 ($t_{icf} \lessapprox t_{cf}$)

In this case assuming that CH can capture one amongst i colliding packets, number of unsuccessful transmissions, W_{2c}, is defined exactly as in (2.33), changing all $\kappa(t_{icf})$ into $\kappa(t_{tot})$. In the non-capturing case analysis becomes much complicated due to three important phenomena. First, arriving traffic will consist of registration packets aggregated during t_{icf} and constantly arriving packets after each slot. Second, because CP length is fixed and small. Further, we cannot consider the system as in steady state during the contention. Third, the average number of requests per slot becomes smaller after each successful transmission. For these reasons we omit the analysis for this case here.

Probability of Sensing Scheduling to Non-existent Nodes

Knowing the average number of unsuccessful nodes registering with a new cluster, for a particular transmission scheme, we can compute the probability that an

OMNG will schedule a measurement request to a node which is nonexistent in a cluster. It is expressed as

$$p_{ss} = 1 - \binom{N_C - \lceil W_{\{x\}} \rceil}{k_m} \binom{N_L}{k_m}^{-1}, \tag{2.36}$$

where $W_{\{x\}} \leq N_C$ is the average unsuccessful number of nodes and $x \in \{1c, 1n, 2c\}$. Now assuming that OSAN can accept only $p_{ss} \leq p_{ss,max}$, to obtain the average node number in the cluster, N_L, which results in such performance, we only need to find N_L by solving (2.36) over $p_{ss,max}$.

Numerical Results

For a representative set of parameters $N_C = 250$, $r_s = 500$, $t_{cp} = 1\,\text{ms}$, $t_{sl} = 0.5\,\text{ms}$, $v = 0.5\,\text{m/s}$ we have compared the expected number of nodes unsuccessful in registration for various channel access strategies. Obviously we observe that $W_{1c} < W_{1n}$ for high t_{icp} (in our case $t_{icp} \approx 6\,\text{s}$). With the prolonged inter-scanning time t_{is} we observe that, in the worst case, maximal number of nodes that will not be able to register to the cluster is less than 6. This means that for the N_C considered here only 2.4% of nodes will have to wait for the next CP.

For the same values of N_C, r_s, t_{cp}, t_{sl}, and v observing p_{ss} for different k_m values for first case of multiple access without capture. Interestingly, if the k_m is greater than W_{1n}, even for a substantial number of nodes within the cluster, when t_{icf} is long, probability of scheduling to a non registered node is moderate. This implies that there is a tradeoff between k_m and time between two scanning events, e.g., for fixed k_m increasing t_{icf} reduces the QoD.

2.5 Hardware Implementation of Cooperative PU Detection

As a result of the analyses of PU detection presented in the previous sections of this chapter, a hardware platform has been developed as a proof of concept for cooperative PU detection. It was a part of AAF project. The AAF demo platform was developed at Delft University of Technology between 2007 and 2008 by graduate students and PhD researchers of the Wireless and Mobile Communications Group and Telecommunication and Remote Sensing Technology Group at the Department of Telecommunications [48].

The whole platform was constructed of two main components: a cooperative spectrum sensing platform based on USRP devices, and Orthogonal Frequency Division Multiplex (OFDM) adaptive carrier selection based on the P25M SDR [49] platform. The spectrum sensing part sends real-time signals on the activity of the PUs (in this case WLAN activity) to SDR P25M platform, which adapts its OFDM waveform based on information obtained, i.e., deactivates carriers on the channels where a PU was detected. Since the primary task of this chapter is the spectrum sensing we will not describe in detail the OFDM modulation part and

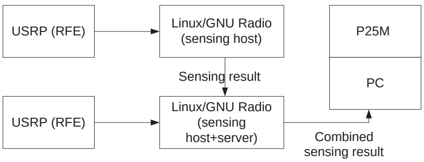

(a)

(b)

Figure 2.10: *AAF Demo platform: (a) schematic representation; and (b) photograph of the whole setup. Stationary PC contains P25M platform, while two laptops are connected to two USRP devices (black boxes in front of laptops), serving as spectrum scanners.*

we refer the reader to [50] for more information. The whole setup is schematically presented in Fig. 2.10a, while the photograph of the setup is given in Fig. 2.10b.

Specifically, the spectrum sensing part is constructed of two PCs running Ubuntu Linux with complete GNU Radio installed, connected to individual USRP with 2.4 GHz daughterboard [51]. Each laptop runs its own spectrum sensing programme written with the help of GNU Radio. Both laptops are connected via the Samba protocol to exchange sensing data, while one of the laptops serves as a sensing server and combines spectrum sensing information from both of GNU radio programs. In the setup a simple measurement combining is performed, see Section 2.2.2. The outcome of the measurement is sent again via the Samba protocol to the PC hosing the P25M SDR platform as a vector of zeros and ones, where ones symbolize carrier occupancy by PU. An example GUI of the spectrum scanner (server side) is shown in Fig. 2.11. Individual USRP devices could scan up to 3 MHz of spectrum at a time. Detection threshold θ is set manually based on experiments to maximize QoD.

Two limitations of the presented setup is the lack of RFE at the P25M, and simplified spectrum sensing measurement result. Since at the time of AAF Demo platform development we had access to USRP's 2.4 GHz daughter board only. Spectrum sensing results using USRP were not reliable enough. It was due to the fact that USRP at was simply too slow to perform accurate measurement in real-time in whole 2.4 GHz range.

We note that the development of the platform was still ongoing while this thesis was written. Therefore we were not able to include any measurement results obtained with this cooperative spectrum sensing system. However we feel that building cooperative spectrum sensing system using off-the-shelf equipment is possible.

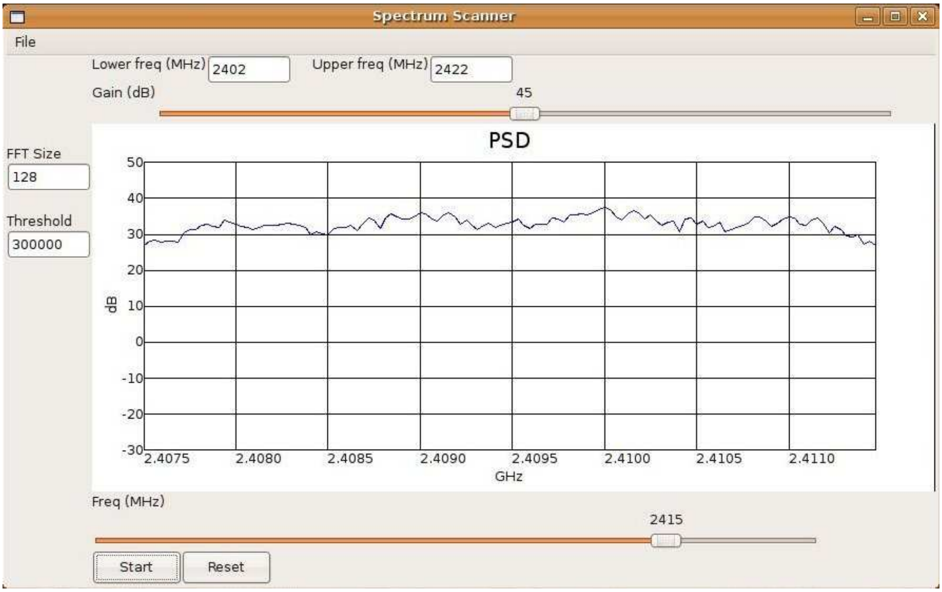

Figure 2.11: *Graphical User Interface of the spectrum scanner of the AAF platform.*

2.6 Chapter Summary and Discussion

Theoretical issues related to the PU detection were introduced in this chapter. Techniques to improve the process based on log-likelihood combining in cooperative detection were also introduced. It has been concluded that novel techniques proposed in this chapter outperform many cooperative PU detection systems. Later we have explored protocol issues of spectrum sensing, that is, how to distribute optimally the detection process among multiple nodes in OSA network. We have concluded that in Random scanning scheduling, by slightly reducing the observation time of the PU activity, an OSA network will save a lot in terms of energy consumption. Also, in this chapter a formal protocol has been proposed that facilitates the cooperative PU detection process. Finally a hardware implementation of a cooperative PU detection has been presented and discussed. Results presented in this chapter will be used in the subsequent chapters that will discuss protocol performance and design of link and transport layers.

In the next chapter we will provide general results on the OSA network performance, particularly related to blocking probability using results obtained here.

Chapter 3

General OSA Network Performance

I am a patient boy, I wait (...),
My time is like water down a drain.
Everybody's moving (...), please don't leave me to remain

Fugazi, "Waiting Room", from the album "13 Songs", Dischord Records

3.1 Introduction

We explained in the previous chapter the fundamental issues related to spectrum sensing in the OSA setup. Now, given the physical layer properties of OSA as described in Chapter 2, we need to understand what is their impact on higher layer protocols. Before we start with the work related to the link layer design which is described in Chapter 4, we need to look at OSA networks from a broader perspective. Here we would like to understand two fundamental issues: i) what level of blocking OSA network might expect, given a certain distribution of channel utilization by the PU, and ii) what channel access strategy, given certain channel utilization by PU on each channel, minimizes collision probability with the PU. These insights will be used to design a PU friendly MAC protocol. Our objective is also to design a protocol which would be easily controlled in terms of levels of interference induced to PU. The novelty of our approach is that we were able to define harmful interference aton the packet level, in contrast to the most common solution where interference is defined at the physical level. We will compare this protocol with other design approaches in Chapter 4.

Particularly, the content of this chapter is structured as follows. In Section 3.2 we analyze in detail blocking probabilities for OSA networks given different channel access schemes. A simple analytical model is presented, accompanied by detailed simulations. The guidelines and presented results are then used in Chapter 3.3 to design a simple MAC protocol with the objectives described earlier. Finally, the chapter is summarized in Section 3.4.

3.2 OSA Network Blocking Probability Analysis

In this section we will focus on a general performance issues related to the operation of OSA networks. By general performance we mean what level of blocking OSA network might experience. Here we distinguish between two types of blocking: i) *Type I blocking*, when all channels are busy, occupied either by a PU, OSA network, or both; and ii) *Type II blocking*, due to the arrival of a PU when OSA network was using the channel.

We will proceed with finding blocking probabilities for OSA networks using a simple Markov chain analysis. More detailed model will be assessed with simulations.

3.2.1 Markov Chain Analysis

Here we assume that the traffic from all the OSA nodes can be aggregated into one stream, and OSA packets are generated such that inter-arrival time and packet lengths are exponentially distributed with parameters λ_D and μ_D, respectively. OSA network accesses M PU channels, independently and randomly occupied by individual PUs (which is a normal case for most of the network analysis). For simplicity of the analysis we assume that OSA network has no queue, where arriving blocked packets could be stored. Interestingly, this assumption holds true, e.g., in IEEE 802.22 networks [52; 53], where switching to another vacant TV channel is not possible, after the operation of the incumbent was detected, where all remaining channels are already occupied by the PUs. Finally the Markov analysis of OSA networks is possible when we assume that arrival and departure process of the PU is memoryless, which is true for some of the PU channels, see Appendix A for detailed discussion.

For the case of one PU channel to which OSA network has access to, the infinitesimal generation matrix for deriving blocking probabilities is defined as

$$\mathbf{Q}_{P,m} = \mathbf{Q}_{p,m} - \mathbf{\Lambda}_{p,m}, \tag{3.1}$$

where

$$\mathbf{\Lambda}_{p,m} = diag\left(\sum_{i=1}^{4} \mathbf{Q}_{p,m}[1,i], \ldots, \sum_{i=1}^{4} \mathbf{Q}_{p,m}[4,i]\right), \tag{3.2}$$

$$\mathbf{Q}_{p,m} = \begin{bmatrix} 0 & \lambda_D & 0 & \lambda_{p,m} \\ \mu_D & 0 & \lambda_{p,m} & 0 \\ \mu_{p,m} & 0 & 0 & \mu_D \\ \mu_{p,m} & 0 & 0 & 0 \end{bmatrix}. \tag{3.3}$$

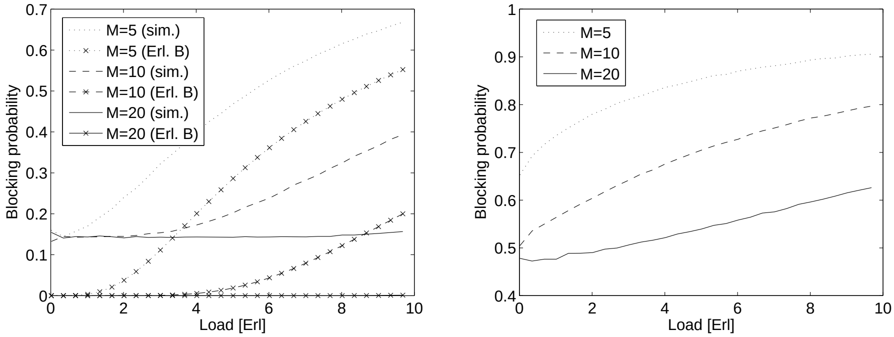

(a) *Uniform channel utilization* **(b)** *Non-uniform channel utilization*

Figure 3.1: *Simulation of blocking probability for M={5,10,20} where OSA network was using RND algorithm and: (a) each channel was utilized by PUs equally with parameters $\lambda_{p,m} = 1$ and $\mu_{p,m} = 3$; and (b) channels are utilized non-uniformly by PUs, i.e., $\forall m > 2$, $\lambda_{p,m} = \lambda_{p,m-1} - \lambda_{p,1}/2$, $\lambda_{p,1} = 20$ and $\mu_{p,m} = 3$. Plots of blocking probability with Erlang B formula for the respective number of channels are shown for comparison.*

In the above Markov chain state 1 describes *channel free*, state 2 *channel occupied by OSA network*, state 3 *channel occupied by PU* and state 4 *arrival of PU while channel was serving OSA network*. Solving this chain we get steady state probability vector $\mathbf{B}_{b,m}$. Type I blocking in this case is

$$\begin{aligned} p_{bl,1} &= 1 - \mathbf{B}_{b,m}(1) \\ &= 1 - \frac{\mu_{p,m}(\lambda_{p,m} + \mu_D)}{\lambda_{p,m}(\lambda_D + \mu_D + \lambda_{p,m} + \mu_{p,m}) + \mu_{p,m}\lambda_D + \mu_D}, \end{aligned} \tag{3.4}$$

and Type II blocking is

$$p_{bl,2} = B_{\lambda_D} \frac{\lambda_{p,m}}{\mu_D + \lambda_{p,m}}. \tag{3.5}$$

In (3.5) term $\frac{\lambda_{p,m}}{\mu_D+\lambda_{p,m}}$ represents the fraction of secondary packets that were dropped due to the interference caused by the arrival of PU on the channel m and B_{λ_D} is the fraction of OSA traffic that was admitted to the PU channel. Finally the total blocking probability is equal to $p_{bl,t} = p_{bl,1} + p_{bl,2}$.

We note that similar procedure of constructing $\mathbf{Q}_{P,m}$ for M PU channels is based on specifying all possible states of interaction between PUs and OSA network. However due to its non-symmetric nature it is hard to provide a closed form expression for blocking probability. Instead we will explore such system with simulations in Section 3.2.2.

But before we proceed with the simulations of such system we need to remark the following. In Markov chain analysis we assume that from the set of free PU

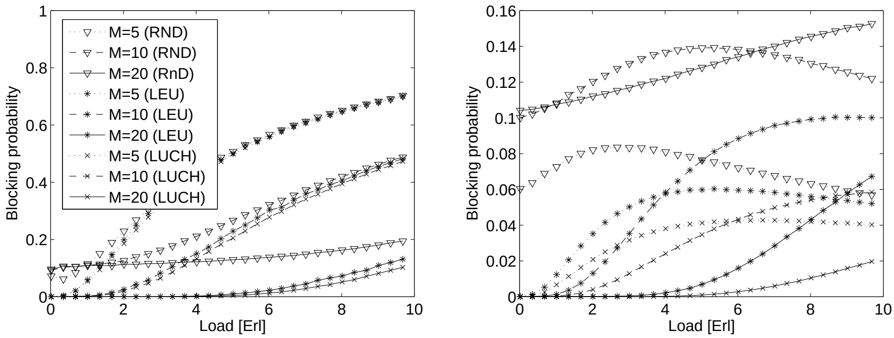

(a) **(b)**

Figure 3.2: *Simulation of (a) blocking probability and (b) type II blocking probability for* $M=\{5,10,20\}$ *for different channel access schemes. Channels are utilized non-uniformly by PUs, i.e., for* $m = 1, \ldots, M/2$, $\forall m > 2$, $\lambda_{p,m} = \lambda_{p,m-1} - \lambda_{p,1}/2$, $\lambda_{p,1} = 20$ *and* $\mu_{p,M} = 3$. *Rest of the channels are considered unoccupied by PUs.*

channels OSA network chooses a channel randomly. We call this access scheme as *Random* (RND) channel access. However we can also think of two other access schemes:

1. *Least-used* (LU), when OSA network chooses channel m with the smallest $\lambda_{p,m}$; whenever PU arrives on a chosen channel blocking occurs;

2. *Least-used with Channel Hopping* (LUCH), when OSA chooses a channel according to LU scheme. Whenever it finds out that PU has arrived, it tries to choose another channel with the smallest $\lambda_{p,m}$, and continues to transmit the rest of the data there. With no more option of channel hopping blocking occurs.

Such channel access based on the knowledge of duty cycle of PUs aims at minimizing Type II blocking. This observation is confirmed by simulations, provided in the next section.

3.2.2 Simulation Results

All simulations were performed using code written in C++, and each simulation ran for 100000 seconds. In our program all OSA network packets were offered to a pool of M PU channels, each having specified arrival and departure parameters. No radio propagation phenomena were implemented in the simulator and all simulations were done assuming perfect PU detection.

In case of M primary channels having uniform duty cycle, and OSA using RND access scheme, blocking probability is plotted in Fig. 3.1a. It is interesting to see that for this set of parameters OSA network, even for the low load, experiences significant blocking probability of ≈ 0.15. Simulation results for non-uniform traffic, also for RND scheme, are shown in Fig. 3.1b. There, not surprisingly, we observed much higher blocking probability than in Fig. 3.1a.

Results of the simulations for the probability of blocking with different access schemes are depicted in Fig. 3.2a. A simulation scenario was constructed such that it closely mimicked the operation of OSA network, i.e., PU channels with non-uniform utilization and a set of free unlicensed channels. For three different sets of channels we see that LUCH algorithm outperforms two other access schemes. What is interesting to see, however, that for the moderate number of channels the difference in blocking probability between LU and LUCH is rather small (less than 0.01). The difference between LU and LUCH is more visible in the case of $M = 20$ channels and it is due to the fact that the secondary packets have more opportunities to switch to different channels. In Fig. 3.2b plot for Type II blocking is shown. For $M = 5$ difference in Type II blocking is small for a moderate load from OSA network. But for $M = 20$ this difference is quite significant (around 0.2). However while LUCH is the most efficient compared to the other two algorithms the difference in terms of blocking probability between LU and LUCH in many scenarios is negligible. We have to emphasize that LUCH algorithm might on the other hand increase signalling traffic on the control channel since OSA network must schedule the hopping of all the packets.

Given the above results our primary objective is to plug the channel adaptability, described above, and physical layer issues discussed in Chapter 2, into more detailed MAC protocol. This will allow us to gain more insights into the operation of OSA. The discussion is given in the next section.

3.3 OSA and the Design of MAC Protocol

In the previous section we have analyzed a very general case of OSA network. However a more in depth setup is needed to account for additional overhead and protocols, such as collision resolution strategies. In this section we will design a very specific MAC protocol taking into account general OSA properties described in Section 3.2. We will start with the system model, where we anchor OSA network in a more realistic setup.

3.3.1 System Model

Let every Mobile Station (MS) belonging to the OSA network request radio resources from the BS. Every MS has no packet buffering [47], is synchronized with other MSs and the channel is slotted. The total traffic generated by the OSA network expressed in packets per slot, is Poisson distributed with parameter λ_D. All packets have equal length. Also, each node obtains immediate feedback whether transmission was successful on a dedicated broadcast channel [47; 54]. We as-

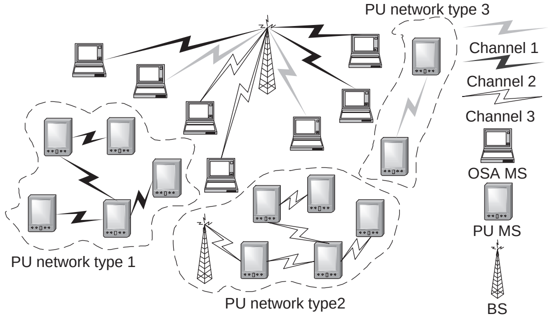

Figure 3.3: *Symbolic representation of the OSA network system model, where multiple MSs contend on multiple channels (here $M = 3$) for the access to the OSA network's BS, normally used by PUs of these bands. We note that PU networks can be ad-hoc or infrastructure based.*

sume that the broadcast channel is always available to the OSA network. The OSA network have access to a set of M channels (corresponding to, e.g., OFDM carriers), while each of the channels is also *randomly* occupied by the proprietary PU of that channel (Fig. 5.1 shows an example system model for $M = 3$). By PU, we mean an ad-hoc or infrastructure based network consisting of a number of MS, operating on channel $m \in \mathbb{M}$ licensed exclusively to PU by the radio regulator[1]. Here, we also assume that channel occupancy by the PU is described by a Poisson process with parameter $\lambda_{p,m}$, its transmission is slotted, and the OSA network is synchronized with the PU (a similar assumption was made in [55]). We approximate PU's operation as a slotted system, with Poisson arrival traffic, where the slot length is equal to the occupancy period of the PU. Finally, we assume that $\lambda_{p,m}$ is known to each of the OSA MSs.

According to the algorithm proposed in [56], each OSA user, before transmitting a request packet, chooses randomly on which OFDM carrier to transmit[2]. Whenever there is collision in a slot j, an OSA MS immediately chooses another carrier randomly, and in slot $j + 1$ tries to transmit the packet (this procedure is called *fast retrial* in [56]). If the packet is still not transmitted, after S successive trials it is backlogged for a random amount of time. The value of S is given *a priori* to the network and is specific to the network operation environment, e.g. level of frequency reuse in cellular-type OSA.

Since an OSA network has to operate under the shadow of the PU network, it should behave in such a way that it will not cause *excessive interference* to the PU on a channel m. The interference for PU will occur, in the OFDM scenario described here, when both the PU and the OSA users try to transmit simultaneously

[1]Refer to ECN architecture from Section 2.1.2.

[2]We note that the algorithm analyzed here can also be applied to classical FDMA networks. However we follow the naming from [56], thus we use the term OFDM throughout this chapter.

in a slot. A radio regulator allowing operation of an OSA network on a specific channel can restrict users to transmit such that the probability of interference I_m to the PU on channel m is

$$I_m = p_{a,m} p_m \leq \alpha_{i,m}, \tag{3.6}$$

where $p_m = 1 - \exp(-\lambda_{p,m})$ is the probability of channel occupancy by the PU on channel m, $p_{a,m}$ is the probability of gaining slot access on channel m by an OSA network user, and $\alpha_{i,m}$ is the *interference limiting factor* on a channel m.

We note that we aim at analyzing the performance of a single OSA network under these circumstances. We note however that the analysis presented here can easily be extended to a multiple OSA systems.

3.3.2 Collision Analysis

Let us assume that the total arriving traffic on channel m, $\lambda_{T,m}$, is the sum of newly generated traffic, fast retrial traffic and backlogged traffic from the OSA network. Although fast retrial traffic does not follow a Poisson distribution, we will assume it is distributed in a Poisson manner, since such an assumption is the norm in the analysis of Aloha-type protocols [47]. The total arrival rate at slot b in channel m is then [56],

$$\lambda_{T,m}[b] = \lambda_m + p_{c,m} \gamma \lambda_{T,m}[b-1], \tag{3.7}$$

where $p_{c,m}$ is the ratio of collisions to total trials of the OSA network on channel m (OSA network user collision probability), $\lambda_m = \rho_m \lambda_D$, $\rho_m > 0$ is the traffic splitting coefficient on channel m, such that $\sum_{i=1}^{M} \rho_i = 1$, and

$$\gamma = \frac{\sum_{b=0}^{S-1} p_{c,m}^b}{\sum_{b=0}^{S} p_{c,m}^b} \tag{3.8}$$

is the ratio of fast retrials to the number of collisions in the previous slot. Therefore, we can write $\lambda_{T,m}$ for the steady state in compact form as

$$\lambda_{T,m} = \frac{\lambda_m}{1 - \frac{1-p_{c,m}^S}{1-p_{c,m}^{S+1}} p_{c,m}} = \lambda_m \frac{1 - p_{c,m}^{S+1}}{1 - p_{c,m}}. \tag{3.9}$$

Because operation on each channel is independent and utilization of channels by the PU is non-uniform, the total OSA network throughput is defined, using [57, (1)] as

$$R = \sum_{i=1}^{M} \lambda_{T,i}(1 - p_{c,i}). \tag{3.10}$$

As we noted earlier, channel occupancy by each PU is different thus the coefficient ρ_m allows access to PU channels non-uniformly, in contrast to the uniform random channel selection analyzed in [56], minimizing the probability of collision with PU traffic. We observe that throughput is maximized only when (see the proof in Appendix B)

$$\rho_m = \frac{1 - p_{b,m}}{\sum_{i=1}^{M} 1 - p_{b,i}}. \tag{3.11}$$

In (3.9), total traffic is affected by the ratio of collisions to total trials. In the following paragraphs we will analyze $p_{c,m}$ depending on the procedures used to transmit packets of the OSA network during multiple transmissions in a slot, i.e., packet capture and spectrum sensing.

Collision Probability without Packet Capture

With the assumption of slotted access and synchronization between PU and SU, the OSA network will experience collisions not only due the channel occupancy by PU but also as a result of to its own traffic.

Ratio of collisions to total trials can be defined as [56]

$$p_{c,m} = 1 - \frac{\mathrm{E}[|Q|]}{\mathrm{E}[|Q|] + \mathrm{E}[|V|]} = 1 - \exp(-\lambda_{T,m} - \lambda_{p,m}), \tag{3.12}$$

where operator $\mathrm{E}[|X|]$ denotes expected number of event X, Q denotes success and V denotes collision. For the OSA network $\mathrm{E}[|Q|] = \lambda_{T,m} \exp(-\lambda_{T,m}) \exp(-\lambda_{p,m})$, i.e., one arrival from OSA user and no arrivals from the PU, while $\mathrm{E}[|Q|]+\mathrm{E}[|V|] = \lambda_{T,m}$, i.e., total expected arriving traffic by the OSA network[3].

Now solving $\lambda_{T,m}$ using (3.6) with $p_{a,m} = p'_{c,m}$ taking into account $\alpha_{i,m} \leq p_m$ we get

$$\lambda_{T,m} \leq -\log\left(\frac{\exp(\lambda_{p,m})(1 - \alpha_{i,m}) - 1}{\exp(\lambda_{p,m}) - 1}\right) = \lambda_{R,m}, \tag{3.14}$$

which defines the maximum traffic that can be offered on PU channel m for the OSA network. Whenever the offered traffic is higher, then each node can randomly discard each newly generated packet with a probability

$$p_\alpha = \lambda_{T,m}/\lambda_{R,m} - 1. \tag{3.15}$$

Such a handling of packets allows for saving its Poisson behavior [47, problem 3.11]. The value of p_α is transmitted to each MS by BS on a feedback channel, based on the knowledge of total number of OSA users and λ_D.

[3]Since the arrivals of the PU and packet generation by the OSA network are independent, the ratio of packet collisions to total trials will be equal to, according to inclusion-exclusion formula,

$$p_{c,m} = 1 - (1 - p'_{c,m})(1 - p_m) = 1 - \exp(-\lambda_{T,m} - \lambda_{p,m}), \tag{3.13}$$

where $p'_{c,m} = 1 - \exp(-\lambda_{T,m})$, and thus (3.12) is equivalent to (3.13).

Collision Probability with Packet Capture

Due to the fading phenomenon even if $n > 1$ users were transmitting in a slot, receiver is able to receive the packet when interference caused by $n-1$ transmitting nodes was smaller than the predefined threshold. Such packet capture increases the throughput possibly minimizing fast retrial and backlogged traffic.

Let us assume that signal amplitude received by BS from PU on channel m is Rayleigh distributed with average received power $P_{t,m} = \bar{P}_{t,m}/r^{\delta}$, where transmitted power $\bar{P}_{t,m}$ decays with a factor δ on distance r from OSA BS, see Fig. 2.4b and the model in Section 2.2.2. We assume that thermal noise can be neglected, i.e., "ideal" contention-limited design [54], since the dominating interference in each slot comes from transmitted packets by the OSA and PU network users. Moreover let us assume that distance r between the OSA network and PU transmitters is such that each user of the OSA network observes the same average received power $P_{t,m}$. Received amplitude of the transmitted packet by a OSA network user to the BS is also Rayleigh distributed, with the same average power for each user, equal to $P_{o,m}$. This network model is equivalent to the case when all MS of the OSA network were placed on a ring around BS of the OSA.

For an arbitrary fading scenario, ratio of collisions to total trials in presence of packet capture is defined as [54, (4)]

$$p_{c,m,\bar{x}}(\varphi) = \sum_{n=1}^{\infty} \frac{\lambda_x^n}{n!} \exp(-\lambda_x) \Pr\left[\frac{P_{tst}}{P_{n,\bar{x}}} < \varphi\right], \tag{3.16}$$

where φ is the threshold level[4] and the $P_{tst}/P_{n,\bar{x}}$ is the ratio of the power of the test packet to the interference power of n users each transmitting with an average power of $\bar{x}$, and generating Poisson traffic with the parameter λ_x. Assuming incoherent addition of n Rayleigh distributed phasors we have [54, (20)]

$$\Pr\left[\frac{P_{tst}}{P_{n,\bar{x}}} < \varphi\right] = \int_0^{\varphi} \int_0^{\infty} f_{P_{tsts}}(xz) f_{\bar{x},n}(x) x dx dz, \tag{3.17}$$

where

$$f_{\bar{x},n}(x) = \frac{1}{\bar{x}^n} \frac{x^{n-1}}{(n-1)!} \exp\left(\frac{-x}{\bar{x}}\right) \tag{3.18}$$

denotes gamma PDF with shape parameter $n-1$ and the scale parameter $\bar{x}$ of $X \triangleq P_{n,\bar{x}}$ — sum of n interferers powers (denoted also as $X \sim \mathcal{G}(n-1, \bar{x})$). While $f_{P_{tst}}(z)$ denotes PDF of $Z \triangleq P_{tst} \sim \mathcal{G}(1, P_{o,m})$ — power of test packet of the OSA network.

[4] In [58] authors have noticed that capture probability depends on the threshold level $\varphi = \varphi_n$, which is a function of the number of interfering sources, i.e., it has to be adaptive to the number of interfering sources. However, throughout this chapter we will refer to a fixed threshold φ for the sake of simplicity.

Packet Capture without Spectrum Sensing It has to be noted that even if the incoming OSA traffic has been limited artificially by p_α, still OSA network can experience collision due to the presence of PU MSs. Since the independence of the PU and the OSA network operation is assumed, we analyze only two types of packet collisions in the presence of packet capture: i) in the presence of OSA sources only, denoted as $p_{c,m,P_{o,m}}(\varphi)$, and ii) in the presence of PU network only, denoted as $p_{c,m,P_{t,m}}(\varphi)$. Using (3.17) we have

$$\begin{aligned}\Pr\left[\frac{P_{tst}}{P_{n,P_{t,m}}}<\varphi\right] &= \int_0^{\varphi}\frac{nP_{t,m}\left(\frac{nP_{t,m}+P_{o,m}}{P_{o,m}}\right)^{-n}}{xP_{t,m}+P_{o,m}}dx\\ &= 1-\left(\frac{P_{o,m}}{\varphi P_{t,m}+P_{o,m}}\right)^{n}. \end{aligned}\tag{3.19}$$

Now applying (3.19) to (3.16) to compute $p_{c,m,P_{t,m}}(\varphi)$ and to compute $p_{c,m,P_{o,m}}(\varphi)$ using (3.19) with $P_{t,m}=P_{o,m}$ in (3.16), we get, after some simplification

$$\begin{aligned}p_{c,m} &= 1-(1-p_{c,m,P_{o,m}}(\varphi))(1-p_{c,m,P_{t,m}}(\varphi))\\ &= 1-\exp\left(-\lambda_{T,m}\frac{\varphi}{\varphi+1}-\lambda_{p,m}\frac{\varphi P_{t,m}}{\varphi P_{t,m}+P_{o,m}}\right),\end{aligned}\tag{3.20}$$

which for the case of $\varphi\to\infty$ reduces to (3.13) as expected.

Packet Capture with Spectrum Sensing To preserve system from random packet discarding while $\lambda_{T,m}>\lambda_{R,m}$, the OSA network can detect when the PU was present before transmitting a packet. This allows for proper packet scheduling at each OSA node, i.e., having more control over the packets to remove from the queue to satisfy (3.6).

Specifically in every slot of length l, each node will observe the PU signal for $s<l$ time (thus reducing R in comparison to no detection case by Ms/l). After carrier observation the OSA node will decide whether the PU user was present or not. The OSA users will claim no slot whenever PU is transmitting. Here we will connect results obtained in Chapter 2, and assume that nodes perform energy detection to find the PU[5].

For generality of our analysis we assume detection of signals in the presence of AWGN with known parameters. Moreover we assume that the signal from the PU is deterministic and unknown. Let us also assume that each node is individually detecting the presence of PU. For a given decision threshold θ of channel m, the probability of false alarm when the PU is absent can be computed with the help of (2.4), replacing θ with θ_m as

$$p_{f,m}=(1-p_m)p_f. \tag{3.21}$$

[5]The offset in timing information and turnaround time [59] (time of switching from transmission to sensing) for spectrum sensing can be accommodated by guard bands, which we assume here as negligible in comparison to spectrum sensing phase and packet length.

Thus the ratio of collisions to total trials due to the presence of the PU, the OSA packets, and the 'imaginary' collision due to false alarm is given by,

$$p_{c,m} = 1 - (1 - p_{c,m,P_{o,m}}(\varphi))(1 - p_{c,m,P_{t,m}}(\varphi) - p_{f,m}). \tag{3.22}$$

Let us now focus on the analysis of the interference introduced to the PU by the OSA network. In this case probability of misdetection can be computed as,

$$p_{\xi,m} = 1 - p_m^{-1} \sum_{n=1}^{\infty} \frac{\lambda_{p,m}^n}{n!} \exp(-\lambda_{p,m}) p_{d,m,n}, \tag{3.23}$$

Where

$$p_{d,m,n} = \int_0^{\infty} Q_u(\sqrt{2\gamma}, \sqrt{\theta_m}) f_{\bar{\gamma},n}(\gamma) d\gamma, \tag{3.24}$$

can be computed similarly as 2.5, replacing $f_\gamma(x)$ with $f_{\bar{\gamma},n}(\gamma)$. Because in this case distribution of $f_{\bar{\gamma},n}(\gamma)$ has integer shape parameter we can evaluate (3.23) with the help of [33, (18)–(23)] as

$$P_{d,m,n} = \frac{1}{(n-1)!\bar{\gamma}2^{n-1}} \left(\zeta + \beta_p \sum_{i=1}^{u-1} \frac{(\theta_m/2)^i}{2i!} {}_1F_1\left(n, i+1, \frac{\bar{\gamma}\theta_m}{2\bar{\gamma}+2}\right)\right), \tag{3.25}$$

where $\beta_p = (n-1)! \exp(-\nu_m/2) \left(2\bar{\eta}/(\bar{\eta}+1)\right)^n$, and ${}_1F_1(.,.,.)$ denotes confluent hypergeometric function, and

$$\zeta = 2^{n-1}(n-1)! \frac{\bar{\gamma}^{n+1}}{\bar{\gamma}+1} \exp\left(-\frac{\theta_m}{2\bar{\gamma}+2}\right) \sum_{i=0}^{n-1} \epsilon_k \left(\frac{1}{1+\bar{\gamma}}\right)^i L_i\left(-\frac{\bar{\gamma}\theta_m}{2\bar{\gamma}+2}\right), \tag{3.26}$$

where $L_n(.)$ is a Laguerre polynomial of degree n, and $\epsilon_k = 1$ for $i < n-1$ and $\epsilon_k = 1 + 1/\bar{\gamma}$ otherwise.

With energy detection capability nodes can reduce their traffic splitting coefficients to $\rho_m = (1 - p_{\xi,m}) / \sum_{i=1}^{M} 1 - p_{\xi,i}$, which in the limiting case,

$$\rho_m = \lim_{\forall i\, p_{\xi,i} \to 0} \frac{1 - p_{\xi,m}}{\sum_{i=1}^{M} 1 - p_{\xi,i}} = \frac{1}{M}, \tag{3.27}$$

implying that in the case of perfect detection of the PU on the channels the OSA user can randomly choose a channel for transmission.

Having computed $p_{d,m}$ we can observe the gain $\Gamma_{R,m} = \lambda'_{R,m} - \lambda_{R,m}$ in introducing energy detection mechanism with $\lambda'_{R,m}$ which is the maximum allowed traffic computed using (3.14) with $p_{a,m} = p_m p_{\xi,m}$. We get

$$\Gamma_{R,m} = \begin{cases} \log\left(\frac{\exp(\lambda_{p,m})(p_{d,m}\alpha_{i,m} - p_{d,m}) + p_{d,m}}{\exp(\lambda_{p,m})(\alpha_{i,m} - p_{d,m}) + p_{d,m}}\right), & p_{d,m} \neq 0 \\ \infty, & p_{d,m} = 0 \end{cases}. \tag{3.28}$$

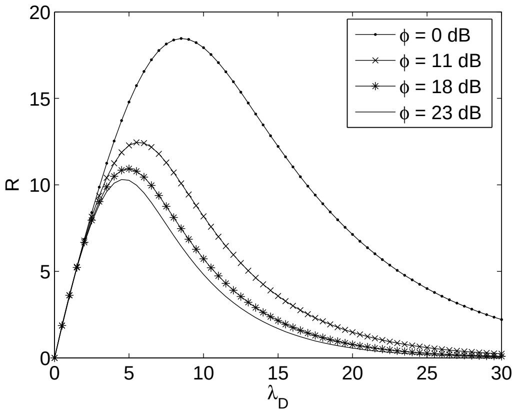

Figure 3.4: *Throughput R in the presence of the OSA network packet capture. Configuration: $P_{o,m} = 23$ dB, $P_{t,m} = 16$ dB, $M = 20$, where first 10 channels are PU free and the rest is occupied non-uniformly by PU, with the rates given by vector $\mathbf{\Lambda_m} = [2, 4, \ldots, 20]$, where $\mathbf{\Lambda_m}(i) = \lambda_{p,i}$, for the corresponding channels $m = \{11, ...20\}$.*

3.3.3 Numerical Results

We have performed a set of numerical experiments to study the performance of the proposed protocol. In Fig. 3.4 we have plotted the throughput in the case of packet capture. System configuration is mimicking the real OSA network scenario, where some channels are free of PU, while others are occupied, but each of them to a different degree. As expected, throughput is decreasing with the increase of φ.

In Fig. 3.5 we have compared throughput of the OSA network using the uniform channel selection and traffic splitting coefficients. We have varied number of PU channels to which OSA network has access to, where for each channel we have fixed $\lambda_{p,i} < \lambda_{p,i+1}$. As expected, splitting the traffic between channels depending on the arrival rate of the PU gives a substantial increase in the throughput R, especially when the number of channels are larger and if arrivals of the PU vary highly between channels.

We have also plotted throughput of the OSA network in the case of packet capture and spectrum sensing, see Fig. 3.6. We clearly observe the decrease in throughput when the time-bandwidth product u becomes small. This implies that for a fixed OFDM subcarrier bandwidth W, with the decrease of integration time we observe very high probability of false alarm, e.g., for $W = 1\,\text{kHz}$ and $s = 1\,\text{ms}$ $(u = 1)$ and $\theta_m = 5\,\text{dB}$ probability of false alarm is 0.9179.

In the next step we plotted the curves for probability of PU detection $1 - p_{\xi,m}$, as a function of the threshold, see Fig. 3.7. We observe an increase in probability of detection with the increase of offered traffic, i.e., increase of collision by PU.

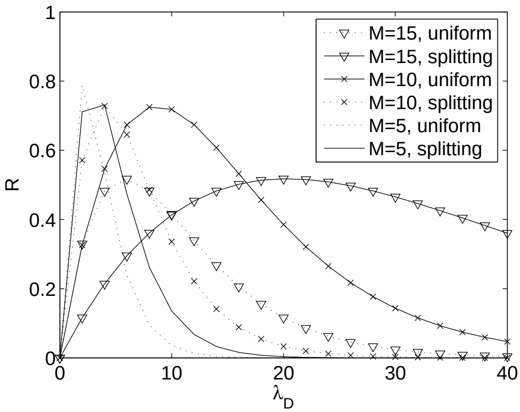

Figure 3.5: *Throughput comparison between uniform channel usage by the OSA network and using traffic splitting coefficients. Configuration: no packet capture, $M = 20$, where all PU channels are occupied according to $\mathbf{\Lambda_m} = [1, \ldots, M]$*

This leads to an interesting conclusion that higher the offered traffic by PU, higher is the probability of interference, but lower is the throughput of the OSA network on that OFDM carrier. Also interestingly, probability of detection of colliding packets transmitted according to the Poisson traffic for a given threshold and $\bar{\gamma}$ is much higher in comparison to one signal only being transmitted.

We also plotted $\Gamma_{R,m}$ in function of $\alpha_{i,m}$ for fixed value of $\lambda_{p,m}$, see Fig. 3.8. As expected $\Gamma_{R,m} \to \infty$ as $1 - p_{\xi,m} \to 0$. We also observe that for relatively high value of $\alpha_{i,m}$, even for low detection probability, the OSA network can gain from energy detection.

3.4 Chapter Summary and Discussion

We have given analytical expressions for computing blocking probability for the general OSA network model. By simulation we have proven that Least-used with Channel Hopping algorithm minimizes packet loss, in comparison with Random and Least-used algorithms.

Moreover, we have analyzed an OSA network in the presence of the PU and with fast retrial capability under the OFDM setting. OSA network nodes harness the holes in the spectrum usage under the shadow of the activity of the PUs. We analyzed mechanisms of spectrum sharing with and without packet capture capability and with spectrum sensing. We applied OFDMA-based Slotted Aloha protocol for accessing the PU channels, which is simple and easily implementable. We have given a simple way to avoid and control collisions when the traffic generated by the OSA is higher. The contributions of this chapter also include the

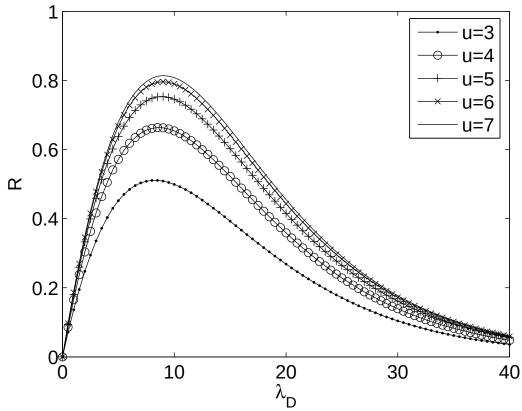

Figure 3.6: *Throughput R in the presence of the OSA network packet capture and spectrum sensing for different values of u. Configuration: $P_{t,m} = 10\,dB$, $P_{o,m} = 5\,dB$, $\varphi = 30\,dB$, $M = 10$, $\mathbf{\Lambda_m} = [0.15, 0.3, \ldots, 1.5]$ (see notation from Fig. 3.4), and threshold value $\theta_m = 5\,dB$. We assume here that $s \ll l$.*

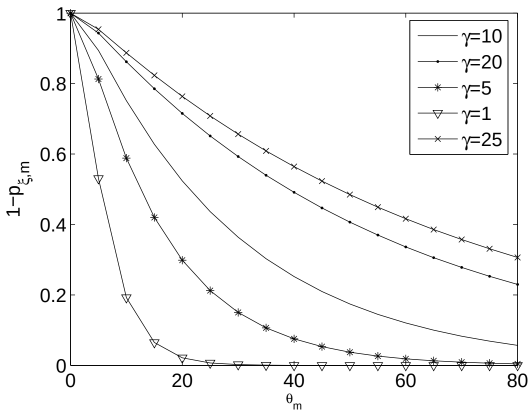

Figure 3.7: *Probability of detection for $u = 2$, $\lambda_{p,m} = 0.5$, for different values of $\bar{\gamma}$ as a function of θ_m.*

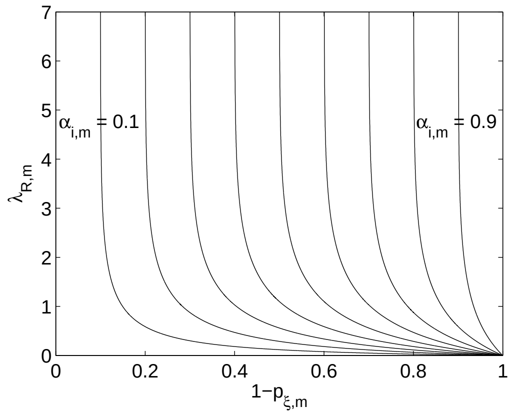

Figure 3.8: *$\Gamma_{R,m}$ as a function of $1 - p_{\xi,m}$ for $\lambda_{p,m} = 7$. Curves from left to right are plotted for $\alpha_{i,m} = \{0.1, 0.2, \ldots, 0.9\}$.*

effective use of the PU channel by using the spectrum sensing. We proved that scheduling the OSA traffic to the least used PU channel reduces the collision and increases the OSA throughput, which is in line with conclusions drawn from the first part of the chapter.

Now, given the initial results for OSA network performance, we will continue further with these analyses in the next chapter. Specifically, in this chapter we have analyzed a very special case of OSA MAC — where one dedicated CC is used, e.g., as a feedback channel for collision resolution. As we show in the next chapter this is the most widely used approach for OSA MAC implementation. However, we will show that it is not the most efficient solution.

Chapter 4

OSA MAC Protocol Performance

Die Konkurrenz
Die Konkurrenz schläft nicht

Wir Sind Helden, "Die Konkurrenz", from the album "Soundso", EMI Music 2007

4.1 Introduction

Given the theoretical foundation of the PU detection in Chapter 2, and general performance of OSA networks in Chapter 3 we can finally develop a foundation for the analysis of the MAC protocols in the OSA context. As we have explained in Section 1.3 the PU detection process is a crucial and distinctive feature of every OSA network. Its performance has certain implications on the upper layers of the protocol stack. This chapter will investigate this aspect carefully.

Our starting point for the analysis is the multichannel MAC comparison framework presented in [60] extending to OSA. A detailed physical layer model is added, with fading, PU activity, PU detection and packet capture. Using this model, we show that it is not needed to have a control channel solely dedicated to the OSA network. It is due to the fact that PU activity on such a channel does not degrade OSA throughput significantly if the OSA data packets are large enough or the number of OSA channels is small. We also show that the throughput achieved in the OSA network scales linearly with PU activity. However, depending on how efficiently the MAC design claims the free spectrum the throughput gain varies. We also show that for any OSA MAC there is an optimal point between high PU detectability and obtained throughput. When the PU detector is designed properly the SU network using any OSA MAC will not gain much from fading potentially allowing packet capture when the PU channel losses are higher. We considered multiple MAC schemes for comparisons. Finally, after the analysis and through simulation studies out of all the OSA MACs considered, the Multiple Rendezvous Control Channel MAC performs best for all the test configurations considered in this chapter.

We emphasize that none of the studies so far have focused on this issue holistically, specifically, on the question of how MAC design and PU detection quality impacts the OSA network performance. We note that the only works we found that focus on assessing the performance of spectrum sharing in general are [61; 62]. They however neglect many of the implementation details.

The content provided here has the following structure. We begin the chapter with brief prerequisites for the analysis in Section 4.2, listing a set of requirements for the operation of any MAC in OSA networks and giving a brief survey of state of the art in OSA MAC design. Then we present an analysis for the operation of all possible multichannel MAC protocols. Next analytical results for the throughput assessment of distributed OSA multichannel MAC designs, particularly from the physical layer perspective, are given in Section 4.3. Simulation results for delay, throughput and interference to the PU, are introduced in 4.4. Finally, in Section 4.5 we conclude the chapter with a brief summary of the results obtained.

4.2 A General OSA MAC Overview

We present a general overview of OSA MAC. However, before we start analyzing the issues of MAC operation we need to briefly outline what are the essential requirements for these protocols in OSA networks. This will drive our analysis and further comparisons for all the MAC protocols considered in the OSA context.

4.2.1 Requirements for Distributed OSA MAC protocol

Since OSA MACs need to work in a different context of the PHY layer, it is better to have a general view of the requirements. Here we list the essential requirements of OSA MACs. In the next section we will describe in more detail certain features of these protocols, referring to an existent OSA MAC design. These features are as follows.

1. *Efficient distribution of PU sensing data*: Information about the PU of the licensed band should be exchanged even when OSA network is saturated by its own traffic. Further, each packet about PU activity must be transported immediately to each of the OSA network nodes in the vicinity of the PU node; see Section 2.4.2 for more discussion on this aspect.

2. *Multichannel operation*: As we have outlined in Section 1.3 another inherent feature of OSA operation is the use of multiple channels for communication. Under the current radio regulation, since spectrum charts are channelized, availability of enough bandwidth of a single continuous channel cannot be guaranteed at any point of time. Intuitively, the probability that enough

bandwidth will be vacated from the PU hold increases with the increase of number of channels considered for the operation.

3. *Short channel switching time*: Time for switching from one channel to another, when PU activity is detected by OSA network node must be negligible and should effectively introduce no additional latency.

4. *Half-duplex transmission*: Each OSA node should either transmit or receive at any instant. Further it should either send or receive data or send or receive signalling. This is due to the fact that usually not every node in a network can support full duplex operation, i.e., full spectrum sensing capability. Full spectrum sensing capability means that nodes are equipped with two antennas, i.e., one each for transmission and reception of data, and for spectrum sensing and signalling.

5. *Scalability with increase in PU channels*: The gain from introducing more primary channels to OSA network should be proportional to the number of channel introduced. However in the most classical case, when one dedicated control channel has been assigned for signalling exchange it becomes saturated with the increase of signalling packets [63]. One of the ideas to mitigate this problem is to construct a dynamic common control channel which will have different bandwidth depending on the number of users in all bands of OSA network at any instant. One of the candidates for such a channel is UWB. However it has to be noted that throughput of UWB decreases profoundly with distance. This would simply mean that maximal distance between neighbouring nodes of CRN will be limited to UWB transmission distance. Such limitation is caused by low power levels in which UWB nodes are allowed to transmit.

4.2.2 OSA MAC Classification

Given the requirements we now give an extensive overview of the available OSA MAC protocols, identifying all important features that are distinct to the OSA operation and need to be modelled such as, multichannel OSA design and PU detection.

In Table 4.1 we have listed different OSA MAC designs found in the literature[1]. The features of the identified MAC protocols, that are important in the context of OSA, are described in detail in the following sections. More discussions on the identified features can also be found in [64; 65].

[1] We are aware of the existence of MAC for IEEE 802.22 WRAN [83] and proprietary OSA MACs found in the OSA devices of Shared Spectrum Company, Philips and Microsoft, but since their specifications are not public they are not mentioned here.

Table 4.1: *OSA MACs versus their Features, See Also [64, Tab. 1],[65, Tab. 2]*

Protocol	Bootstrapping	Type	Scanning	RFEs
DOSS [66]	Yes	DCC	Yes	3
Su *et. al.* [67]	No	DCC	Yes	2
Motamedi *et. al.* [68]	No	DCC	Yes	2
SCA-MAC [69]	No	DCC	Yes	2
Nan *et. al.* [70]	No	DCC	Yes	2
C-MAC [71]	Yes	DCC	Yes	1
AS-MAC [59]	Yes	DCC	Yes	1
ESCAPE [72]	No	DCC	Yes	1
MMAC-CR [73]	No	DCC	Yes	1
DC MAC [74]	No	DCC	Yes	1
HC-MAC [75]	No	DCC	Yes	1
Choi *et. al.* [76]	No	DCC	No	2
Shu *et. al.* [77]	No	DCC	No	2
BB-OSA [78]	No	DCC	No	1
OS-MAC [79]	No	DCC	No	1
OSA-MAC [80]	No	DCC	No	1
HD-MAC [81]	Yes	SPCC	Yes	1
SRAC [82]	No	SPCC	No	1

Centralized versus Distributed Architecture

OSA network architectures can be classified into centralized and distributed. In the centralized architecture, one dedicated network entity is responsible for the management of medium access and functionalities related to channel management. Examples of these architectures for OSA are Common Spectrum Coordination Channel [84], Spectrum Information Channel [85] and DIMSUMNet [86]. For the distributed case, each node of the network decides on the channel access locally. The focus of this chapter is to analyze distributed OSA MACs only[2].

Bootstrapping and Channel Selection

Bootstrapping is the process during which an SU node decides which of the PU channels are suited for opportunistic use. In one scenario, external entities provide information on opportunistically enabled channels. Then, SU consults those entities when it wants to join a network. Other scenarios assume that each node

[2]We note that all centralized protocols that we are aware of organize spectrum access for OSA networks, and [84–86] in particular, use dedicated control channel to coordinate networks. One of the distributed multichannel OSA MAC classes that we analyse here is also based on dedicated control channel principle. Therefore, dedicated channel for control in OSA MAC context can also be treated as a benchmark for assessing effectiveness of centralized spectrum coordination protocols.

finds those channels locally, which can involve a significant amount of spectrum scanning. After finding the channels, each node distributes its set of channels to other users in the network, e.g., via a proprietary protocol. Interestingly, only a handful of proposed OSA MACs consider bootstrapping, e.g., C-MAC [71], AS-MAC [59], DOSS [66] (only for a Control Channel), and HD-MAC [81]. Bootstrapping, which is sometimes also referred to as channel selection [87], is mostly explored in a single channel context. In a multichannel domain, MAC designers usually assume that each OSA node has a pre-programmed list of PU channels for use. We will also assume in our analysis and simulations that the list of channels is known to SUs.

Control Channel Design

After the bootstrapping procedure, the SU network has decided on a set of possible channels. Now, for each data packet transmission the SU transmitter and receiver have to coordinate which channel and time slot they will use for the transmission. This coordination is typically implemented using a *(Common) Control Channel* (CC). From the reliability viewpoint, this CC is a very crucial element of the MAC design, since no SU data communication is possible when it is obstructed.

Using the approach defined in [60, Section II] for the general multichannel MACs, we can identify four classes of CC implementation. For the list of references for each MAC class in the non-OSA case we refer to the original paper [60].

1. *Dedicated (Common) Control Channel* (DCC): Here one channel is dedicated solely to the transport of control messages. All nodes should overhear the control message exchange and data exchanges. As a result, one Radio Front-End (RFE) needs to be dedicated to the exchange of control messages. When only one RFE is used, transmission of control and data packets is time multiplexed, but then the operation of the protocol becomes more complex. The drawback of the DCC approach in the context of OSA is that when a PU is active on the control channel, all SU communication must wait until the dedicated channel becomes free again. If PU activity is organized in long bursts, this can result in long delays. As a result, existing OSA MAC protocols often assume that the CC is always free from PU. Interestingly, the majority of the proposed designs so far are DCC, see Table 4.1.

2. *Hopping Control Channel* (HCC): Here all idle nodes hop across all the channels following a similar pattern. When both the sender and the receiver successfully exchange control messages on the current channel, they stop hopping and start transmitting data. After that, they come back to the original hopping pattern, re-joining the rest of the network. HCC has the advantage that it uses all channels for data transmission and control messaging, whereas in DCC, the CC can be used to transfer only control packets. Also, HCC does not require a single dedicated channel to be free from PU activity always. This MAC class has not been proposed yet in

the OSA context in the literature. We note that in HCC only one control message can be exchanged during one hopping sequence.

3. *Split Phase Control Channel* (SPCC): Here OSA transmission time is divided into alternating control and data phases. During the control phase, all nodes switch their RFEs to the dedicated CC and decide on the channels to use for data transfers in the upcoming phase. Each node stays on the negotiated channel during data transmission phase. The advantage is that the CC can be used during the data phase. Compared to DCC, no extra RFE for the control channel is needed. On the other hand, SPCC requires stronger synchronization to identify the control and the data phases. Only two out of all MAC protocols listed in Table 4.1 belong to the SPCC class.

4. *Multiple Rendezvous Control Channel* (MRCC): Here multiple nodes can exchange control information at the same time using all available channels. Each node knows the hopping pattern of its one hop neighbours. Such hopping pattern is based on the seed of a pseudo-random generator. Once the seed of the receiver is known, the sender can follow the intended receiver on its hopping sequence. MRCC randomly spreads both control and data exchanges across all channels. As a result, MRCC is the most robust adjusting to the unpredictable PU activities. We will illustrate this quantitatively later in this chapter. However MRCC also requires a more stringent synchronization between the hopping users since, they have to keep track of hopping times of one-hop neighbours. In contrast to HCC, it allows to exchange more than one message during the control sequence. Interestingly, none of the MAC designs in OSA context proposed so far belongs to the MRCC class of multichannel MAC protocols. A detailed discussion on the operation of a MRCC MAC proposal for a non-OSA environment can be found in [88].

We can further divide the multichannel MACs into two major groups: with *Dedicated CC*, i.e., DCC and SPCC, and with *Hopping*, i.e., HCC and MRCC. The multichannel MAC analysis framework of [60] will serve us to compare these MAC designs in the context of OSA in Section 4.3 and Section 4.4. Graphical representation of each multichannel OSA MAC class is given in Fig. 4.1.

PU Detection

We can thus classify OSA MAC protocols into a) scanning and b) non-scanning OSAs. From Table 4.1 we can conclude that the majority of the protocols considered here assume to have the scanning under their control. Unfortunately, scanning increases the overhead since nodes cannot transmit when they are scanning. The overhead can be minimized by increasing the hardware complexity, i.e., by introducing a dedicated RFE for scanning only (see Table 4.1 for the list of OSA MAC and their number of RFEs). More importantly, since it is often

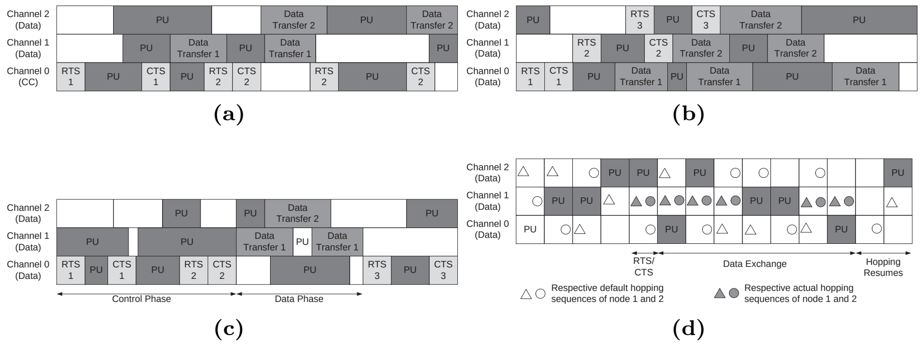

Figure 4.1: *Illustration of the operation of different multichannel MAC types with PU activity on each channel: (a) Dedicated Control Channel, (b) Hopping Control Channel, (c) Split-Phase Control Channel, (d) Multiple Rendezvous Control Channel. Please compare [60, Fig. 1] for the description of the non-OSA multichannel MACs.*

difficult to distinguish SU and PU signals, the whole SU network has to be quiet during sensing which requires *Quiet Period Management* [71]. Scanning or hence quieting the network can be done periodically or before each transmission attempt. The time interval between two consecutive sensing attempts varies, and is often a function of the policy. The more tolerant the PU is to the interference the less often the sensing can be done. Noise, fading, multi-path shadowing and low PU signal levels make the reliable detection process difficult [30]. Suboptimal detectors not only affect the PU QoS levels, but the SU QoS as well. In Section 4.3.2 we will give a detailed model of the PU detector, which will later be used in the global system model for the MAC comparison.

Number of RFEs

Different multichannel MAC designs operate using different number of RFEs. For DCC, this number varies between 1 (one RFE is time shared for control and data exchange) and 3 (one RFE for control data exchange, and two simplex RFEs for data transfer). All SPCC MACs that are proposed use only one RFE, see Table 4.1. We expect that HCC and MRCC will use only one RFE as well.

The number of RFEs has a significant impact on the hardware cost and the power consumption. The energy consumption of a radio depends to a large extent on the amount of time the RFE can be switched off to the sleeping mode. Since none of the classes of MACs considered here have been optimized for sleeping, we can assume that they will never be able to be turned off. As a result, the number of RFEs is roughly proportional to the total power consumption. In the rest of the chapter, we will hence not study the power cost in more detail, and assume that the number of RFEs is 2 for DCC and 1 for the other protocols.

4.3 Analysis

In this section we propose a model to analyze OSA MAC performance from the throughput perspective. First, we give a global overview of the system model. Later we discuss the detailed physical layer model. Finally, we embed them into the multichannel MAC model proposed in [60]. We note that our model possesses the same limitations as that of [60]. Specifically, due to significant involvement of the delay analysis the model is limited to throughput assessment only. Moreover, the work here is limited to a single collision domain and effects such as hidden/exposed terminals are not modelled. However, features that are not captured by this analytical model, e.g., delay and level of interference to the PU, will be studied through simulation in Section 4.4.

4.3.1 Modeling Assumptions

Channel Organization

We evaluate the performance of a OSA network consisting of N nodes operating on a pool of M channels, where each channel can potentially be used by a PU independently with probability p_{bm}. Each channel has a fixed throughput of C Mb/s. SUs can utilize the channels when they are temporarily not in use by the PU, but only when this causes no excessive interference to the PU of any channel $m \in M$.

Time Granularity

The system is analyzed using discrete time slots. As a result, all transmissions within the SU network are slotted and the boundaries between consecutive slots are uniquely identified. Further, for the sake of analyses, slots of the secondary network are assumed to be synchronized with the PU network slots. This means that any PU or SU packet starts at a slot boundary. A slot is long enough to contain one RTS/CTS exchange of the SU network. In Fig. 4.1 a more detailed picture is given since SU transmissions are not synchronized with the PU slot and a PU packet can start in between the RTS and CTS exchange.

Channel Access

Every node has an infinite stream of data to transmit. Distributed access[3] is modelled by generating each channel access with a probability p. Such channel access results in a connection arrangement (RTS/CTS exchange) on the control channel. A successful arrangement is always made when only one user requests a

[3] We note, just as in [60] effects related to PU activity and multiple channel management are much more profound for the operation of any Multichannel OSA MAC than collision resolution strategies. Therefore, the collision resolution procedure, i.e., RTS/CTS exchange, assumed in the model is simplified.

new connection in the network in a given slot and the slot was free from the PU activity. In addition, in case of collisions with the PU or another SU, SU nodes are potentially able to capture the transmitted packet under the condition that the total SINR is larger than a certain threshold φ.

Data Model

After obtaining the channel SU nodes can transmit only one packet (amount of data), which is fragmented into multiple slots with an acknowledgement per fragment. When the transmission has finished, nodes need to perform a new arrangement for the next transmission attempt. For the sake of simplicity of analysis, we assume the packet lengths of secondary network are geometrically distributed with parameter q, i.e. each SU data packet has a mean length of q^{-1} time slots.

PU Detection

To avoid excessive interference with the PU, every slot of length l starts with a scanning period s. At the beginning of the scanning period s, all SU nodes stop their transmission and at the end of that period, each secondary node locally decides if the channel is free from PU activity or not. Every decision is prone to errors. When a SU node does not detect a PU, with probability $1-p_d$, a collision between PU and SU occurs. A capture model determines if the collision results in a lost packet for the SU. A lost fragment has to be retransmitted in the next available slot. Alternatively, an idle slot may be considered busy with false alarm probability p_f. In such a case, the SU postpones its transmission and tries to send the remainder of the packet in the next available slot. In both the cases, when this happens during the data transmission phase, no new arrangement is needed. As a result, the presence of PU only extends the data phase. The probabilities p_f and p_d are functions of s, channel bandwidth W and detection threshold θ. We also assume that all OSA nodes observe the same channel conditions, i.e., the same instantaneous signal level from PU in each slot.

Physical Layer

Signals received by each of the SU nodes are affected by Rayleigh fading and thermal noise. We assume that the channel state is constant for the whole slot length. For the analysis we assume that each SU experiences the same instantaneous PU fading, described by a Rayleigh fading process. SU transmissions are all affected by independent identically distributed Rayleigh fading as well.

4.3.2 Physical Layer Model

We now explain the physical layer model, consisting of a PU detection, packet capture and slot availability in more detail.

PU Detection Errors

Every node of the OSA network at the beginning of every slot will sense to detect the presence of PU on a given channel. We assume energy detection in the presence AWGN and Rayleigh fading, which was extensively described in Chapter 2. For simplicity of analysis we assume single node, non-cooperative PU measurement, which results in p_f and p_d given by (2.4) and (2.7), respectively. Cooperative spectrum sensing will only change the p_f and p_d.

Packet Capture

Fading causes additional packet loss for the OSA. We neglect it since these losses are not specific to the analysis of multichannel MAC design in the context of OSA. However, fading can lead to a throughput increase for the OSA network in the following scenario. Even if the OSA node has mistakenly detected the channel as free from PU activity, if the received PU signal has been in deep fade, the OSA node might be able to successfully transmit its packet (this effect has been observed first in [89]) due to packet capture. Therefore we have introduced the packet capture model to account for this phenomenon in our analysis.

We assume that n colliding OSA packets with average received power P_o (including PU interference of average received power P_t) are added coherently at the OSA node[4]. Also, we omit the impact of noise in the capture, since interference from competing packets will be the dominant factor in the capture process [54, (20.b)]. Having listed all the assumptions, we can now compute the capture probability for the OSA network, as given in the following proposition.

Proposition 1. *Given the coherent addition of signals, with capture threshold φ, $n \in [0, N-1]$ interferers, PU interference power P_t, and SU packet power P_o, the capture probability is*

$$S_{x,n}(\varphi) = 1 - \frac{P_x(n)\varphi}{P_o + P_x(n)\varphi}, \tag{4.1}$$

where

$$P_x(n) = \begin{cases} P_t + nP_o, & x = 1 \text{ (PU+SU interference)}, \\ nP_o, & x = 2 \text{ (SU interference)}. \end{cases} \tag{4.2}$$

Proof. See derivation of (3.17). □

[4]Coherent addition requires phase knowledge of the signals, which might be difficult for the OSA case. However, from the analytical perspective the non-coherent generalization requires the PDF of the sum of unequally distributed exponential variables, i.e., n variables with average parameter P_o and one variable with average parameter P_t, which has no compact form. Further, the resulting PDF needs to be convoluted with the fading distribution of the test packet and integrated, which introduces another challenge.

Slot Availability

Having the analytical formulas for PU detection errors and packet capture, we can compute the probability that a given slot available for SU communication, incorporating all the effects.

Proposition 2. *The possible slot availability for the SU node, given n other SU nodes transmitting, is*

$$\psi(n) = (1 - p_{bm})(1 - p_f)S_{2,n}(\varphi) + p_{bm}(1 - p_d)S_{1,n}(\varphi). \tag{4.3}$$

Proof. A slot can be available to the SU in two distinct cases. First, when there is no PU on the channel and second, when there is one. In both cases, interference effects might reduce the probability that the slot will not be available, but only when the detector properly decides on the channel state. Combining these effects altogether we obtain (4.3). □

4.3.3 Markov Analysis

In Section 4.3.1 we listed system assumptions that allow us to model the multichannel OSA MAC performance as a Markov model where the state space gives the number of channels in use for data communication. More specifically, assumption 2 and 4 define the time granularity of a discrete-time Markov model and assumption 3 and 4 relate to the transition probabilities, i.e., when a successful arrangement results in a new data transmission or when an ongoing data transmission is finished. On top of that, assumptions 1 and 5 allow us to embed the impact of PU activity on the MAC performance. In this section, we will describe the Markov model and show how to embed the physical model derived earlier into it. For the analysis we will focus on one representative OSA MAC from the two OSA MAC groups defined in Section 4.2.2, i.e., DCC for CC OSA MACs, and HCC for Hopping OSA MACs.

State Space and Steady State Channel Occupancy

In the discrete Markov chain model, state $X_t = k$ represents the $2k$ devices (k pairs) involved in the transmission at time t. The state space is then

$$\mathcal{S} = \left\{0, 1, \ldots, \min\left(\left\lfloor \frac{N}{2} \right\rfloor, M\right)\right\}. \tag{4.4}$$

Following this definition of the state space, we can define the steady state vector of the Markov chain $\mathbf{\Pi} = \left\{\pi_0, \pi_1, \ldots, \pi_{\min\left(\left\lfloor \frac{N}{2} \right\rfloor, M\right)}\right\}$. From this, the average utilization per channel, considered as the proportion of time when the channel is occupied by SU, is

$$\tau = \psi(0)\frac{\sum_{i\in\mathcal{S}} i\pi_i}{M}, \tag{4.5}$$

where $\psi(0)$ denotes the slot availability, when a single SU is accessing the channel for data communication. We note that SU collisions only happen during the control message exchange. Also, we note that the computed utilization for the non-OSA multichannel case represented by [60, (4)] has to be decreased by the slot availability, since we assume that when the channel becomes busy during the data phase, the SU just waits until the channel becomes available again on that channel. Hence, although in the steady state computation the SU is residing on a channel m, it is not effectively using it. Without that adjustment the Markov model would consider the PU occupancy as an increase in channel utilization by SU network. Using (4.5) we can finally compute the throughput, by which we mean a total throughput of the OSA network as a whole, i.e., the average throughput of one secondary network consisting of multiple SUs, as

$$R = M_C C \tau \frac{l}{s+l}, \tag{4.6}$$

and

$$M_C = \begin{cases} M-1, & \text{for DCC,} \\ M, & \text{otherwise.} \end{cases} \tag{4.7}$$

The separate definition of the throughput for DCC comes from the fact that for this MAC class one channel is dedicated only to RTS/CTS (control) exchange. Next, in comparison to [60, (9)] the throughput formula has to be reduced by a scanning factor $\frac{l}{s+l}$, given that only a part of the whole slot is used for effective data communication.

Transition Probabilities

To compute the steady state vector, we need to define the transition probabilities, i.e., the probabilities to start a new data transmission after a successful connection arrangement, or to finish the one when the data packet was sent.

Let $S_j^{(k)}$ denote the probability of j new arrangements given k pairs are communicating, and $T_j^{(k)}$ denote the termination probability of j connections, given k pairs are communicating. Then the entries of transition probability matrix $\mathbf{P}$ are

$$p_{kz} = \begin{cases} 0, & \text{if } z > k+1, \\ T_k^{(0)} S_k^{(1)}, & \text{if } z = k+1, \\ T_k^{(k-z)} S_k^{(0)} + T_k^{(k-z+1)} S_k^{(1)}, & \text{if } 0 < z \leq k \text{and } k+z \neq 2\max\{\mathcal{S}\}, \\ T_k^{(k-z)} S_k^{(0)} + T_k^{(k-z+1)} S_k^{(1)} & \\ +T_k^{(k-z)} S_k^{(1)}, & \text{if } k = z = \max\{\mathcal{S}\}, \\ T_k^{(k)} S_k^{(0)}, & \text{if } z = 0, \end{cases} \tag{4.8}$$

We emphasize, that (4.8) corrects the error in transition probabilities of [60, (6)]. There, transmission probability for condition $k = z = \max\{\mathcal{S}\}$ was not considered, that means the data transfer is not possible even after a successful connection arrangement because all channels are busy. This happens with probability $T_k^{(0)}S_k^{(1)}$. When this case is not considered correctly, the resulting matrix $\mathbf{P}$ in [60] is not stochastic, i.e., each row does not sum to 1, which is a necessary condition for finite state Markov chains. We will elaborate on this issue more in Section 4.3.4.

Because of the possible PU operation on each of the M channels, fading effects, and PU detection errors the definitions of $S_j^{(k)}$ and $T_j^{(k)}$ given in [60] need to be changed. The respective definitions follow as below.

Termination Probability $T_k^{(j)}$

The probability $T_k^{(j)}$ that j connections finish the transfer in a given slot is

$$T_k^{(j)} = \binom{k}{j}\{q\psi(0)\}^j\{1-q\psi(0)\}^{k-j}, \tag{4.9}$$

which means that nodes involved in transmission can terminate successfully only when the slot was available for the SUs. We note that we neglect the details of the retransmission policy, which could indeed be included in the termination expression. Our expression is for the simple case where we have an ACK per fragment (one slot) and that we just retransmit the fragment in the next available slot if necessary.

Arrangement Probability $S_k^{(j)}$

Different OSA MAC classes have different mechanisms to arrange a new connection, which is translated into different probabilities in the Markov model to start a transmission. Here we will derive these important probabilities, for each multichannel MAC class individually.

For DCC and HCC the arrangement probability $S_k^{(j)}$ is

$$S_k^{(j)} = \begin{cases} S_{A,x}, & \text{if } j = 1, \\ 1 - S_{A,x}, & \text{if } j = 0, \\ 0, & \text{otherwise}, \end{cases} \tag{4.10}$$

where $S_{A,x}$ is defined below, separately for DCC ($x = 1$) and HCC ($x = 2$).

DCC In case of DCC MAC the average probability of successfully receiving the packet in the presence of interferers is [90]

$$S_{A,x=1} = \sum_{i=1}^{N-2k} \binom{N-2k}{i} p^i (1-p)^{N-2k-i}\psi(i-1). \tag{4.11}$$

Since the successful transmission might happen for only one user, given i users are competing for the channel at the same slot, and summing over all possible amount of interferers i we obtain the expected probability of successful arrangement. The number of interferers is bounded by $N-2k$, since $2k$ users are involved in data transmission and will not compete for the new arrangement.

Equation (4.11) does not prohibit however to have more than one sender-receiver SU pair to access data channel, i.e., more than one user can be successful in capturing the packet. But since we are particularly interested in capture effects between PU and SU, and usually in an OSA setup SUs are nearby while the PU is far away, we have

$$S_{A,x=1} = (N-2k)\,p(1-p)^{N-2k-1}\psi(0). \tag{4.12}$$

We note that using (4.11) in a model will give an upper bound for the OSA network throughput, while using (4.12) will result in a throughput lower bound. For the numerical results we will proceed with the arrangement probability definition of (4.12).

HCC In this case we modify (4.12) as in [60, Section III.B] to take into account the probability that the receiver is available and the that the channel is not used for data communication. Therefore we have

$$S_{A,x=2} = S_{A,x=1}\frac{N-2k-1}{N-1}\frac{M_C-k}{M_C}. \tag{4.13}$$

To make a fair comparison of HCC OSA MAC with DCC OSA MAC, one needs to take into consideration the switching time. As in [60], this is modeled by modifying the average SU data packet length in slots as $q'^{-1} = q^{-1}\frac{l+s}{l+s+t_p}$, where t_p is the channel switching time.

4.3.4 Verification of the Analytical Model

To verify our analytical model we have developed an event-driven simulator in Matlab and Octave which closely mimics the conditions assumed in Section 4.3.1. Our simulator allowed us to track the channels that have been chosen by SUs and PUs during their respective connections (which were not possible in the analytical model). Results of the simulations were generated using the method of batch means for 95% confidence intervals. Each simulation was divided into at least 5 batches, where each batch contained at least 5000 network events (see for example [91] for a similar approach of an analytical model verification).

Comparison of the Proposed Model with [60]

As we have noted in Section 4.3.3, the transition probability matrix of [60, (6)] for comparing non-OSA multichannel MACs was incorrect. Using transition mat-

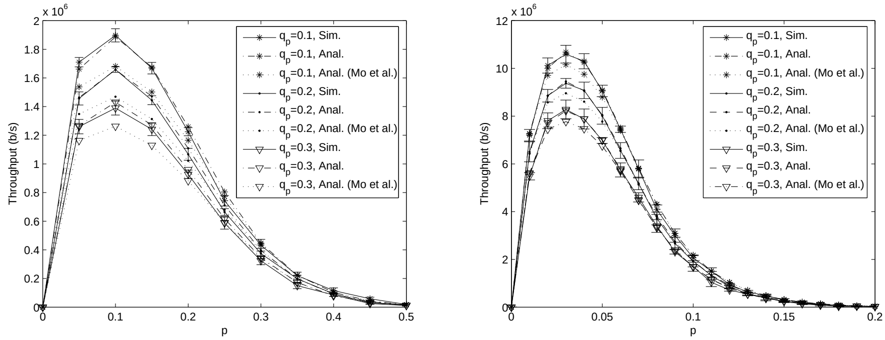

(a) **(b)**

Figure 4.2: *Numerical verification of DCC MAC class throughput with respect to probability of transmit p and different PU activity values p_{bm} for the proposed model and using transition probabilities of Mo et al. [60]; (a) $M = 3$, $N = 12$, $l = 812\,\mu s$ and (b) $M = 12$, $N = 40$, $l = 200\,\mu s$; Common parameters: $C = 2\,Mb/s$, $s = 20\,\mu s$, $N_0 = -90\,dBm$, $P_t = -85\,dBm$, $P_o = -80\,dBm$, $W = 1\,MHz$, $\theta = 17.8\,dB$, $\varphi = 9.5\,dB$.*

rix [60, (6)] for $k = \max\{\mathcal{S}\}$ we have

$$\sum_{i=0}^{k} \mathbf{P}_{k,i} = T_k^{(k)} S_k^{(0)} + T_k^{(k-1)} S_k^{(0)} + T_k^{(k)} S_k^{(1)} + \dots$$
$$+ T_k^{(0)} S_k^{(0)} + T_k^{(1)} S_k^{(1)} = \sum_{j=1}^{k} T_k^{(j)} + T_k^{(0)} S_k^{(0)}$$
$$= 1 - T_k^{(0)} \left(1 - S_k^{(0)}\right) < 1 \text{ if } S_k^{(0)} < 1. \tag{4.14}$$

In the model proposed in this chapter last term of $\sum_{i=0}^{k} \mathbf{P}_{k,i}$ is replaced by $T_k^{(0)} S_k^{(0)} + T_k^{(1)} S_k^{(1)} + T_k^{(0)} S_k^{(1)} = T_k^{(0)} + T_k^{(1)} S_k^{(1)}$, which, after performing simple algebra as in (4.14) results in $\sum_{i=0}^{k} \mathbf{P}_{k,i} = 1$. Interestingly, only in the case of DCC $S_k^{(0)} < 1$; since in HCC, connection arrangement is impossible when all channels are busy ($k = \max\{\mathcal{S}\}$). To observe how severe the error in the original model was, we plotted the throughput of DCC for different access probability values p and different level of PU activities using our simulator and compared them with our model and that of [60] in Fig. 4.2. We can clearly see that for the considered parameter range the mismatch between simulations and analysis presented here using [60, (6)] is visible when the access probability results in the highest throughput (approximately $p = [0.05, 0.25]$ in Fig. 4.2a and $p = [0.025, 0.1]$ in Fig. 4.2b). In contrast to that our proposed model gave a perfect match with the simulations (all points are within 95% confidence intervals).

Table 4.2: *Verification of the Analytical Model for the SU Network Throughput R Mb/s as a Function of PU Activity for $M = 3$, $N = 12$, $C = 2$ Mb/s, $l = 812\,\mu s$ (Top Half) and $M = 12$, $N = 40$, $C = 6$ Mb/s, $l = 200\,\mu s$ (Bottom Half); Common Parameters: $s = 10\,\mu s$, $N_0 = -90$ dBm, $P_t = -85$ dBm, $P_o = -80$ dBm, $W = 1$ MHz, $\theta = 17.8$ dB, $\varphi = 20$ dB (See Text For More Explanation).*

p_{bm}	DCC (sim.)	DCC (anal.)	DCC (sim.)	DCC (anal.)
	q=0.5 kB		q=1 kB	
0.10	(0.94,1.08)	1.08	(1.84,1.94)	1.92
0.25	(0.88,0.92)	0.88	(1.47,1.65)	1.57
0.40	(0.60,0.70)	0.69	(1.18,1.25)	1.22
0.60	(0.36,0.45)	0.48	(0.57,0.70)	0.84
0.80	(0.10,0.15)	0.23	(0.18,0.30)	0.42
0.10	(4.06,4.40)	4.13	(8.24,9.15)	8.46
0.25	(3.30,3.52)	3.40	(6.50,7.04)	6.90
0.40	(2.58,2.75)	2.67	(5.23,5.72)	5.46
0.60	(1.58,2.07)	1.93	(3.27,4.30)	3.96
0.80	(0.73,0.97)	0.96	(1.15,2.26)	1.97
p_{bm}	HCC (sim.)	HCC (anal.)	HCC (sim.)	HCC (anal.)
	q=0.5 kB		q=1 kB	
0.10	(0.87,0.96)	0.87	(1.37,1.60)	1.40
0.25	(0.70,0.79)	0.72	(1.13,1.21)	1.15
0.40	(0.52,0.61)	0.56	(0.81,0.97)	0.91
0.60	(0.27,0.34)	0.36	(0.44,0.56)	0.58
0.80	(0.10,0.14)	0.18	(0.16,0.23)	0.30
0.10	(3.86,4.26)	4.10	(7.52,8.07)	7.64
0.25	(3.38,3.70)	3.38	(6.00,6.70)	6.43
0.40	(2.65,2.89)	2.65	(4.80,5.10)	4.96
0.60	(1.56,1.90)	1.76	(3.18,3.78)	3.29
0.80	(0.85,1.11)	0.88	(1.30,1.79)	1.65

OSA MAC Scaling with PU Activity

Next, we check how the multichannel OSA MACs scale with PU activity, results are presented in Table 4.2. For each scenario, we assume that the channel access is optimized and we achieve this by choosing the access probability p that maximizes the throughput. For $p_{bm} = [0.1, 0.4]$, which are the values of interest, we can see that our model matches the simulation results closely since all values are within 95% confidence intervals. We note, however, that our model has slightly lesser accuracy with the simulations for very high values of PU activity $p_{bm} \geq 0.6$ (see in Table 4.2 for DCC with $M = 3$ and $N = 11$). Also we have observed that the model is sensitive to the selection of transmission probability p, i.e., there is less match with the simulations when the network operates in highly saturated

Table 4.3: *Verification of the Analytical Model for the SU Network Throughput R Mb/s as a Function of Probability of False Alarm for $p_{bm} = 0.068$ (Top Half) and $p_{bm} = 0.20$ (Bottom Half); Common Parameters: $M = 3$, $N = 12$, $C = 2\,Mb/s$, $l = 200\,\mu s$, $s = 10\,\mu s$, $t_p = 100\,\mu s$, $N_0 = -90\,dBm$, $P_t = -85\,dBm$, $P_o = -80\,dBm$, $W = 1\,MHz$, $\varphi = 20\,dB$ (See Text for More Explanation).*

p_f	DCC (sim.)	DCC (anal.)	DCC (sim.)	DCC (anal.)
	q=0.5 kB		q=1 kB	
0.10	(1.11,1.19)	1.13	(1.91,2.07)	1.95
0.20	(1.07,1.15)	1.12	(1.81,1.89)	1.86
0.30	(1.03,1.10)	1.10	(1.63,1.68)	1.73
0.10	(0.88,0.95)	0.96	(1.58,1.67)	1.65
0.20	(0.86,0.96)	0.95	(1.48,1.58)	1.57
0.30	(0.86,0.93)	0.93	(1.39,1.45)	1.46
p_f	HCC (sim.)	HCC (anal.)	HCC (sim.)	HCC (anal.)
	q=0.5 kB		q=1 kB	
0.10	(3.13,3.21)	3.17	(3.20,3.24)	3.22
0.20	(2.83,2.88)	2.85	(2.84,2.90)	2.90
0.30	(2.43,2.47)	2.46	(2.44,2.50)	2.49
0.10	(2.66,2.72)	2.73	(2.75,2.79)	2.76
0.20	(2.37,2.45)	2.44	(2.44,2.48)	2.48
0.30	(2.05,2.11)	2.11	(2.08,2.14)	2.13

conditions.

From Table 4.2 we expect a linear decrease in throughput for the OSA network when the PU activity increases. We will evaluate this closely in Section 4.4.2. We also observe that DCC performs slightly better than HCC for the chosen setup, which is consistent with [60, Fig. 4].

Impact of Sensing on OSA MACs

Next, we verify the correctness of the operation of the model as a function of scanning performance in Table 4.3. While keeping most parameters fixed (see Table 4.3), we vary the detection threshold $\varphi \in \{14.5, 13.9, 13.5\}$ dB, which results in different $p_d = \{0.93, 0.94, 0.95\}$. As in the section above, we assume that the channel access is optimized by choosing the channel access probability p that results in maximum throughput. We perform the verification for an average PU occupancy of 6.8% ($p_{bm} = 0.068$) which corresponds to our measured value in [65, Tab. 1] and Appendix A, and next for a PU occupancy three times larger. Again our model matches the simulation closely since all results are within the 95% confidence intervals, for all values of the detection performance. As expected, the throughput decreases with increasing p_f.

After verifying the important aspects or our model, we proceed in the next

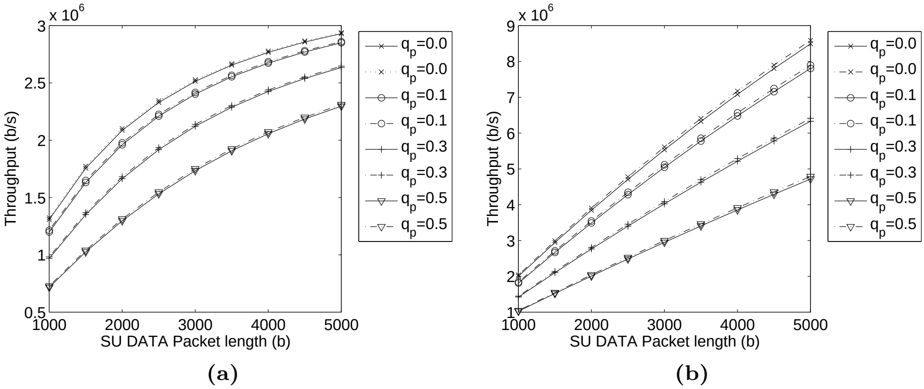

Figure 4.3: *Throughput of DCC with respect to CC availability, when data channels are not occupied by PUs using Eq. (4.11), dashed line, and Eq. (4.12), solid line. Parameters:* $C = 2\,Mb/s$, $p = e^{-1}/N$, $l = 812\,\mu s$, $s = 10\,\mu s$, $N_0 = -90\,dBm$, $P_t = -75\,dBm$, $P_o = -70\,dBm$, $W = 1\,MHz$, $\theta = 14.6\,dB$, $\varphi = 9.5\,dB$, *(a)* $M = 3$, $N = 12$, *and (b)* $M = 12$, $N = 40$.

section to a more detailed performance analysis using only the analytical model.

4.3.5 Numerical Results

Impact of Control Channel Availability

As we have noted in Section 4.2.2, DCC is the most used OSA MAC. It is therefore crucial to observe in isolation how this particular MAC class behaves. What differentiates DCC from other multichannel MACs is that one channel is solely assigned to control information exchange. In this section we will show how unavailability of the CC due to the presence of PU on a channel affects the operation of DCC.

The result is presented in Fig. 4.3. We were particularly interested in the relation between data the packet length q^{-1}, and CC availability p_{bm}. Physical layer parameters are chosen such that the scanning overhead is minimum (only 1.2% of the whole slot), simultaneously resulting in high PU detection performance, i.e., $p_d > 0.91$, $p_f < 0.08$. We will show later in Section 4.3.5 how to optimize the scanning performance. Moreover, the packet capture probability for SU is less than 20%. We have also assumed that all data channels, except for CC, are unoccupied by the PU, to observe the impact of the CC unavailability clearly. Other parameters of the setup used in this section are given in Fig. 4.3.

Interestingly, for large packet sizes even if the CC is highly unavailable, the network can still achieve moderate or high throughput, see Fig. 4.3. This is because the SU nodes do not need many new arrangements for long data transmissions, and even if the CC is highly occupied by the PU, it does not affect the operation of DCC significantly. We clearly see that when the data packet is small the impact of CC unavailability is rather high. This means that SU can control their impact by controlling the data packet size or connection duration. It is also interesting to note that the impact of the CC unavailability on DCC is not linear and is more stringent for high unavailability rates, between 0.8 and 1, since the congestion is worse. Also, by comparing Fig. 4.3a and Fig. 4.3b, we see that the impact is more severe for a higher number of SU channels since the congestion on the control channel is worse as well. Again, SU can adapt to the PU by adapting its number of used channels. Referring to our measurement results [65, Tab. 1], when the average PU activity was only 6.8%, implementing the CC on such a channel is possible when the SU network intelligently adapts the packet size and number of channels in use.

Finally in Fig. 4.3 we have compared the DCC throughput using (4.11), represented by dashed line, and (4.12) represented by solid line. The impact of multiple captures on the control channel in our setup — when access probability p is correctly chosen — is very small and it would not contribute largely to the collisions on data channels as noted in Section 4.3.3.

OSA MAC Comparison of Throughput Scaling with the Number of Channels

Next, we show how the presence of PUs on all M channels affects the throughput of each of the two investigated protocols. The result is presented in Fig. 4.4. As in the previous section, detection quality and capture effects have been set to have minimum impact on the final result so that we can clearly see the effects of data channel unavailability on the OSA network throughput. Here all channels are occupied by the PU uniformly and equally including the CC for DCC. The number of SU users in the setup is always three times greater than the number of channels.

Obviously, higher the PU activity the lower is the throughput for each of the MAC classes. In Fig. 4.4a and Fig. 4.4b we see that for a large number of channels DCC is always better than HCC, independent of the SU data packet size. The reason why HCC scales slower is that it always wastes channel access time, since it can only access a channel every M slots. Both for DCC and HCC the throughput increase slows down with the increase in the number of channels. HCC saturates because of wasting the slots while hopping onto other channels, and DCC because of the congestion on CC. Comparing Fig. 4.4 with [60, Fig. 3], we observe the same trends as in the non-OSA case. Our numerical findings (not presented in Fig. 4.4), show a linear increase in throughput between different PU occupancies. Later, in Section 4.4.2 we will investigate the impact of PU activity on the throughput in more detail analyzing all four OSA MAC classes and taking into account more networking aspects, e.g., queuing.

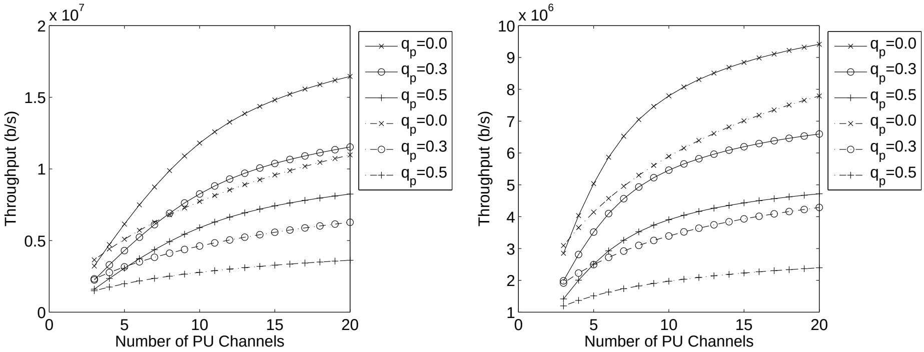

(a) **(b)**

Figure 4.4: *Throughput of DCC (solid line) and HCC (dotted line) as a function of number of channels for different PU activities on each channel and (a) 5 kbyte SU data average packet size, and (b) 10 kbyte SU data average packet size. Values of* C*,* l*,* s*,* N_0*,* P_t*,* P_o*,* W*,* θ*,* φ*, and* p *are the same as in Fig. 4.3a and* $t_p = 100\,\mu s$*. The number of users is always three times larger than the number of channels.*

OSA MAC Comparison of Throughput Scaling with the Number of SUs

In the next experiment we have investigated how increase in number of SUs in the OSA network affects the secondary network throughput. We fixed the number of channels and the probability of transmission and varied only the number of users N. Results are presented in Fig. 4.5.

As expected, with the increase in SUs the network throughput decreases for all the protocols. However, the impact on throughput is more stringent for DCC when the number of users is close to the number of channels, see left part of Fig. 4.5a. When the number of SUs is approximately twice the number of channels, irrespective of the PU activity, network throughput for both protocols is more or less the same.

PU Detection Quality and Packet Capture

As we have noted earlier, the purpose of introducing capture effects into the model is to investigate the impact of the following phenomenon on the system performance. Even when the channel has been detected by the OSA network as occupied by PUs, depending on the channel conditions, the OSA network can still successfully transmit the packet. Similarly, capture can relax the collisions between SU nodes on the CC.

We have performed two numerical experiments, for which results are given in Fig. 4.6, with the parameter setup presented therein. In the first experiment, see Fig. 4.6a, we have computed how different capture probabilities affect the

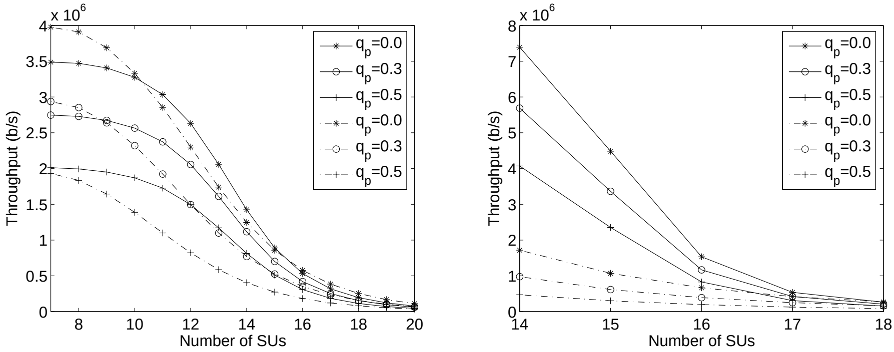

(a) **(b)**

Figure 4.5: *Throughput of DCC (solid line) and HCC (dotted line) as a function of number of SUs for different PU activities on each channel and (a) $M = 3$, and (b) $M = 6$. Parameters: $C = 2\,Mb/s$, $p = e^{-1}$, $l = 812\,\mu s$, $s = 1\,\mu s$, $N_0 = -90\,dBm$, $P_t = -75\,dBm$, $P_o = -70\,dBm$, $W =$ 1 MHz, $\theta = 14.6\,dB$, $\varphi = 9.5\,dB$.*

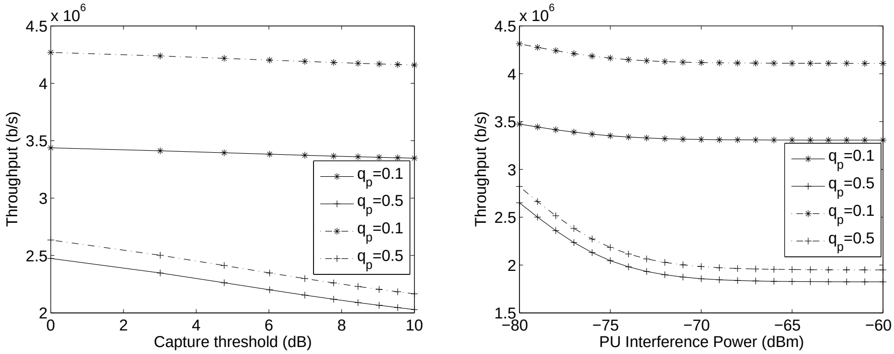

(a) **(b)**

Figure 4.6: *Impact of capture effects on OSA MAC throughput for two different PU activities p_{bm}: (a) throughput of DCC (solid line) and HCC (dotted line) as a function of capture threshold φ for fixed $P_t = -75\,dB$, and (b) throughput of DCC (solid line) and HCC (dotted line) as a function of PU interference power for fixed capture threshold φ = 20 dB. Parameters assumed in both plots: $M = 3$, $N = 20$, $C = 2\,Mb/s$, $l = 812\,\mu s$, $s = 1\,\mu s$, $N_0 = -90\,dBm$, $P_o = -70\,dBm$, $\theta = 19\,dB$, $W = 1\,MHz$, $t_p = 100\,\mu s$, $1/q = 10\,kbyte$ and $p = e^{-1}/N$.*

throughput of DCC and HCC. We have set the PU detector performance, such that it resulted in a very low probability of false alarm, $p_f = 10^{-13.6}$, and low probability of detection, $p_d = 0.63$. We have set p_d such that the phenomenon described in the beginning of this paragraph will be clearly visible. We varied the capture threshold such that it resulted in very high capture probability (left-most part of the plot) to almost no capture (right-most part of the plot). The essential observation is that when the capture probability is very high, it positively affects all protocols. However, when the capture probability drops to a normal level (1-5%), its effect is negligible. Particularly, the positive effect of the capture in the presence of PU interference is more visible, when the PU activity is higher, i.e., the slope of the throughput curve is steeper with higher p_{bm} for both of the analyzed protocols.

In the second experiment, see Fig. 4.6b, we have observed how a potential capture of the PU might affect the SU network throughput. This time we have varied the PU interference power, for the same values of s as in Fig. 4.6a. Varying the PU power results in varying the detection quality, i.e., for the case $p_d = [0.24, 0.99]$, $p_f = 10^{-13.6}$. The capture is mostly visible when the detection quality is small, i.e., when simultaneous transmissions of SU and PU are more probable. With the increase in detection quality effect of capture becomes also negligible. With the increase of PU activity the capture effect becomes less visible. Therefore, we may conclude that when the detector is designed sufficiently well capture from PU will not increase SU network throughput as high as by adding new PU channels to the OSA network, see the results in Section 4.3.5. Thus, due to the minimal effect of the capture on the obtained throughput in the chosen scenarios, we will omit this effect in the simulation model presented in later sections.

Impact of Scanning Length

Since the scanning length is a crucial parameter of every OSA system we quantify how it impacts the performance of multichannel OSA MACs. For energy detection increasing the observation time improves the detection performance, i.e., it improves p_d, simultaneously decreasing p_f (see Section 4.3.2). For the given channel bandwidth W and PU interference power P_t we have varied the observation time $s = [1, 50]\,\mu$s. Simultaneously, we have adapted the sensing threshold as $\theta = 10^{7.31} s\,\mu\mathrm{s}^{-1}$ (linear value), which resulted in the following detection performance range for the considered range of s with $p_f = [0.23, 0.02]$ and $p_d = [0.82, 0.93]$. For these detector operating conditions, we have plotted the throughput of DCC and HCC in the case of $M = 3$, $N = 12$ and two different slot lengths l. The results are presented in Fig. 4.7.

The most essential observation is that with the increase in the observation time, the throughput first increases due to lower false alarm probabilities, but then decreases again. This is due to the fact that the scanning length overhead s starts to dominate over the usable slot l, reducing the effective throughput of the SU, see (4.6). This is particularly visible for small slot sizes, compare Fig. 4.7a

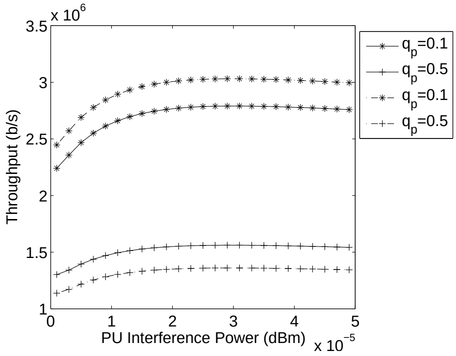

(a)

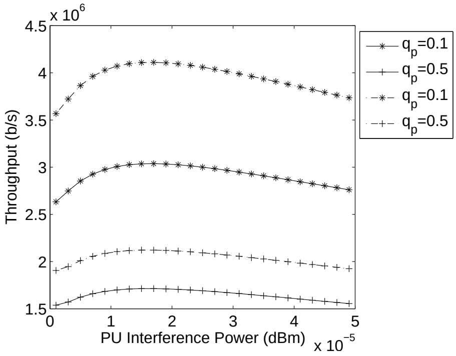

(b)

Figure 4.7: *Throughput of DCC (solid line) and HCC (dashed line) as a function of scanning length s for different channel availability rates and (a)* $l = 200\,\mu s$ *slot size, and (b)* $l = 812\,\mu s$ *slot size;* $W = 1\,MHz$, $P_o = -80\,dBm$, $P_t = -85\ \ dBm$, $N_0 = -90\,dBm$, $\varphi = 9.5\,dB$, $N = 12$, $M = 3$, $C = 2\,Mb/s$, $p = e^{-1}/N$, $1/q = 5\,kbyte$ *data packet size and* $t_p = 100\,\mu s$.

and Fig. 4.7b. With the highest detection performance for $s = 50\,\mu$s in the setup, sensing constitutes 9% of $l = 812\,\mu$s slot, while for $l = 200\,\mu$s it results in 25% overhead. Therefore, the scanning period s should be carefully chosen for any OSA multichannel MAC, since improving detection performance for decreasing p_f does not always increase throughput. Every OSA MAC class is affected equally by this phenomenon. We can therefore formulate the optimization problem as

$$\max R \text{ subject to } p_d \geq \alpha_i, \tag{4.15}$$

where α_i is the detection constraint that the OSA network needs to fulfil, while accessing PU channels. The parameter that we want to optimize is R with respect to s. We know that p_d is a non-linear, step-like function, where computation of this probability is in a summation form and $p_d \to 1$ as a in (2.7) increases. We also know that R is a function of p_f. Finding an optimal solution in this form is difficult, and it involves using heuristics such as first finding a convex envelope and later the optimal value of p_d that satisfies α_i [92], which is beyond the scope of this chapter. However, we can think of the other simple heuristics for solving (4.15). First we find $a_{max} = \lfloor sW \rfloor - 2$ that fulfils $p_d = \alpha_i$ and we compute R using (4.6). We then increase a_{max} by 1 and compute the new throughput. If the new throughput is larger than the old one, we perform increasing a_{max}, otherwise we terminate and the resulting R from the last step is the optimal throughput R_{opt}. The optimization procedure is also depicted in Algorithm 1. We have performed a similar procedure in Fig. 4.7, where we compute R for every s in the considered range. Then, the maximum value of the throughput obtained

Algorithm 1: Optimization Heuristics for (4.15)

Input: $R_1 := 1$, $R_2 := 0$, $C, N, M, l, \theta, \varphi, W, P_o, P_t, N_0, p, q, p_{bm}, t_p$
Output: R_{opt}
Find $a_{max} := \lfloor sW \rfloor - 2$ that results in $p_d = \alpha_i$;
while $R_1 - R_2 > 0$ **do**
  Compute $R_1 := R$ using (4.6) with a_{max};
  $a_{max} := a_{max} + 1$;
  Compute $R_2 := R$ using (4.6) with a_{max};
$R_{opt} = R_2$;

in the figure transforms to the optimal sensing time. Please note that, as we mentioned before, in the upper range of s in Fig. 4.7 results in a big overhead for the slot and therefore s should also be upper bounded to a reasonable value, e.g., less than 50 μs, corresponding to the data part of the slot l.

4.4 Simulations

In this section we discuss the simulation results to compare the four different OSA MAC designs. In the simulation model we introduce queuing and a more detailed PU activity model that were difficult to assess analytically.

First, we study the throughput for the four OSA MAC designs introduced earlier. Simulation results are given as a function of sensing performance and as a function of the PU activity that is modelled through average channel utilization and PU packet length. Next, we focus on simulating the delay performance for each of the four MAC classes, again as a function of PU activity and scanning performance. Finally, we measure the expected collision probability with the PU, which we consider to be an important performance metric in the context of OSA networking. We start with introducing the simulation setup.

4.4.1 Simulator Description

We have developed a coarse-grained time-slotted simulator in Matlab, which extends the work of [60] with OSA related features like PU traffic and PU detection. Matlab was a design choice since we needed a rapid prototyping functionality and overall control over the simulator development process. The simulation environment is coarse-grained, since it omits all the transient effects related to connection arrangement, i.e., the backoff mechanism. This simplification gives enough information on the interactions between individual SUs and between SUs and PUs, while resulting in fast development time. The smallest time scale observed in the simulator is on the RTS/CTS transaction scale, which means that the smallest time-slot considered is long enough to transmit a RTS/CTS control handshake.

This interaction is fully described by the probability of a new successful connection arrangement p_{sa} that captures collision effects due to backoff mechanisms in a simple way. This probability p_{sa} is related to the probability p to access the channel in the analytical model of Section 4.3. Similar to the assumptions taken in [60], we assume that the probability to have a successful contention in the OSA network is $p_{sa} = e^{-1}$, which mimics the optimal operation of the slotted ALOHA protocol. For more explanation we refer to [60, Section V], where the justification of introducing such simulator is presented in more depth.

We now summarize the simulator features here. They are grouped in two sets: multichannel MAC related aspects and OSA related features. The multichannel MAC related features are as follows.

1. *Queuing:* In the analytical model no assumption on the buffering have been taken since only throughput was modelled. The simulator implements packet buffering and only backlogged packets can contend for the medium. The queuing delay is monitored for the delay analysis.

2. *Traffic generation:* In the simulator we have assumed fixed length packets (5 slots or 1024 bytes) for the OSA network while the inter-arrival times are geometrically distributed.

3. *SPCC model:* As in [60], the simulator implements contention resolution between multiple SPCC pairs that use the same data channel when all data channels are utilized.

4. *Receiver selection*: In the simulation we assume that each receiver has only one transmitter. Although the case where multiple transmitters contend for a single receiver has been studied in [60], we believe it is not important to our study, which focuses particularly on the impact of PU traffic on the OSA network.

The OSA related features of the simulator are as follows.

1. *Channel occupancy:* Each channel is assumed to be occupied with PU packet-based traffic, and the average PU occupancy level is the same for all channels. The distribution of the PU traffic is described by a geometric on/off process. The simulator allows us to vary the average length of the channel, i.e., *'on'* and *'off'* periods. The difference in average on the period length for the same average PU channel utilization is denoted as *PU burstiness*, where more burstiness represents shorter average on times. We vary the PU packet size from 10 to 100 slots.

2. *Detection errors:* As in the analytical model of Section 4.3 every slot is preceded by a scanning period of varying length, after which the OSA node individually decides about the channel occupancy. Detection performance is a function of the length of the scanning period, the noise and PU signal

levels and the fading process. We use the same energy detection model described by (2.4) and (2.7). For simplicity, we assume that every OSA node observes the same propagation conditions, such that the PU occupancy decision is the same for all OSA nodes. Parameters used were as follows: channel bandwidth $W = 1\,\text{MHz}$, PU interference power $P_t = -85\,\text{dBm}$, $N_0 = -90\,\text{dBm}$ and $\theta = 10^{7.31} s\,\mu\text{s}^{-1}$ (linear value). For these settings we simulated a scanning performance ranging from $p_f = [0.2, 0.01]$ and $p_d = [0.89, 0.93]$.

3. *Interference to PU:* Since level of harm to the PU introduced by the OSA network is of utmost importance in the context of OSA networks, we monitor the probability of PU interference (collision) in the simulator.

4. *Fading:* Since the capture effect was shown to be small if p_d is sufficiently high, we did not embed capture in the simulation model.

4.4.2 Simulation Results

Having introduced the simulation setup we now present the simulation results. Focus is on throughput analysis, delay analysis, and interference to the PU.

OSA Network Throughput Analysis

To assess the maximum possible throughput an OSA network can achieve we simulate the saturation conditions. In Fig. 4.8 the OSA network throughput is shown to decrease linearly with PU channel utilization, for all four considered MAC designs. This linear decrease with PU activity is expected since each slot occupied by the PU cannot be used by the OSA network. Since not all OSA MAC designs access the channel the same way, they grab the available white spaces with varying efficiency. This explains the different slopes for the different MAC designs. In Fig. 4.8a we plot the throughput for different scanning lengths, resulting in different performance of the PU detection. As mentioned earlier in the analysis section, a careful optimization of the scanning performance can result in a significant throughput increase. This is also visible in Fig. 4.8a and the throughput penalty for worse scanning performance is similar for the four MACs.

We plotted the impact of varying the PU packet size in Fig. 4.8b, for a scenario with $M = 12$ channels and $N = 40$ OSA users. Surprisingly, HCC and MRCC achieved a larger throughput when the PU packet size is larger (solid line). This is because those MAC protocols contend on the same channel they will use for the following data transmission if the contention was successful. If the channel is not free, they just hop onto another channel, and if they find the next one free they will be able to send their data packets with a high probability if the PU ‘on’ and ‘off’ times are longer. DCC however contends on another channel and needs to be lucky to find both control and data channel free from PU activity. A successful contention for DCC does not mean that the chosen data channel is

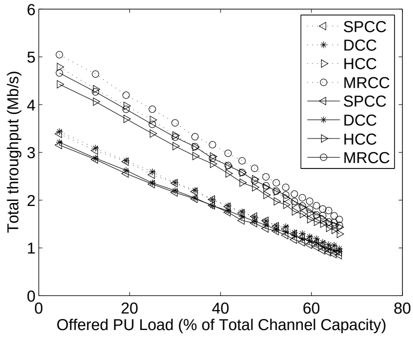

(a)

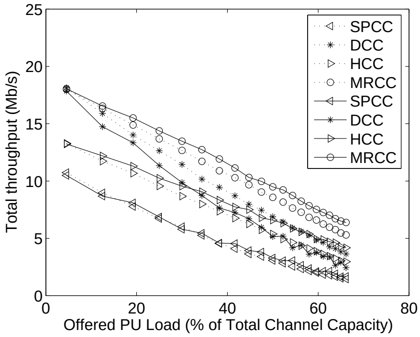

(b)

Figure 4.8: *Simulated impact of the PU channel occupancy on the throughput of OSA network exploiting different OSA MACs: (a)* $M_C = 3$ *channels and* $N = 20$ *OSA users with different PU detection (solid:* $p_f = 0.2$ *and* $p_d = 0.89$*; dashed:* $p_f = 0.01$ *and* $p_d = 0.93$*) and PU average packet size of 10 slots, and (b)* $M = 12$ *channels and* $N = 40$ *OSA users with different PU packet sizes (dashed: 10 slots; solid: 100 slots) and good PU sensing with* $p_f = 0.01$ *and* $p_d = 0.93$*. Common parameters:* $C = 2$ *Mb/s,* $l = 812\,\mu s$*.*

free. Note that we do not monitor the data channel PU activity in the simple MAC designs considered. As a result, DCC's performance suffers a lot when the PU packet sizes are longer. We also note that in the simulations we put the *stick limit* [60] to 50 slots, which means that if the data packet was not sent after 50 slots, a new connection arrangement is needed.

OSA Network Delay Analysis

To observe the impact of PU occupancy on the OSA network delay, we monitor the OSA network delay for the scenario where in the load of the OSA network is 15% of the total channel capacity; it is shown in Fig. 4.9. First, we study the scenario of $M = 3$ channels with $N = 20$ OSA users in Fig. 4.9a. In this case, a total load of 15% of the total channel capacity is equivalent to 45 kbps per flow. When the PU occupancy increases, all protocols suffer from an increased network delay. The impact is however the largest for SPCC and DCC, since they employ a dedicated channel for control that is prone to congestion. In Fig. 4.9a we also see the impact of the scanning performance on the delay. Similar to the throughput analysis, we see that a suboptimal scanning increases the delay significantly for all MAC designs.

In Fig. 4.9b we study the delay for a network with $M = 12$ channels and $N = 40$ users. In this scenario also 15% of the total channel resource is used, which corresponds to 90 kbps per flow. We note that the delay performance

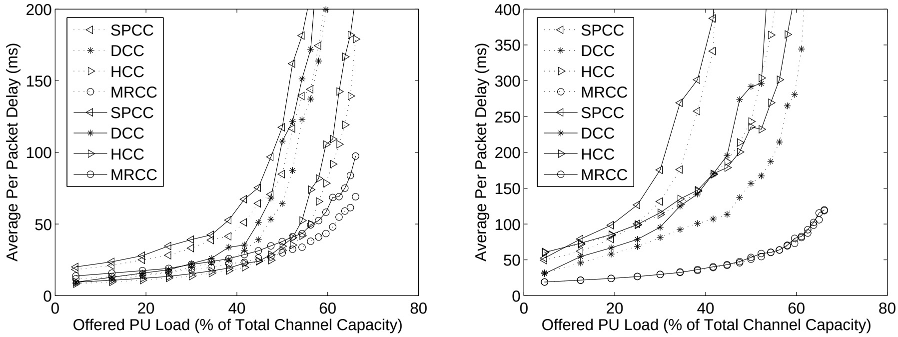

(a) **(b)**

Figure 4.9: *Simulated impact of PU channel occupancy on OSA network delay, for different OSA MACs: (a)$M = 3$ channels and $N = 20$ OSA users with different PU detection (solid: $p_f = 0.2$ and $p_d = 0.89$; dashed: $p_f = 0.01$ and $p_d = 0.93$) and PU average packet size of 10 slots and (b) $M = 12$ channels and $N = 40$ OSA users with different PU packet sizes (dashed: 10 slots; solid: 100 slots) and good PU sensing with $p_f = 0.01$ and $p_d = 0.93$. Common parameters: $C = 2$ Mb/s, $l = 812\,\mu s$.*

of MRCC is similar to the first scenario, because the load is also 15%. SPCC and DCC however suffer from a larger delay since their control channel becomes more congested when the number of data channels increases. HCC on the other hand performs suboptimally since it visits every channel only every 12 slots, and since the packet size is only 5 slots, all the channels are not occupied during the remaining $12 - 5 - 1 = 6$ slots. In Fig. 4.9b we also study the impact of the PU ‘on and ‘off time distribution. Interestingly, the delay is larger when the PU occupancy increases. This is because when the PU occupies the channel for a longer duration, the OSA nodes have to wait for longer time until they can access the channel. Another observation is that the MRCC and HCC MACs are not so sensitive to the packet size of the PU network. This is because they perform contention on the same channel as that of data transmission. When the channel is found to be idle, they can hence both contend and immediately send data packets if contention was successful. Because of the burstiness, when idle, the PU channel remains idle for the remaining 5 slots with a high probability. As a result, both protocols hardly have to wait for the long PU packets to be transmitted first, since they simply hop onto the next channel when a channel is occupied. Since all the 12 channels are assumed to be independent, one of the next hops will end up in an idle channel. Again, SPCC performs worst among all the classes considered.

Table 4.4: *Main Results: VL - Very Low, L - Low, M - Moderate, H - High*

	DCC	HCC	SPCC	MRCC
PU Channels Scalability	L	L	VL	H
Impact of Average PU Activity	M	M	H	L
Impact of PU Activity Duration	H	L	H	L
Induced PU Interference	H	M	M	M
Impact of scanning	M (if properly designed)			
Impact of packet capture	M (if properly designed)			

OSA Network Impact on PU

The last simulation study focuses on the probability to harm the PU, which is the new and very important performance metric in the OSA context. We define harm to the PU as the probability that a slot occupied by a PU transmission is also used by the SU, causing part of the PU data packet to be lost. For that, we consider a network of $M = 3$ channels with $N = 20$ OSA users. The PU occupies the channel for 50% of the time, while the on times are 10 slots or 100 slots. We simulate a scenario where the total OSA network load is 15% of the total channel capacity. All differences in interference are hence due to the way the channel access is organized. The results are given in Fig. 4.10a. The curves are obtained by varying the probability of false alarm p_f from 0.01 to 0.2 and the usual energy detection model is used to adjust the p_d and the scanning overhead. With increase in p_f the detection performance p_d decreases, as expected, causing more interference to the PU. The p_d ranges from 0.93 to 0.89. We see in Fig. 4.10a that the true impact on the PU is always low (best p_d would result in 7% harm), since the OSA network does not use all the available channel resources. Interestingly, we see that the interference to the PU decreases significantly when the PU activity in a given slot depends on the activity of that PU in the previous slot. If that dependency is the case, most of the SU packets will not be sent because the RTS/CTS exchange before the data packet could not be sent as well, preventing more potential harm to the PU during data activity. This is more visible for MRCC and HCC, since those protocols do network arrangement and data transmission on the same channel. As a result, the probability to harm the PU during a data packet is much lower since this can only happen when the PU was not detected during the control phase. When the PU 'on' and 'off' times are large, the probability that PU activity changes during the SU data transfer is small. We also note that DCC does not benefit as much from this because DCC transmits data and control messages on different channels.

We also plot the harm to the PU for a scenario with a large number of channels and users in Fig. 4.10b. The same load of 15% is used, and because of that the

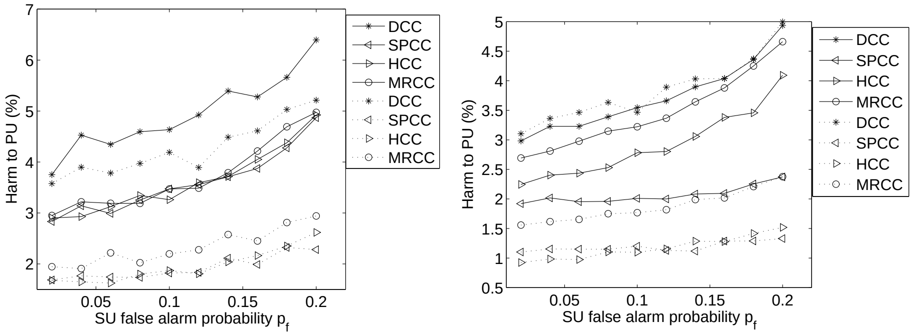

(a) **(b)**

Figure 4.10: *Interference to the PU for the four OSA MAC protocols, as function of p_f computed from the analytical model. PU 'on' and 'off' time considered are 10 slots (solid line) and 100 slots (dashed line), for a PU occupancy of 50%: a) $M = 3$ channels and $N = 20$ users with 15% channel load, and b) $M = 12$ channels and $N = 40$ users with 15% channel load. Common parameters: $C = 2\,Mb/s$, $l = 812\,\mu s$.*

probability to harm the PU does not increase, although more channels are in use. Compared to the previous scenario, we see that SPCC performs better but this is due to the fact that SPCC achieves a throughput lower than 15% of the total capacity (we recall that during the control phase $M - 1$ of the channels cannot be used). Because of that, the channel is accessed less frequently and the probability to harm the PU is low. Next, we see that MRCC interfere with the PU more than HCC in the simulations. This is because of the assumption that no collision happens in HCC (collision resolution is hidden by assuming a fixed probability p_{sa} to gain access to the channel successfully). In HCC all users contend on the same channel, while in MRCC this contention is spread across channels. As a result, during the control phase MRCC can harm the PU with a higher probability, i.e., up to $Mp_{sa}(1 - p_d)$ (assuming contention on every channel), while HCC only interferes with probability $p_{sa}(1 - p_d)$. In reality, the interference should however happen with the same probability. Finally, in Fig. 4.10b, we note that again, that SPCC, MRCC and HCC have a lower interference when the 'on' and 'off' durations of the PU are longer. For DCC, the interference does not vary as a function of PU traffic patterns.

4.5 Conclusions

This chapter presented a very detailed performance study of OSA MAC Protocols. By means of an analytical model as well as detailed simulations we were able to assess different OSA MAC designs in a cohesive manner. This is the first study that performs such a detailed assessment since the Control Channel design in OSA context is often neglected.

We draw many important conclusions from our study. First, we show that the negative impact of PU activity on the Control Channel can be mitigated by transmitting long SU packets of decreasing the number of channels used. Next, although the scanning length and capture effects have equal impact on all the OSA MAC classes considered here a proper insight into these effects in the OSA context has been obtained. As a result, we have shown that the impact of capture on the OSA network throughput is small when the PU detector is properly designed. The impact of the scanning configuration was however large and there is a single optimal point of operation. All OSA MAC classes scale linearly with the increase of PU activity, but MRCC achieves the highest throughput since it can use the available white spaces more efficiently. Interestingly, the throughput achieved by MRCC is higher when the PU activity is organized in longer 'on' and 'off' periods. Delay increases steeply with PU activity when the network becomes congested for all OSA MACs. Again, MRCC achieves the lowest delay. Further, MRCCs delay is also not significantly affected by the PU packet lengths ('on' and 'off' periods). We conclude that from the OSA network perspective MRCC is the best OSA MAC protocol since it achieves the highest throughput and lowest delay for any PU activity pattern, while causing a low interference to the PU (especially when the PU has long 'on'/'off' times). MRCC is the most efficient in finding and using the random white spaces. Moreover its implementation complexity is comparable to the other multichannel MAC classes. Major conclusions are also summarized in Table 4.4.

We have shown that OSA MACs that spread requests among all possible channels, e.g., MRCC, performs best among all proposed OSA MAC classes. However the hopping sequence of MRCC implemented in the simulator is not adaptable to the level of activity of PUs on each of the channels, since we have assumed that all channels have been utilized in the same way by the PUs. In the case of non-uniform channel utilization, as a future work, our plan is to extend MRCC with adaptability mechanisms.

Given the insights on the OSA MAC operation we will proceed further with the investigation of OSA networks. In the next chapter we will look into higher layers of the OSI protocol stack.

Chapter 5

Performance of TCP over OSA Links

I must move fast, you understand me

The Smiths, "Frankly, Mr. Shankly", from the album "The Queen Is Dead", Rough Trade, 1985

Knowing all the major effects of the MAC operation in the OSA network, the next logical step would be to investigate the performance of higher layer protocols, specifically those related to transport layer. At the time of preparing the thesis this issue had not been explored thoroughly, as we have pointed out in Chapter 1. Given the proliferation of TCP in the current Internet we would not expect any new design for TCP implementation to happen. Therefore all potential MAC protocols working on the OSA link would need to transfer existing TCPs *ergo* OSA network designers need to understand the relation between existing TCPs and OSA link. This chapter investigates this issue and results presented here draw many important conclusions helpful in the design of effcient TCP transmission over OSA links. The novelty of the approach presented here is that we look at the OSA network design from the cross-layer perspective. That is, the TCP transfer analysis presented in this chapter correlate features related to spectrum sensing, analyzed in Chapter 2, with the OSA link dynamics at the MAC layer, presented in Chapter 4.

Some of the conclusions to be drawn from the analysis presented here are as follows. First, with highly dynamic OSA links, i.e., with highly active PUs, all TCPs with Selective Acknowledgments utilize the available capacity with efficiency $> 95\%$. Second, the length of the active period of the PU has more impact on the channel usage efficiency by any TCP than non-activity. And finally, sensing time and false alarms have severe impact on the TCP performance.

This chapter is structured as follows. We start with a brief literature review on TCP in Section 5.1. Then we introduce all known flavors of TCP in Section 5.2, that will be investigated in OSA context in subsequent chapters. The impact of varying capacity of OSA links on TCP was investigated in Section 5.3, while physical layer effects in OSA setup on TCP have been investigated in Section 5.4. The chapter is concluded and briefly summarized in Section 5.5.

5.1 The Need for Research on TCP Performance for OSA

To briefly recapitulate, in this thesis we look at the OSA link as a wireless link with time varying bandwidth, constructed of a set of independent channels, each of possibly different capacity. Individual channels are occupied by the PU on a random basis. During PU presence, the channel is not available for use by the SU, while the information on the availability of the channel is given with a certain confidence. This results in transmission errors for the OSA user when it is trying to access a channel that is mistakenly believed to be available (simultaneously causing disruption for the PU communication). It also results in underestimation of OSA link capacity, since the SU might believe that the channel is occupied by the PU, when it is actually free of PU activity. When information on the channel availability is gathered by the communicating OSA node itself, it has to take additional time to scan the channel. However, even in cooperative OSA links (where PU and SU can negotiate the channel use), or when PU activity is non-existent (where only SU contends for the channel), individual OSA users will experience similar time variations in channel availability, see Chapter 2.

Given this characteristic of the OSA link as nothing but a time-varying capacity link, research on the performance of TCP over such paths has been studied in many different contexts, e.g., packet marking strategies for best effort traffic in a Differentiated Services environment [93], bandwidth allocation in high speed optical networks [94], interplay of wireless link characteristics and TCP design [95], and vertical handovers and slowly adaptive competing traffic [96–99]. What makes our work unique, is that we were able to determine the performance of real-world TCP implementations over a OSA link model extrapolated from measured channel data, as given in Appendix A. Our simulations were performed using Network Simulator (NS) version 2.29 [100], with Linux-TCP enhancements [101], and additional bug-fixes. The Linux-TCP enhancement makes it possible to use actual source code of the Linux operating system's (version 2.6) TCP stack in NS, in addition to the TCP implementations available in plain NS. The behavior of TCP implementations from plain NS can differ significantly from current real-world TCP stack performance [102], but the Linux-TCP implementation behavior was shown to be very similar to actual Linux. As Linux' TCP implementation closely follows the latest TCP developments, our results should be representative of what can be expected from a modern, up-to-date real-world TCP stack.

We also note that although there seems to be a large number of papers related to link layer protocol performance in OSA networks, see Chapter 4 and the references therein, authors do not evaluate them with any real transport protocols (either TCP or UDP). Only in [74], the performance of proposed distributed channel coordination MAC for OSA network was assessed using TCP, not specifying, however, what TCP flavor was used for evaluation.

5.2 Overview of Modern TCP Flavors

TCP has constantly evolved since it's original conception. A good overview in the context of wireless networks is given in [103]. Many versions (or so called *flavors*) of TCP are currently in use, but probably the most commonly used TCP in the Internet today is New Reno [104], which improves the Fast Recovery Algorithm of its ancestor Reno [105]. In the congestion avoidance phase, New Reno (and Reno) probe the network by additively increasing the sending rate by a segment per round-trip time, until a packet loss occurs. Thus, they use packet loss as an indicator of congestion, causing a periodic oscillation of the congestion window, which reduces throughput.

A promising new TCP variant is Vegas [106]. In the congestion avoidance phase, Vegas constantly measures the round-trip time of the connection, calculates from this the actual and expected segment flow rate, and from this the number of segments that (it believes) are queued in the network. Two parameters, called α and β control the size of the congestion window. Per round-trip time, when the calculated number of queued segments is less than α, the congestion window is increased by one segment, if greater than β, the window is decreased by one segment, else the window is not changed. The default values of α and β are 1 and 3, so Vegas in essence attempts to keep between 1 and 3 segments queued in the network. Because Vegas avoids congestion, it does not suffer from Reno's congestion window oscillations, and achieves better throughput in certain scenarios.

Most modern TCP stacks employ selective acknowledgments [107] (SACKs), which allow a TCP receiver to indicate up to 3 blocks of segments that have been correctly received. Old-style cumulative acknowledgments only allow the receiver to indicate the highest in-order segment received. The more precise SACK information enables the sender to re-transmit only those segments actually missing, and can result in much improved performance, especially in more dynamic network environments where multiple losses may occur more frequently, e.g., OSA links. In this chapter, we mainly consider SACK enabled TCP stacks, as these are the common case today.

Because of their different characteristics, especially in the congestion avoidance phase, these TCP flavors can be expected to perform differently over OSA links. Reno more aggressively probes the network and as a result, many packets are typically buffered in the network, perhaps allowing it to instantly grab capacity of a OSA link with packets already in the network. On the other hand, Vegas attempts to keep between only 1 and 3 segments queued in the network, which avoids oscillations in the congestion window and rate, but this may limit is ability

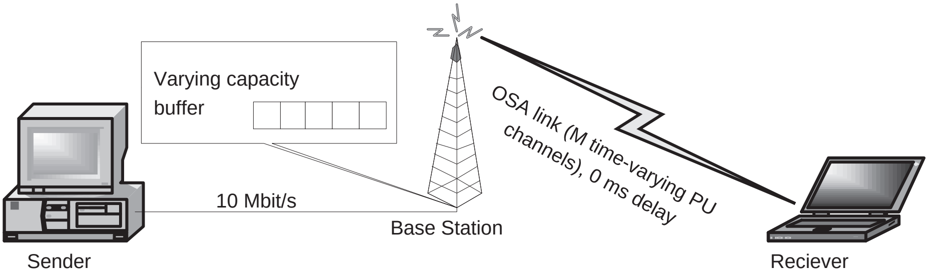

Figure 5.1: *Basic OSA network setup used for TCP performance evaluation.*

to grab additional bandwidth. Also, Vegas' view of the network capacity may be disrupted by greatly varying RTT [108] due to abrupt capacity changes of OSA links.

5.3 Impact of OSA Link Dynamics on TCP Performance

5.3.1 Simulation Setup

To investigate the performance of different TCP flavors in a OSA environment, we have constructed a basic simulation scenario shown in Fig. 5.1. A sender is connected to BS by means of a wired connection, representing the Internet with IPv4. The receiver is connected to the BS via a OSA link of varying capacity. The BS buffers and forwards packets. A TCP connection is established between the sender and receiver, and an infinite flow of TCP segments travel from sender to receiver, while TCP acknowledgments flow in the opposite direction. We simulate the TCP connection, of which we discard the first 100 seconds, to remove the effect of TCP's startup phase. We record the number of segments TCP managed to transfer in the subsequent 10000 seconds. All simulations, as noted earlier, were performed using NS version 2.29, with TCP-Linux enhancement.

The wired connection has a fixed capacity of 10 Mbit/s and a constant delay representing the (simplified) delay a packet incurs while traveling the Internet. In addition to these delays, packets incur a transmission delay according to the current bit rate of a link, and queuing delays depending on occupancy and maximum size of the buffer in the BS. The bit rate of the wired link is chosen such that the OSA link is the bottleneck link. On the OSA link, a packet incurs no propagation delay.

The OSA link is constructed as follows. From the BS to the receiver, the BS has access to M channels, where each individual channel has equal capacity. The sum of all channel capacities is 2.4 Mbit/s. In addition, a small non-time-varying channel of 0.1 Mbit/s is always available to the BS, making the maximum and minimum available capacity 2.5 and 0.1 Mbit/s, respectively. Moreover, individual channels are occupied randomly and independently of each other by the PU, according to an exponential distribution, where parameters for arrivals and departures ($\mu_{p,1} = \mu_{p,2} = \ldots = \mu_{p,M} = \mu_p$ and $\lambda_{p,1} = \lambda_{p,2} = \ldots = \lambda_{p,M} = \lambda_p$, respectively), are the same for every OSA channel. Thus, $1/\mu_p$ and $1/\lambda_p$ are the average 'on' and 'off' period of a channel. In the other direction, from the receiver to the BS, TCP acknowledgments can be transmitted by the receiver at a constant 2.5 Mbit/s rate. Furthermore, the BS' PU detection is perfect, and no errors occur on the wireless link. In Section 5.4 we will analyze the impact of these phenomena on TCP in detail.

In the simulations, the delay of the fixed link is varied between 5 and 100 ms, and the size of the BS's buffer between 5 and 100 packets, giving a wide range of network configurations one might encounter in the real world. For the OSA link, $1/\lambda_p, 1/\mu_p \in \{1.5, 5.5\}$ s, and it consists of $M \in \{3, 12\}$ channels. We have chosen the values of $1/\lambda_p$ and $1/\mu_p$ different than those extracted from measurements in Appendix A, resulting in a more dynamic OSA link, but representing possible combinations of arrivals and departures of the PU on a OSA link.

Given the fixed total capacity of 2.4 Mbit/s of these channels, individual channels are 200 kbit/s in 12 channel models, and 800 kbit/s in the 3 channel models. As discussed in Section 5.2, we mainly consider the Linux implementation of Reno and Vegas, but also simulate NS' implementation of New Reno, and Reno with selective acknowledgments (referred to as 'Sack' in the following). For Linux' New Reno and Vegas, and NS' Sack, the receiver uses selective acknowledgments, whereas for NS' New Reno it does not. The receiver sends one acknowledgment per received packet, i.e., no delayed acknowledgments, as this was shown to produce behavior closer to that of the actual Linux OS [101], that dynamically adapts its acknowledging strategy. The maximum segment size of TCP is set to 960 bytes, resulting in packets of 1000 bytes, after the IP header is added. We set the maximum congestion window to 1000 packets, well beyond the (maximum) bandwidth delay product (BDP) of the path, as setting it close to the BDP is not possible for a link of varying bandwidth. Finally, we set the minimum retransmission timeout to 0.2 s for all TCPs, as this is current practice. The BS buffer is a simple first in first out queue that drops arriving packets when it is full. We simulated all combinations of the above parameters.

Finally, for all simulations, we calculate the total OSA link capacity C_{tot} that was available to TCP over the entire measured period (from t_1 to t_2 s), and the number of bytes TCP actually managed to transfer in this period, referred as C_{act}. From these, we calculate the efficiency ϵ of TCP as

$$\epsilon = \frac{C_{act}}{C_{tot}} = \frac{A_c(t_2) - A_c(t_1)}{\int_{t_1}^{t_2} C_\Sigma(t)dt} \in [0, 1], \tag{5.1}$$

where $C_\Sigma(t)$ is the total available OSA link rate at time t (bytes/s), and $A_c(t)$ is the number of bytes acknowledged at the sender at time t.

In summary, we simulate a single long-lived bulk TCP transfer over a network path where the OSA link is the bottleneck link, and measure the achieved efficiency. We compare the achieved efficiency of number of TCP flavors, and see which performs best and why for our simulated OSA link environments. We do not look at fairness among multiple TCP connections, nor do we consider short lived TCP connections, e.g., web-traffic. We simulate a OSA link with optimal and instantaneous PU occupancy measurements, without any wireless loss.

5.3.2 Simulation Results

Discussion of Models

Fig. 5.2 shows TCP efficiency achieved by all TCP flavors in all 3 and 12 channel models. The efficiency is plotted as a function of wired link delay, for a (reasonable) buffer size of 50 packets. We can see that all TCPs achieve higher efficiency in 12 channel models, compared to their performance in 3 channel models, under otherwise equal conditions. The reason for this is the smaller link capacity change in 12 channel models when a channel becomes available or unavailable[1]. Therefore, in the 12 channel models there is a relatively larger buffer to potentially i) grab capacity by transmitting packets queued in the buffer when the OSA link capacity is increased, and ii) absorb packets when link capacity is decreased until the sender can lower sending rate. Additionally, there is a low probability, due to the features of the exponential distribution, that more than one PU channel will change state simultaneously (or at almost the same time). Thus, the 12 channel model capacity will usually change by 200 kbit/s at a time, whereas in the 3 channel models, the granularity of change is 800 kbit/s, see Section 5.3.1.

Looking at the rate at which OSA link capacity changes occur, TCPs achieve better performance on links with long 'on' and 'off' periods, than on links with short 'on' and 'off' periods (compare, e.g., Fig. 5.2e and 5.2h). This is not surprising, as TCP needs to adapt less often because the OSA link changes capacity less often (for a given interval). Also, once TCP has converged to the new link capacity, it can operate there for a longer time.

Comparing the average duration of 'on' and 'off' periods, we see that for short delay, all TCPs perform better in the 12 channel model when $1/\lambda_p = 1.5$, $1/\mu_p = 5.5$, than when $1/\lambda_p = 5.5$, $1/\mu_p = 1.5$, achieving almost 100% efficiency in the former, see Fig. 5.2f and 5.2g). In this case, 'on' periods are easier to adapt to than short 'off' periods. Interestingly, the opposite becomes true as end-to-end delay increases. Here, we see performance start to drop beyond delays of approximately 80 ms for the link with $1/\lambda_p = 1.5$, $1/\mu_p = 5.5$, whereas for the link with $1/\lambda_p = 5.5$,$1/\mu_p = 1.5$, efficiency is unaffected by end-to-end delay (given a buffer size of 50 packets).

[1] Recall individual channels are 200 kbit/s in 12 channel models, versus 800 kbit/s in 3 channel models, and they become (un)available independently of each other.

This is due to the following. For our 12 channel link models, *when end-to-end delay is large*, it is easier to utilize an 'on' period using packets from the buffer, than it is to adapt the sending rate to even a short 'off' period. A decrease in link capacity ('off' period) will likely lead to packets being lost as the BS buffer overflows. Loss leads to (multiplicative) reductions of the congestion window, and possibly even time-outs. We can conclude that, overall, grabbing extra bandwidth is easier for TCPs (as it is actually achieved by the BS buffer) than reducing the sending rate (while maintaining high efficiency). For the 12 channel models, λ_p has a greater effect than μ_p, and when $1/\lambda_p$ is small, TCP performance suffers most.

This effect can also be clearly seen in Fig. 5.5, where the number of buffers required at the BS to achieve 95% efficiency is plotted against the delay of the wired link, e.g., Internet delay. Focusing on the TCPs that employ selective acknowledgments in Fig. 5.5a–5.5c we can see the following. For the 12 channel models, for large delays, the number of required buffers is mostly determined by the duration of the 'off' period, as the curves are grouped according to the value of λ_p. The same cannot be said of the 3 channel models. Here, λ_p and μ_p both affect TCP performance. This is due to the relatively smaller buffer, compared to the change in link capacity, which is typically 800 kbit/s for 3 channel models. The buffer does not contain sufficient packets to keep the OSA link saturated after a capacity increase, until the sender can increase its rate, whereas it does for 12 channel models. As a result, the effect of an 'on' period is not hidden, as it was in the 12 channel case.

Discussion of BS Buffer Size and End to End Delay

Fig. 5.3 shows the required buffer capacity at the BS, to achieve a given efficiency. We observe that for short delays, $\lessapprox$20 ms, all TCP flavors achieve similar, high efficiency, >95%, if 10 or more buffers are available at the BS. For these delays, a small buffer already results in maximum performance, and no significant gain in efficiency can be achieved by increasing the buffer. Not too surprisingly, very small buffers (5 packets) can still adversely affect performance. On the other hand, for increasing end-to-end delay, all TCPs can improve their performance when a larger buffer is available at the BS. In our simulations, a buffer size of 100 packets allows greater than 95% efficiency for all TCP flavors in all models.

Although buffer size can alleviate the effect of end-to-end delay, simply increasing the number of buffers at the BS will not always result in efficiency approaching 100%, though one can get close. In e.g., the 3 channel model for $1/\lambda_p = 5.5$ s and $1/\mu_p = 1.5$ s, it is clear there is a certain part of the capacity that cannot be utilized no matter how large the buffer is chosen, see Fig. 5.4, which shows the efficiency Linux' New Reno achieves (best performance of all TCPs in this case). This is also true, though to a lesser extent, for the equivalent 12 channel model.

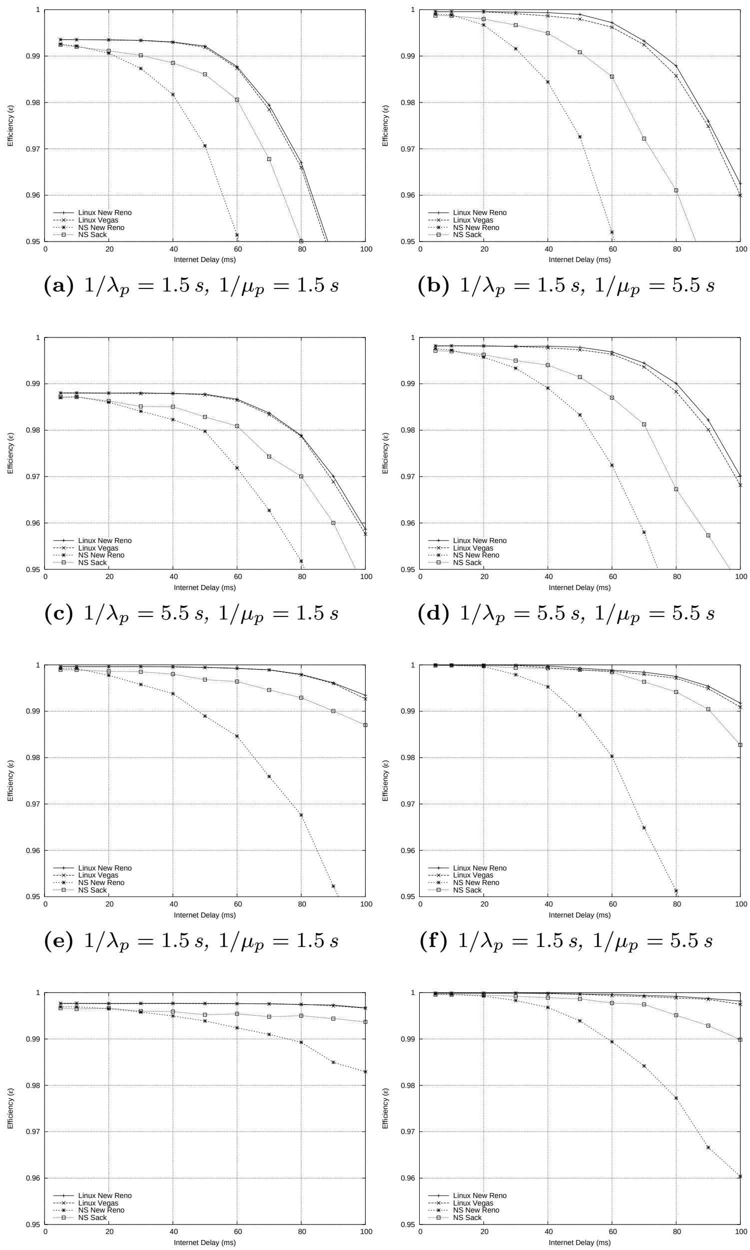

(a) $1/\lambda_p = 1.5\,s$, $1/\mu_p = 1.5\,s$

(b) $1/\lambda_p = 1.5\,s$, $1/\mu_p = 5.5\,s$

(c) $1/\lambda_p = 5.5\,s$, $1/\mu_p = 1.5\,s$

(d) $1/\lambda_p = 5.5\,s$, $1/\mu_p = 5.5\,s$

(e) $1/\lambda_p = 1.5\,s$, $1/\mu_p = 1.5\,s$

(f) $1/\lambda_p = 1.5\,s$, $1/\mu_p = 5.5\,s$

(g) $1/\lambda_p = 5.5\,s$, $1/\mu_p = 1.5\,s$

(h) $1/\lambda_p = 5.5\,s$, $1/\mu_p = 5.5\,s$

Figure 5.2: *TCP efficiency of all analyzed TCP flavors as function of wired link delay for BS buffer size of 50 packets and (a)–(d) 3 channel model, (e)–(h) 12 channel model.*

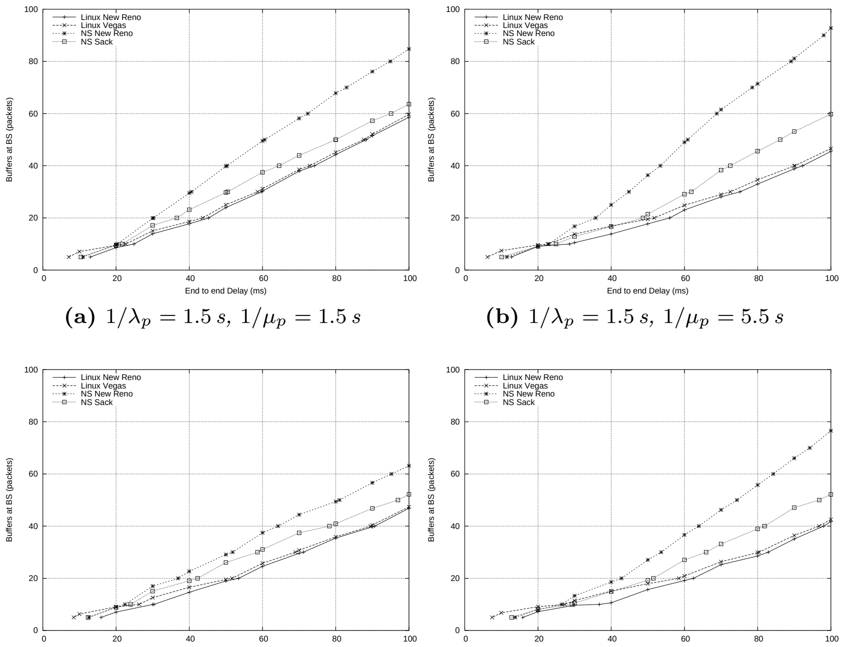

(a) $1/\lambda_p = 1.5\,s$, $1/\mu_p = 1.5\,s$ **(b)** $1/\lambda_p = 1.5\,s$, $1/\mu_p = 5.5\,s$

(c) $1/\lambda_p = 5.5\,s$, $1/\mu_p = 1.5\,s$ **(d)** $1/\lambda_p = 5.5\,s$, $1/\mu_p = 5.5\,s$

Figure 5.3: *Buffers required to achieve 95% efficiency, shown for all TCP flavors grouped per link; 3 channel model. The data points are acquired via linear interpolation of the measured data.*

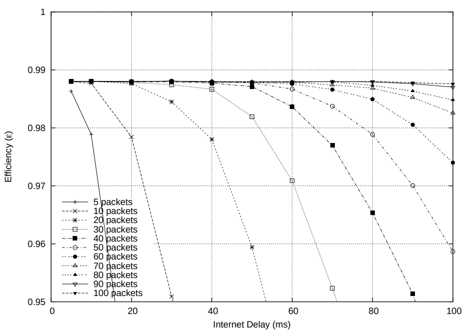

Figure 5.4: *Effect of increasing buffer size at the BS for Linux New Reno; 3 channel model with* $1/\lambda_p = 5.5\,s$, $1/\mu_p = 1.5\,s$.

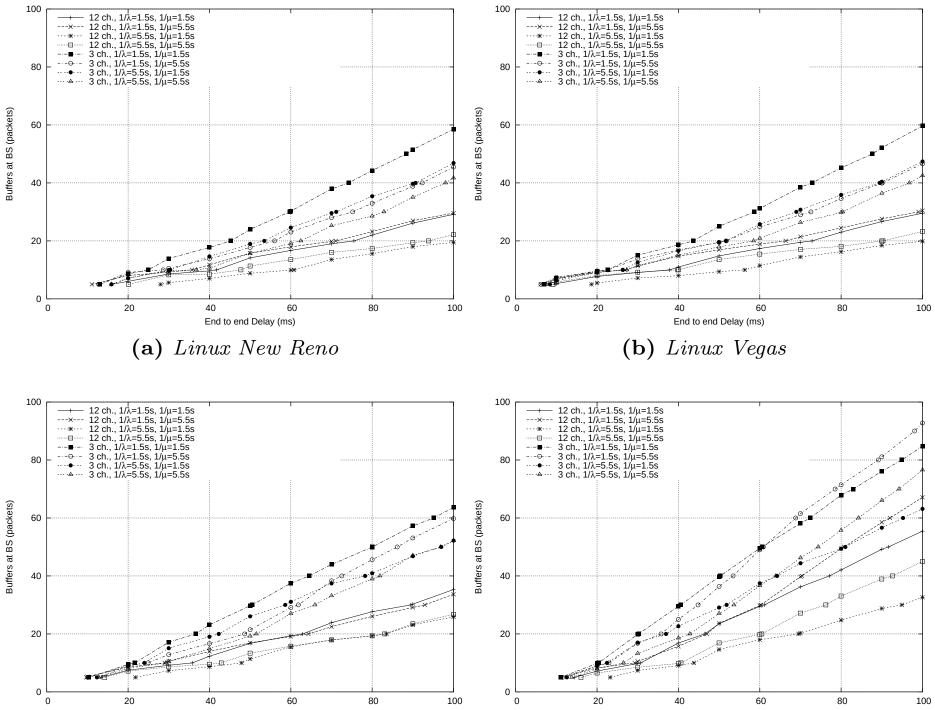

(a) *Linux New Reno* **(b)** *Linux Vegas*

(c) *NS Sack* **(d)** *NS New Reno*

Figure 5.5: *Buffers required to achieve 95% efficiency, for all models, grouped by TCP flavor. The data points are acquired via linear interpolation of the measured data.*

Discussion of TCP Flavors

Overall, Linux New Reno and Linux Vegas perform best in all models, for all delays and buffer sizes, but especially for large delays. Linux New Reno outperforms Linux Vegas for smaller buffer sizes, but their performance becomes indistinguishable as buffer size is increased beyond 50 packets, see Fig. 5.2a–Fig. 5.2d and Fig. 5.2e–Fig. 5.2h. The efficiency difference is usually no more that a few percent points. TCP Linux New Reno just beats Linux Vegas for 12 channel links, and outperforms Linux Vegas more clearly for links with 3 channels. Linux Vegas uses the default configuration parameters for Vegas, which are quite conservative. Linux Vegas may be able to grab bandwidth more aggressively, and thus perform better, if its parameters are set to more aggressive values.

It is a bit puzzling why Linux Vegas and Linux New Reno perform similarly. We would expect that (Linux) Vegas requires less buffers to achieve it's optimal performance, and would thus outperform (Linux) New Reno for small buffers and small delays. As end-to-end delay increases, we would expect the situation to change, as Vegas is unable to adapt quickly enough to changing OSA link capacity. However, as a rule, our simulations do not show this. We speculate that this is due to the Linux implementation of Vegas deviating significantly from the regular Vegas, as is indicated in the comments of the source code of Linux' Vegas, which describe more aggressive settings. We have also run simulations with NS' implementation of Vegas, which does show the expected behavior (not shown here) in some cases, but behaves erratically in others.

Comparing NS New Reno and Sack, in all 12 channel links except for the case that $1/\lambda_p = 5.5\,\mathrm{s}$, $1/\mu_p = 1.5\,\mathrm{s}$ see Fig. 5.2g, Sack outperforms New Reno by a large margin, for large delays. For $1/\lambda_p = 5.5\,\mathrm{s}$, $1/\mu_p = 1.5\,\mathrm{s}$, their performance is much closer, as New Reno's performance is quite good. A similar effect can be seen in the 3 channel models. This means that selective acknowledgments cannot improve performance in models with long 'off' and short 'on' periods as much as in the others. Selective acknowledgments especially help performance in scenarios with multiple non-consecutive losses in the same round-trip time of data. In our simulations, this occurs when link capacity suddenly drops and the buffer subsequently overflows as packets continue to arrive at the old rate, but drain at a lower (new) rate. In the case link capacity increases, it is the (number of packets in the) buffer and the rate at which a TCP can increase its sending rate that determine performance, and these are identical for New Reno and Sack.

Finally, comparing achieved efficiency of NS's TCP implementation (Sack) with the TCP-Linux ones, we see that for short end-to-end delays, NS predicts the performance quite accurately. However, for large end-to-end delays, NS does not fare so well. This is due to improvements that are in Linux' TCP implementations, but not in the NS implementations we simulated, see, e.g., [101]. These have a larger effect, e.g., when end to end delay is large and when packet loss is more frequent.

Summarizing, we have seen that both Linux New Reno and Linux Vegas perform very well for all link models, but only if a large buffer is available at the BS. We have also seen that selective acknowledgments are essential to good performance in scenarios with large end-to-end delay. All TCPs perform well for short end-to-end delays, say, under 20 ms, even for quite small buffers. From comparing TCP performance in various models, we can conclude that the average 'off' period has a much stronger effect on efficiency than the average 'on' period.

5.4 Impact of PU Detection on TCP Performance

In the previous section we have analyzed the behavior of TCP in OSA links, where we have assumed perfect detection of the PU and error-free OSA links. This assumption allowed us to focus on the impact of the duty cycle distribution on TCP. In the following section we will investigate the impact of the PU detection process on TCP throughput, assuming a noisy OSA link.

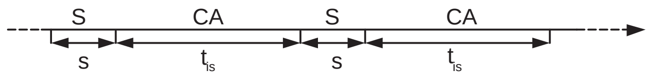

Figure 5.6: *Scanning cycles used by the SSLL. Note that the length of the channel observation (scanning) s is not negligible in comparison to the inter-scanning length t_{is}; S – scanning phase, CA – channel access phase.*

5.4.1 System Model

We have assumed earlier that the BS obtains perfect and immediate information about the availability of each PU channel in the OSA link. However, in real OSA networks, the BS, or the receiver itself, will be obliged to make a decision on the presence of the PU, based on its own radio measurements of a noisy PU channel.

In these analysis we assume that the BS performs energy detection of the PU transmitted signal, just as it was analyzed in Chapter 2. We reduce our OSA model described in Section 5.3.1 to the BS and receiver only, since detection errors will only occur on the wireless link. The detection process is logically performed by a Scanning Subsystem of the Link Layer (SSLL), described in Chapter 2. Without loss of generality, we assume that the OSA link contains only one PU channel, free from PU activity, however, the BS does not know that. Detection is performed periodically after fixed intervals, see Fig. 5.6. Specifically after the scanning phase, a period of channel observation by the SSLL, follows the channel access phase, a period of TCP packet transmission (compare this with the OSA MAC model presented in Chapter 4). The length of the scanning and channel access phase are not necessarily equal, but are the same for individual cycles. When the SSLL decides that the PU channel is free, it allows TCP packets waiting in the BS buffer to be transmitted. TCP packets are secured by a Link Layer (LL) Stop and Wait ARQ mechanism [109]. The following derivations are assumed for the TCP steady state, i.e., a long lasting TCP connection with an infinite source of data.

5.4.2 Analytical Model

If we do not take congestion related TCP packet loss into account, and assume a wireless link of infinite accessible capacity, the maximum throughput TCP can achieve depends only on the packet loss probability, segment size and RTT [110]. To get an idea of how detection errors affect TCP throughput between the BS and a receiver, we recall the simple SQRT model for estimating maximum achievable TCP throughput R_{TCP}, where

$$R_{TCP} = \frac{MSS}{RTT}\sqrt{\frac{3}{2p_{ep}}}, \tag{5.2}$$

p_{ep} is the packet error probability, MSS is the TCP segment size, and RTT is the TCP packet round-trip time. We formulate RTT in our network scenario as

$$RTT = 2t_{sr} + n_f t_{pa} N_F + s + t_w, \tag{5.3}$$

where t_{sr} denotes one-way packet delivery time (including transmission, propagation, packet queuing and processing delay), n_f is the average number of LL frame retransmissions, N_F is the number of LL frames per TCP packet, t_{pa} is the delay of the ARQ protocol, introduced by LL frame retransmissions, and finally t_w is the average delay that a packet incurs when an improper decision is made by the SSLL[2].

Each individual scanning decision may result in an error, thus limiting channel access (increasing RTT) by a multiple of the inter-scanning interval t_{is}, see Fig. 5.6. The average time a TCP packet must wait to gain access to the channel after successful detection of the PU by the SSLL can be computed as

$$t_w = \lim_{k\to\infty} \sum_{j=1}^{k} p_f^j t_{is} = \frac{t_{is} p_f}{1 - p_f}, \tag{5.4}$$

where p_f is the probability of false alarm given by (2.4). We note that although our model assumes the absence of the PU, real systems have to be designed such that a particular probability of detecting the PU on a OSA link can be achieved, limiting the probability of introducing interference to the PU system by the OSA device. The probability of detection is defined as in (2.3). From (2.3) we observe that p_d is also a function of the observation time, thus with a fixed threshold the OSA device would have to enlarge the scanning period s to gain the same detection probability, *ergo* increasing RTT.

The average number of LL frame retransmissions is given as [109]

$$n_f = (1 - p_{ef}) \sum_{i=1}^{n_{f,max}-1} i p_{ef}^i + n_{f,max} p_{ef}^{n_{f,max}}, \tag{5.5}$$

where $n_{f,max}$ is the maximum number of retransmissions of one LL frame. Finally, the packet error probability is computed as

$$p_{ep} = 1 - p_{cf}^{N_F}, \tag{5.6}$$

where p_{cf} denotes the probability of correct frame reception at LL after at most $n_{f,max}$ retransmissions. This can be written in compact form as

$$p_{cf} = (1 - p_{ef}) \sum_{i=0}^{n_{f,max}} p_{ef}^i = 1 - p_{ef}^{n_{f,max}+1}, \tag{5.7}$$

where p_{ef} denotes the LL frame error rate. Here, we assume that the probability of LL frame error is uniformly distributed over all frames.

[2]We are aware of other TCP throughput analytical models, such as [111; 112]. However, we have chosen SQRT as a simple, but sufficiently accurate model of TCP.

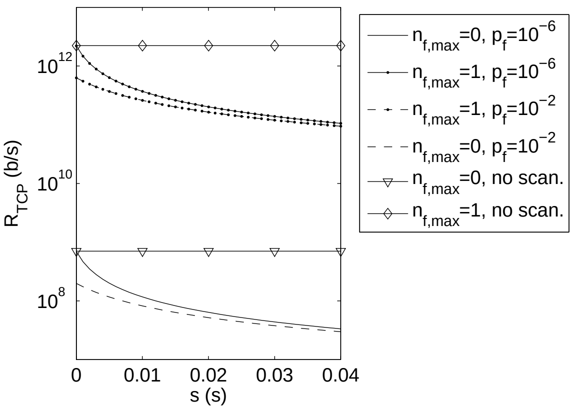

Figure 5.7: *TCP throughput as a function of scanning length. SSLL detection threshold θ is adapted to the observation period s such that the probability of false alarm is constant; input parameters: $p_{ef} = 10^{-7}$, $N_F = 2$, $W = 0.5\,MHz$, $MSS = 512\,bytes$, $t_{sr} = t_p = 10\,ms$.*

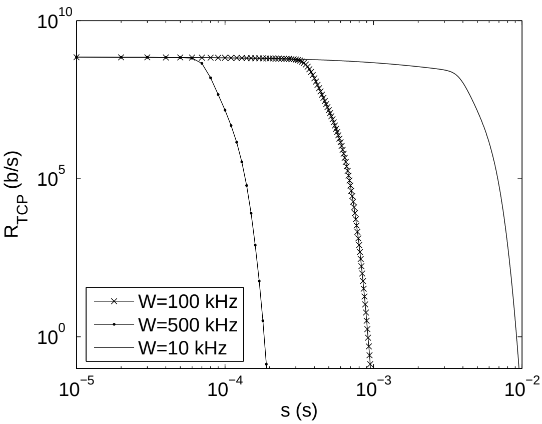

Figure 5.8: *TCP throughput as a function of scanning length; input parameters: $p_{ef} = 10^{-7}$, $N_F = 2$, $MSS = 512\,bytes$, $t_{sr} = t_p = 10\,ms$, $\theta = 40\,dBm$.*

Numerical Results

Analyzing Fig. 5.7, with the increase of the maximum number of retransmissions, the probability of packet drop decreases significantly. However for $n_{f,max} > 2$ (not shown in Fig. 5.7) we do not observe any significant gain in comparison with $n_{f,max} = 1$, which leads to the conclusion that one retransmission is enough for the OSA ARQ protocol. We also note that the impact of an incorrect detection by the SSLL on R_{TCP}, is not very significant when T_o is large, since the length of the scanning phase is the dominating component for increasing the RTT, i.e., $s \gg t_w$ in (5.3). Comparing to a situation with perfect detection and no scanning, we can easily observe the capacity decrease due to the introduction of scanning.

Fig. 5.8 plots achievable TCP throughput versus the scanning time, for a fixed SSLL detection threshold θ. With the increase of the scanning period p_f becomes higher, which directly results in a significant increase of the RTT, resulting in $p_f = 1$ and reducing throughput to zero. The increase of observation time might occur in the case when OSA node needs to preserve a high probability of detection, for a fixed threshold, particularly when the SNR of the received PU signal is small.

5.5 Chapter Summary and Discussion

In this chapter we have investigated the performance of a number of TCP flavors in an OSA environment. We can conclude that modern, real-world TCP stacks can achieve better than 95% efficiency on OSA links with widely varying characteristics, under a very wide range of network configurations, if i) a large (but not unrealistically so) buffer is available at the BS, and ii) the receiver employs Selective Acknowledgments. We have also seen that TCPs have trouble adapting to even brief reductions in capacity, if end-to-end delay is large. This implies that the probability of false alarm, a parameter of the OSA link's Primary User (PU) detection process, may have a larger effect on throughput than is apparent from our theoretical analysis of TCP's steady state behavior. Our simulations also do not account for this, as we assumed perfect detection of the PU. This remains as future work.

We have also analytically evaluated the impact of the scanning process on TCP throughput. We conclude that even for very high probability of false alarm, the maximum achievable TCP steady state throughput is not significantly affected. The scanning interval has the greatest effect, as it increases the round-trip time, which reduces achievable TCP throughput. On the other hand, it cannot be arbitrarily decreased, because it may decrease the probability of detection, for which a minimum is prescribed by the radio regulator.

Chapter 6

Conclusions

Через Річку, Через Гай

The Ukrainians, “Cherez Richku, Cherez Hai”, from the self-titled album, Cooking Vinyl Records, 1991

In this era of networking and miniaturization of the communicating devices there is no hesitation for us to say that the world will be networked sooner than later. It is a world that has shrunken by humongous amount of networked devices. Where will all those devices are placed in the communication spectrum? The only *mantra* is to reuse and reuse and reuse the spectrum — in time and space. OSA is a tiny part in this direction; of course we claim it to be the right direction. Let us see how best we have done our duty and what our contribution to this task at hand is.

First let us recapitulate the work presented so far. Given the importance of the OSA, as sketched in Chapter 1, many research topics have been identified that were of utmost importance to the successful deployment of the OSA networks. In the beginning we have found that protocol-related issues of OSA, especially for Layer 2 and 4 of the OSI Reference Model were least explored and somehow lagging behind those related to the physical layer. While understanding the importance of protocol design for OSA was primary concern, the aim of this thesis was also to explore certain performance aspects of the protocols for OSA networks and to design them in a most efficient way.

Particularly, the focus of this thesis was on the design of efficient MAC protocols for OSA networks taking into account physical layer characteristics of OSA operation. Moreover, given the operation of the proposed OSA MAC protocol, we wanted to answer how the properties of a OSA link affect the operation of contemporary TCP implementations. We know that TCP is the *de facto* transport layer protocol used in the Internet.

The goal of the thesis was somewhat ambitious and we believe that we achieved it. We drew many important conclusions while executing the work as part of this thesis and through the results achieved. We will now summarize them in Section 6.1. Later we will elaborate on the directions for future research in the area of OSA protocol design and performance evaluation in Section 6.2.

6.1 Summary of the Results

This thesis has been structured in three major parts, each one addressing the specific research topic. They are:

1. *Physical layer properties of OSA transmission*, (Chapter 2) particularly addressing the spectrum sensing;
2. *Layer 2 OSI Reference Model protocol design*, (Chapter 3 and 4), addressing the general OSA network and, OSA MAC performance and its implications;
3. *Layer 4 OSI Reference Model protocol design*, (Chapter 5) addressing the TCP performance associated with the design of OSA MAC and OSA physical layer properties.

Each of the above is a complete and independent work under the general assumptions and scenarios considered. The conclusions we derive from these three important parts have been presented here. Most important conclusions are given in the boxes.

6.1.1 Physical Layer Properties of OSA Transmission

One may notice that we have taken a bottom-up research approach in this thesis so as to explore protocol issues of OSA. We focused on the physical properties of OSA networks and in particular the detection process of the PU. In the early stages of this work it was known that reliable PU detection is a difficult task for each OSA node individually. Therefore a cooperative PU detection process has been investigated.

To mitigate the consequence of destructive propagation effects on the reliability of the PU detection, nodes in the OSA, networks should cooperate and fuse their measurement results cooperatively as much as possible and whenever it is possible.

In parallel to the physical layer work we have performed a detailed investigation of system design of OSA networks. We have anchored our system design on the structure of future emergency networks and we have observed, specifically, the following.

Structure of future emergency networks allows us to implement cooperative spectrum sensing.

Knowing that cooperation is the only solution for robust spectrum sensing our aim was to design a simple cooperative PU detection system that outperforms other existing fusion methods available in the literature. Our contribution lies in proposing a novel fusion detection technique, based on log-likelihood combining. It has been compared for different scenarios with other known cooperative detection techniques, which led to an important conclusion.

Log-likelihood combining outperforms all existing weighted measurement combining methods, especially in the low SNR region and low number of nodes in the OSA network.

In parallel to the work on pure physical layer properties of PU detection, we have analyzed how scheduling of measurements amongst OSA network nodes should be performed such that most of the time free channel should be brought forth by the detection process and in turn utilized by OSA network. We have analyzed two essential approaches, i.e., random and fixed (round robin) scheduling. We have found the following.

Random scheduled spectrum sensing requests achieve asymptotically the same performance as the round robin scheduler, with the increase in number of sensing nodes or with the decrease in inter-scanning (non-observable) period.

Our final contribution is the implementation of the analyzed cooperative spectrum sensing techniques. Unlike the many reported research work found in the literature on the PU detection, we implemented one of the well known cooperative PU detection techniques.

We have demonstrated that cooperative spectrum sensing can be implemented using commercial off the shelf equipment.

6.1.2 OSA MAC Performance and Design

After understanding the effects of radio layer and the general behaviour of the OSA link, we approached the design and performance evaluation of OSA networks in general and the OSA MAC protocols in particular. First we wanted to know how the general behaviour of the PU, i.e., its temporal and generally random activity, affects the throughput of the OSA network. The first step was to analyze different channel access strategies based on the activity levels of the PUs and compute the OSA network blocking probability. We specifically found the following.

In MAC for OSA networks channel access based on the channel occupancy statistics achieves much higher performance than with the random channel access strategies. The improvement is particularly visible when there is disparity in channel utilization by PUs or when higher number of the PU channels are available.

However, due to the complexity of the analysis we were able to assess the OSA network performance in complex network setups, i.e., involving many nodes and many PU channels, only through simulations. Summarizing,

Implementing non-uniform channel utilization and smart channel access policies in the Markov analysis of OSA networks, and assessing the blocking probability or throughput are very involved, since the transition probability matrix has to be constructed individually for a given number of channels.

After understanding the impact of intelligent channel access strategies we proceeded with designing the first OSA multichannel MAC protocol. Apart from implementing smart channel access strategies, that have been analyzed earlier, in this design we have defined a novel co-existence metric for OSA network based on level of packet collision with the PUs. Our contribution here is characterized as follows.

Interference constraints in OSA channel access can also be defined on a packet level basis. Such approach greatly simplifies OSA MAC design.

Further, we have tried to incorporate some of the functionalities of packet communication implicating from the physical layer, e.g., packet capture, in the protocol design. We have observed the following relation.

Packet capture, i.e., throughput increase by utilizing constructive propagation effects has far less impact on the OSA network throughput than adding more PU channels to the OSA network. This makes the OSA node deign simpler.

In the next step, to understand some of the issues related to OSA MAC operation we have performed extensive analyses of all possible implementations of multichannel OSA MACs. In the initial stages of research we have found that most popular implementation is based on dedicated control channel (DCC). During the course of this research work we were led to interesting observations. They are listed here.

DCC MAC performs worse than other known multichannel MACs like MRCC. Further, DCC and HCC perform differently depending on the network setup. Finally, all classes of OSA MACs scale down linearly with the increase in PU channel activity.

We have noted above that one of the contributions of this thesis was to propose a novel interference metric induced by OSA network to PUs, based on packet collision level. We have evaluated all OSA MACs from this perspective as well.

Hopping based OSA MACs reduce the probability of interference with the PU.

Moreover, we have tested the relation between PU detection quality and protocol performance. It was important, since high quality spectrum sensing, referred to in this thesis as QoD, is usually obtained by increased PU channel observation time.

Sensing time should be strictly optimized to result in the highest network throughput, since delay introduced by long sensing time (increasing probability of false alarm), introduces high network delay.

6.1.3 TCP over OSA Links Performance

Finally, using the foundation on OSA MAC through research results the thesis focused on the performance of the protocols of the higher layers and in particular Layer 4 of the OSI Reference model. By performing extensive and detailed simulations that took into account real life OSA link behaviour, we were able to draw some important conclusions on the performance of TCP protocol.

The first question which we wanted to answer was how much capacity any TCP implementation can actually obtain in the OSA setup. Since the OSA MAC protocols cannot regulate the capacity an OSA link can offer, it was imperative to see how TCP deals with varying capacity OSA link. With a metric for the TCP efficiency proposed in this thesis we have found the following.

All modern implementations of TCP with ACK utilize most of the capacity, i.e., not less than 95%, of the OSA link when a reasonable buffer size at the BS is available.

Another important conclusion that we were able to draw was related to the impact of physical layer on the performance of the TCPs. Knowing the importance of spectrum sensing in OSA context we have shown the following.

Delay induced by scanning has far more impact on the TCP throughput than OSA link errors.

Finally, we have shown that for a TCP in steady state, increasing observation time to improve PU detection results in rapid throughput degradation of TCP performance beyond a certain point.

6.2 Directions for Future Work

In the light of the results presented above we can strongly say that efficient and QoS-enabled communication in the OSA context can indeed be achieved. However, we strongly feel that the results presented here are just a small fraction of the results for OSA networking and protocol design that needs to be solved. The solutions proposed here are too small compared to the amount of problems that are still holding up the deployment of OSA networks. It is not enough to understand deeply OSA networks operation on the protocol level. We will now outline some of the issues worth investigating.

In case of PU detection, it has been assumed for simplicity that a central entity performs measurement combining. Although such assumption is the most straightforward and easiest to implement, more robust methods like distributed measurement combining might be considered. That is, nodes would share information on the results of the measurements and converge to the common measurement result such that there is no need for referring to a single point of contact.

OSA MAC analysis leaves many open research issues as well. In this thesis multichannel protocol classes have been compared. Based on these analyses some conclusions have been drawn, i.e., MRCC is the best multichannel OSA MAC comparing with other OSA MAC classes. As a logical next step would be important to implement MRCC and compare its operation with the general results obtained in this thesis. Further, all results have been obtained in the case of one hop communication only. Therefore, it would be indeed interesting to observe the operation of any of the OSA multichannel MACs in the multihop scenario. Also, broadcasting properties of MRCC need to be improved, since at this moment sending packets to multiple terminals at the same time is difficult.

In case of TCP performance investigation in the OSA networks, we have limited ourselves to the network setup consisting of one sender-receiver pair, where sender communicated with the receiver connected in turn connected to the BS. Therefore more general OSA network models are needed, i.e., with more receiving nodes connected to the same BS. Analyses of fairness, where multiple nodes compete for the same OSA link are also needed.

Appendix A

Spectrum Occupancy Measurements

To get some insights into channel activity pattern of the PUs we performed measurements independently of the ones already been available in the literature [24; 113–115]. What we were particularly interested in is the dynamics of PU activity.

To measure the channel occupancy statistics we have set up the following experiment. A Rhode&Schwartz ESPI07 spectrum analyzer (SA) was connected through the Ethernet port to a PC, on which Matlab 7.0 was used as an interface with the SA. Simultaneously, the SA was connected with a 400 MHz band cross-dipole antenna through a ZX60-3018G power amplifier. The antenna was placed on the roof of the 11th floor building of the University of Twente's Electrical Engineering department. The entire measurement was performed on March 13 2007, between 11 AM and 8 PM.

First we have observed coarsely a wide range of channels for user activity to be able to choose a group channels for a close watch and to analyze it later in detail. The frequencies we have chosen to measure are listed in Table A.1. According to the Agentschap Telecom's (a Dutch Radio regulator) radio frequency plan, the first four bands were mobile communication channels. In the last band we have spanned a wide range of frequencies—all of them assigned to a different type of mobile communication. We refer the reader to to [116] for more details. After selecting the frequency ranges, each of them were divided into frequency bins with a bandwidth resolution (BR) of 1 kHz except for the last one, which had 100 kHz BR. Also, each measurement had 10000 samples of data, where the inter-sample period (ISP) was between 120 and 145 ms, see Table A.1 for details. This corresponds to approximately 24 minutes of observation for each frequency bin. One measurement sample represents the average signal power observed in one ISP.

Table A.1: *Measured Frequency Ranges with the Respective Inter-sample Period (ISP) and Bandwidth Resolution (BR).*

Frequency range [MHz]	ISP [ms]	BR [kHz]
[446,04; 446.05]	145	1
[446,05; 446,06]	144	1
[446,075; 446,085]	113	1
[446,065; 446,075]	143	1
[459.62; 467,82]	120	100

Table A.2: *Results of the PU Channel Observations in the Considered Frequency Range.*

Feature	Value
Mean channel utilization	6.8%
Always busy bins	1.7%
Always free bins	15.7%
Bins with PU duty cycles	82.6%
Mean number of busy bins in a slot	21.1%
Standard deviation of busy bins in a slot	2.3%
Number of free bins (Max)	85%
Number of free bins (Min)	16.6%
Average 'on' time	4.3 s
Average 'off' time	58.9 s

The estimated noise floor for 1 kHz BR was $N_0 = -115\,\text{dBm}$ and $N_0 = -90\,\text{dBm}$ for 100 kHz BR.

Before proceeding with the analysis of the measured data, we have filtered all measurements with a moving average filter with window of 5 to reduce the impact of noise on the analyzed data. The filter size has been chosen experimentally to represent the optimal relation between noise filtering and possible information loss. For each frequency bin in the measured ranges we have extracted periods of signal activity (known as the 'on' period) and non-activity (known as the 'off' period). As an activity threshold we have chosen a value of $\theta_f = N_0 + 10\,\text{dBm}$ to account for additional signal fluctuations.

The first question related to PU activity patterns is to determine or define when a PU is considered to be present. Our measurement indicated that only 1.7% of the frequency bins were busy the all the time, and hence could not be used by SUs at all. Also, 15.7% of all the observed frequency bins was free during the whole observation time. Therefore, the remaining 82.6% of all the frequency bins showed 'on' and 'off' patterns. The average 'on' time was 4.3 s which is relatively short in the context of OSA since claiming and freeing spectrum is typically considered to operate at a slower pace. Therefore, when a SU cannot time-share a frequency bin with a PU, it can only achieve a spectrum utilization of 15.7%. A striking fact

Table A.3: *Percentage of occurrence of given value (top part) and average values of distributions' parameters (bottom part) given in seconds; λ, σ, a, b, k are the parameter symbols of the respective distributions.*

	$\alpha = 0.05$		$\alpha = 0.1$	
	'on'	'off'	'on'	'off'
No activity	57,2%	39,6%	58,7%	41,68%
Unknown	42,5%	31,2%	41%	31,5%
Exponential	0,17%	23,4%	0,13%	20,3%
Rayleigh	—	1,5%	—	1,2%
Uniform	0,04%	4,2%	0,08%	4,8%
Weibul	—	0,04%	—	—
No activity	—	—	—	—
Unkown	—	—	—	—
Exponential	λ = 15,18	λ = 21,58	λ = 18,61	λ = 22,95
Rayleigh	—	σ=4,95	—	σ=16,01
Uniform	a=0,12 b=53,76	a=0,13 b=153	a=0,12 b=88,92	a=0,15 b=156,6
Weibul	—	λ=5,7 k=0,13	—	—

is that the total channel utilization of the measured frequency range during whole observation time was only 6.8%. So, when time-sharing is possible, the SUs can achieve a utilization of 93.2%, which is a significant improvement compared to 15.7%, compared to the case where always free frequency bins are considered. The average number of busy bins was 21.1% (of the total measured frequency range), with a standard deviation of 2.3%. The minimum and the maximum number of free bins in a frequency pool shows that between two consecutive measurements, variation in available frequencies can be large. Also, interestingly, the average 'on' time is much smaller than the average 'off' time, which means that the channel vacated by PU can stay free for a considerable amount of time.

As a next step, having vectors of 'on' and 'off' values we have performed a set of Kolmogorov-Smirnov tests to determine which continuous distribution fits the obtained data the best. Our tests involved Exponential, Log-Normal, Gamma, Normal, Rayleigh, Uniform and Weilbull distributions (we note that some distributions might also be of interest like Erlang, hyper-Erlang and mixed distributions [117], however we have decided to focus on the most common ones). For statistical significance, we have not taken into account vectors that contained less than 30 elements. Our tests were performed for two significant level values of $\alpha = \{0.1, 0.05\}$. Parameters of tested distributions were obtained using Maximum Likelihood Estimation. The preliminary results for one frequency range are given in Table A.3.

Although we have measured only a small piece of the whole radio spectrum this result already gives some significant insights on what to expect from the PU traffic properties. First, the majority of the traces had no identified type of distribution. Secondly, the exponential distribution, usually assumed in the analysis of OSA MACs, has only a reflection in a handful of the identified activities. Also, we can see that for the used exponential distribution, individual idle times are pretty large. This means that the channel once determined to be idle will remain idle with a high probability.

Appendix B

Optimal Channel Access

Lemma 1. *Channel access procedure in multichannel multiaccess protocols based on the arrival rates of the PU minimizes collision probability, in contrast with (random) uniform channel selection.*

Proof. First we introduce the term $\mathcal{M} \triangleq \sum_{i=1}^{M} p_{\mathbf{A},i}\ p_i$ where $p_{\mathbf{A},i}$ is the observed probability of choosing a channel i by OSA network using channel access procedure of type $\mathbf{A}$, and p_i is the probability of a PU user arriving on channel i.

Knowing $p_{b,m}$ for each PU on its channel m, one can express the normalized channel arrival probability for each PU as $\rho_m = \frac{p_{b,m}}{\sum_{i=1}^{M} p_{b,i}}$, and $\sum_{i=1}^{M} \rho_i = 1$. Let us take $\rho_1 \leq \ldots \leq \rho_M$, and analyze two access schemes here. In the *random* access scheme, $\mathbf{A} := \mathbf{RND}$ the OSA user chooses each channel uniformly randomly with probability $p_{\mathbf{RND},i} = 1/M$. In the *Least Used First* scheme[1], $\mathbf{A} := \mathbf{LeU}$, OSA user chooses each channel with probability $p_{\mathbf{LeU},i} = \frac{1-p_m}{\sum_{i=1}^{M} 1-p_i} = \tilde{\rho}_i$, $\sum_{i=1}^{M} \tilde{\rho}_i = 1$, such that $\tilde{\rho}_1 \geq \ldots \geq \tilde{\rho}_M$. Therefore, we only need to prove using $\mathcal{M}$ that

$$\sum_{i=1}^{M} \tilde{\rho}_i \rho_i \leq \frac{1}{M} \sum_{i=1}^{M} \rho_i. \tag{A.1}$$

Using Chebyshev's sum inequality [119]

$$n \sum_{i=1}^{n} a_i b_i \leq \left(\sum_{i=1}^{n} a_i \right) \left(\sum_{i=1}^{n} b_i \right) \tag{A.2}$$

for $a_1 \leq \ldots \leq a_n$ and $b_1 \geq \ldots \geq b_n$ replacing $n = M$, $b_i = \rho_i$ and $a_i = \tilde{\rho}_i$ we get (A.1). $\square$

[1] This algorithm is similar to the channel assignment scheme proposed for optical switches in All-Optical Networks [118].

We note that while $\rho_i \to 1/M$ or $M \to \infty$, gain from introducing access schemes for OSA network based on PU activity is negligible, in comparison to random access scheme.

Bibliography

[1] P. Hansell, S. Kirtay, I. Inglis, J. Pahl, and S. Munday, “Evaluating spectrum percentage occupancy in licence-exempt allocations,” Office of Communications,” Tech. Rep. 1606/LEM/R/3, July 7, 2007. [Online]. Available: http://morse.colorado.edu/~tlen5520/ho/OfcomSpecOcc.pdf

[2] E. Noam, “Taking the next step beyond spectrum auctions: Open spectrum access,” *IEEE Commun. Mag.*, vol. 33, no. 12, pp. 66–73, Dec. 1995.

[3] C. Jackson, “Dynamic sharing of radio spectrum: A brief history,” in *Proc. IEEE DySPAN’05*, Baltimore, MA, Nov. 8–11, 2005.

[4] J. Mitola III, “Cognitive radio for flexible mobile multimedia communications,” in *Proc. IEEE MOMUC’99*, San Diego, CA, Nov. 15–17, 1999.

[5] R. Thomas, L. DaSilva, and A. MacKenzie, “Cognitive networks,” in *Proc. IEEE DySPAN’05*, Baltimore, MA, Nov. 8–11, 2005.

[6] J. Mitola III and G. Q. Maguire, Jr., “Cognitive radio: Making software radios more personal,” *IEEE Personal Commun. Mag.*, vol. 6, no. 4, pp. 13–18, Aug. 1999.

[7] J. Mitola III, “Cognitive radio: An integrated agent architecture for software defined radio,” PhD Dissertation, Royal Institute of Technology, Stockholm, Sweden, May 2000. [Online]. Available: http://www.it.kth.se/~jmitola/Mitola_Dissertation8_Integrated.pdf

[8] S. Haykin, “Cognitive radio: Brain-empowered wireless communnications,” *IEEE J. Select. Areas Commun.*, vol. 23, no. 2, pp. 201–220, Feb. 2005.

[9] R. V. Prasad, P. Pawełczak, J. Hoffmeyer, and S. Berger, “Cognitive functionality in next generation wireless networks: Standardization efforts,” *IEEE Commun. Mag.*, vol. 46, no. 4, pp. 72–78, Apr. 2008.

[10] N. Devroye, P. Mitran, and V. Tarokh, "Limits on communication in a cognitive radio channel," *IEEE Commun. Mag.*, vol. 44, no. 6, pp. 44–49, June 2006.

[11] P. G. Cook and W. Bonser, "Architectural overview of the SPEAKeasy system," *IEEE J. Select. Areas Commun.*, vol. 17, no. 4, pp. 650–661, Apr. 1999.

[12] J. Place, D. Kerr, and D. Schaefer, "Joint tactical radio system," in *Proc. MILCOM'00*, Los Angeles, CA, Oct. 22–25, 2000.

[13] M. McHenry, E. Livsics, T. Nguyen, and N. Majumdar, "XG dynamic spectrum access field test results," *IEEE Commun. Mag.*, vol. 45, no. 6, pp. 51–57, June 2007.

[14] P. Camana, "Integrated communications, navigation, identification avionics (ICNIA) – the next generation," *IEEE Aerosp. Electron. Syst. Mag*, vol. 3, no. 8, pp. 23–26, Aug. 1988.

[15] J. Hoffmeyer, D. Stewart, S. Berger, B. Eydt, F. Frantz, F. Granelli, K. Kontson, D. Murotake, K. Nolan, P. Pawełczak, R. V. Prasad, R. Roy, M. Scoville, D. Sicker, D. Swain, and P. Tenhula, "Definitions and concepts for dynamic spectrum access: Terminology relating to emerging wireless networks, system functionality, and spectrum management," IEEE Standards Activities Department," 1900.1-2008 Standard, Oct. 2, 2008.

[16] Q. Zhao and B. M. Sadler, "A survey of dynamic spectrum access: Signal processing, networking, and regulatory policy," *IEEE Signal Processing Mag.*, vol. 24, no. 3, pp. 79–89, May 2007.

[17] S. Pollin, "Coexistence and dynamic sharing in cognitive radio networks," in *Cognitive Wireless Communication Networks*, E. Hossain and V. K. Bhargava, Eds. New York, NY: Springer, 2007.

[18] V. Kawada and P. Kumar, "A cautionary perspective on cross-layer design," *IEEE Wireless Commun. Mag.*, vol. 12, no. 1, pp. 3–11, Feb. 2005.

[19] D. Kliazovich, M. Devetsikiotis, and F. Granelli, "Formal methods in cross layer modeling and optimization of wirelesss networks: State of the art and future directions," in *Heterogeneous Next Generation Networking: Innovations And Platform*, S. Kotsopoulos and K. Ioannou, Eds. Idea Group Inc., 2008, in press.

[20] C. N. Mathur and K. Subbalakshmi, "Digital signatures for centralized DSA networks," in *Proc. First IEEE Workshop on Cognitive Radio Networks (IEEE CCNC 2007 Workshop)*, Las Vegas, NE, Jan. 11, 2007.

[21] R. Chen, J.-M. Park, and J. H. Reed, "Defense against primary user emulation attacks in cognitive radio networks," *IEEE J. Select. Areas Commun.*, vol. 26, no. 1, pp. 25–37, Jan. 2008.

[22] C. Nanjunda and K. Subbalakshmi, "Cognitive networks: Towards self-aware networks," in *Security Issues in Cognitive Networks*, Q. H. Mahmoud, Ed. New York, USA: Wiley, 2007.

[23] P. Pawełczak, R. V. Prasad, L. Xia, and I. Niemegeers, "Cognitive radio emergency networks — requirements and design," in *Proc. IEEE DySPAN'05*, Baltimore, MA, Nov. 8–11, 2005.

[24] M. McHenry, "NSF spectrum occupancy measurements project summary," Shared Spectrum Company, Vienna, VA, Tech. Rep., August 2005. [Online]. Available: http://www.sharedspectrum.com/?section=measurements

[25] C2000 network homepage (in Dutch). [Online]. Available: http://www.c2000.nl

[26] "Service specification group services and applications," Mobile Broadband for Emergency and Safety Applications Project, Statement of Requirements TS 70.001 V3.11, Oct. 2000. [Online]. Available: http://www.projectmesa.org/ftp/Specifications/MESA_70.001_v3.1.1_SoR.doc

[27] Safecom program homepage. [Online]. Available: http://www.safecomprogram.gov

[28] F. R. Wentland, "Summary of public outreach efforts concerning state and local public safety spectrum management policies and procedures," Public Safety Wireless Advisory Commitee, Tech. Rep., May 2004. [Online]. Available: http://ntiacsd.ntia.doc.gov/pubsafe/documents/finalpsreport.pdf

[29] Wireless deployable network system homepage. [Online]. Available: http://www.widens.org

[30] T. Yucek and H. Arslan, "A survey of spectrum sensing algorithms for cognitive radio applications," *IEEE Commun. Surv. and Tut.*, Apr. 2007, accepted for publication.

[31] R. Tandra and A. Sahai, "Fundamental limits on detection in low SNR under noise uncertainty," in *Proc. WIRELESSCOM'05*, Maui, HI, June 13–16, 2005.

[32] H. Urkowitz, "Energy detection of unknown deterministic signals," *Proc. IEEE*, vol. 55, no. 4, pp. 523–531, Apr. 1967.

[33] F. F. Digham, M.-S. Alouini, and M. K. Simon, "On the energy detection of unknown signals over fading channels," in *Proc. IEEE ICC'03*, Anchorage, AK, May 11–15, 2003.

[34] ——, "On the energy detection of unknown signals over fading channels," *IEEE Trans. Commun.*, vol. 55, no. 1, pp. 21–24, Jan. 2007.

[35] T. S. Rappaport, *Wireless Communications: Principles and Practice.* Upper Saddle River, NJ, USA: Prentice Hall, 2002.

[36] D. Cabrić, A. Tkachenko, and R. W. Brodersen, "Spectrum sensing measurements of pilot, energy, and collaborative detection," in *Proc. IEEE MILCOM'06*, Washington, DC, Oct. 23–25, 2006.

[37] W. Wang, L. Wang, W. Zou, and Z. Zhou, "On the distributed cooperative spectrum sensing for cognitive radio," in *Proc. IEEE ISCIT'07*, Sydney, Australia, Oct. 16–19, 2007.

[38] R. Viswanathan and P. K. Varshney, "Distributed detection with multiple sensors: Part I—fundamentals," *Proc. IEEE*, vol. 85, no. 1, pp. 54–63, Jan. 1997.

[39] A. Ghasemi and E. S. Sousa, "Collaborative spectrum sensing for opportunistic access in fading environments," in *Proc. IEEE DySPAN'05*, Baltimore, MA, Nov. 8–11, 2005.

[40] E. Visotsky, S. Kuffner, and R. Peterson, "On collaborative detection of TV transmissions in support of dynamic spectrum sharing," in *Proc. IEEE DySPAN'05*, Baltimore, MA, Nov. 8–11, 2005.

[41] P. K. Varshney, *Distributed Detection and Data Fusion.* New York: Springer-Verlag, 1996.

[42] P. Pawełczak, R. V. Prasad, H. Nikookar, and I. Niemegeers, "Performance analysis of periodical spectrum sensing for dynamic spectrum access networks," in *Proc. AWIN'05 (IEEE GLOBECOM'05 Workshop)*, St. Louis, Mo, Nov. 28 – Dec. 2, 2005.

[43] P. Pawełczak, C. Guo, R. V. Prasad, and R. Hekmat, "Cluster-based spectrum sensing architecture for opportunistic spectrum access networks," Delft University of Technology, Tech. Rep. IRCTR-S-004-07, Feb.12, 2006. [Online]. Available: http://dutetvg.et.tudelft.nl/~przemyslawp/files/osa_arch.pdf

[44] M. P. Olivieri, G. Barnett, A. Lackpour, A. Davis, and P. Ngo, "A scalable dynamic spectrum allocation system with interference mitigation for teams of spectrally agile software defined radios," in *Proc. IEEE DySPAN'05*, Baltimore, MA, Nov. 8–11, 2005.

[45] N. C. Beaulieu and Q. Xie, "An optimal lognormal approximations to lognormal sum distributions," *IEEE Trans. Veh. Technol.*, vol. 53, no. 2, pp. 479–489, Mar. 2004.

[46] F. Hoeksema, M. Heskamp, R. Schiphorst, and K. Slump, "A node architecture for disaster relief networking," in *Proc. IEEE DySPAN'05*, Baltimore, MA, Nov. 8–11, 2005.

[47] D. Bertsekas and R. Gallager, *Data Networks.* Upper Saddle River, NJ, USA: Prentice Hall, 1992.

[48] S. B. Raghunathan, M. van den Oever, R. Doost-Mohammady, P. Pawełczak, I. Budiarjo, M. Heskamp, Q. Zhang, A. Kokkeler, H. Nikookar, Z. Qin, R. Hekmat, and L. P. Lighart, "Dynamic spectrum access AAF platform," Chicago, IL, USA, 2008, IEEE DySPAN'08 Demonstration Session.

[49] Innovative Integration P25M Memo. [Online]. Available: http://www.innovativedsp.com/products/p25m.htm

[50] I. Budiarjo, "Adaptive baseband processing for cognitive radio," PhD Dissertation, Delft University of Technology, Delft, the Netherlands, May 2009.

[51] Universal Software Radio Peripheral Home Page. [Online]. Available: http://www.ettus.com

[52] C. Cordeiro, D. Cavalcanti, and S. Nandagopalan, "Cognitive radio for broadband wireless access in TV bands: The IEEE 802.22 standard," in *Cognitive Radio Communications and Networks: Principles and Practice*, A. M. Wyglinski, M. Nekovee, and Y. T. Hou, Eds. Amsterdam, The Netherlands: Elsevier, Inc., 2010, to be published.

[53] *Draft Standard for Wireless Regional Area Networks Part 22: Cognitive Wireless RAN Medium Access Control (MAC) and Physical Layer (PHY) Specifications: Policies and Procedures for Operation in the TV Bands*, IEEE Std. P802.22 Draft 1.3, Nov. 2008.

[54] J. C. Arnbak and W. van Blitterswijk, "Capacity of slotted aloha in Rayleigh-fading channels," *IEEE J. Select. Areas Commun.*, vol. 5, no. 2, pp. 261–269, Feb. 1987.

[55] Q. Zhao, L. Tong, and A. Swami, "Decentralized cognitive MAC for dynamic spectrum access," in *Proc. IEEE DySPAN'05*, Baltimore, MA, Nov. 8–11, 2005.

[56] Y.-J. Choi, S. Park, and S. Bahk, "Multichannel random access in OFDMA wireless networks," *IEEE J. Select. Areas Commun.*, vol. 24, no. 3, pp. 603–613, Mar. 2006.

[57] L. Zhou, Y.-D. Yao, H. Heffes, and R. Zhang, "Investigation of slotted ALOHA under Nakagami fading with synchronized and asynchronous cochannel cells," *IEEE Trans. Wireless Commun.*, vol. 52, no. 6, pp. 1462–1651, Jan. 2004.

[58] D. Dardari, V. Tralli, and R. Verdone, "On the capacity of slotted aloha with rayleigh fading: The role played by the number of interfereres," *IEEE Commun. Lett.*, vol. 4, no. 5, pp. 155–157, May 2000.

[59] S. Sankaranarayanan, P. Papadimitratos, and A. Mishra, "A bandwidth sharing approach to improve licensed spectrum utilization," *IEEE Commun. Mag.*, vol. 43, no. 12, pp. S10–S14, Dec. 2005.

[60] J. Mo, H.-S. W. So, and J. Walrand, "Comparison of multi-channel MAC protocols," *IEEE Trans. Mobile Comput.*, vol. 7, no. 1, pp. 50–65, Jan. 2008.

[61] C.-T. Chou, S. Shankar N, H. Kim, and K. G. Shin, "What and how much to gain by spectrum agility?" *IEEE J. Select. Areas Commun.*, vol. 25, no. 3, pp. 576–588, Apr. 2007.

[62] Y. Xing, R. Chandramouli, S. Mangold, and S. Shankar N, "Dynamic spectrum access in open spectrum wireless networks," *IEEE J. Select. Areas Commun.*, vol. 24, no. 3, pp. 626–637, Mar. 2006.

[63] S.-L. Wu, C.-Y. Lin, Y.-C. Tseng, and J.-L. Sheu, "A new multi-channel mac protocol with on-demand channel assignment for multi-hop mobile ad hoc networks," in *Proc. IEEE I-SPAN'00*, Dallas, TX, USA, Dec.7–9, 2000.

[64] P. Pawełczak, S. Pollin, H.-S. W. So, A. Motamedi, A. Bahai, R. V. Prasad, and R. Hekmat, "State of the art in opportunistic spectrum access MAC design: Research challenges," in *Proc. ICST/IEEE CrownCom'08*, Singapore, May 15-17, 2008.

[65] P. Pawełczak, S. Pollin, H.-S. W. So, A. Bahai, R. V. Prasad, and R. Hekmat, "Quality of service of opportunistic spectrum access: A medium access control approach," *IEEE Wireless Commun. Mag.*, vol. 15, no. 5, pp. 20–29, Oct. 2008.

[66] L. Ma, X. Han, and C.-C. Shen, "Dynamic open spectrum sharing MAC protocol for wireless ad hoc networks," in *Proc. IEEE DySPAN'05*, Baltimore, MA, Nov. 8–11, 2005.

[67] H. Su and X. Zhang, "Cross-layer based opportunistic MAC protocols for QoS provisioning over cognitive radio wireless networks," *IEEE J. Select. Areas Commun.*, vol. 26, no. 1, pp. 118–129, Jan. 2008.

[68] A. Motamedi and A. Bahai, "MAC protocol design for spectrum-agile wireless networks: Stochastic control approach," in *Proc. IEEE DySPAN'07*, Dublin, Ireland, Apr. 17–20, 2007.

[69] A. C.-C. Hsu, D. S. L. Wei, and C.-C. J. Kuo, “A cognitive MAC protocol using statistical channel allocation for wireless ad-hoc networks,” in *Proc. IEEE WCNC’07*, Hong Kong, Mar. 11–15, 2007.

[70] H. Nan, T.-I. Hyon, and S.-J. Yoo, “Distributed coordinated spectrum sharing MAC protocol for cognitive radio,” in *Proc. IEEE DySPAN’07*, Dublin, Ireland, Apr. 17–20, 2007.

[71] C. Cordeiro and K. Challapali, “C-MAC: A cognitive MAC protocol for multi-channel wireless networks,” in *Proc. IEEE DySPAN’07*, Dublin, Ireland, Apr. 17–20, 2007.

[72] X. Liu and Z. Ding, “ESCAPE: A channel evacuation protocol for spectrum-agile networks,” in *Proc. IEEE DySPAN’07*, Dublin, Ireland, Apr. 17–20, 2007.

[73] M. Timmers, A. Dejonghe, L. Van der Perre, and F. Catthoor, “A distributed multichannel MAC protocol for cognitive radio networks with primary user recognition,” in *Proc. ICST/IEEE CrownCom’07*, Florida, USA, Aug. 1–3, 2007.

[74] J. Zhao, H. Zheng, and G.-H. Yang, “Distributed coordination in dynamic spectrum allocation networks,” in *Proc. IEEE DySPAN’05*, Baltimore, MA, Nov. 8–11, 2005.

[75] J. Jia, Q. Zhang, and X. Shen, “HC-MAC: A hardware-constrained cognitive MAC for efficient spectrum management,” *IEEE J. Select. Areas Commun.*, vol. 26, no. 1, pp. 106–117, Jan. 2008.

[76] N. Choi, M. Patel, and S. Venkatesan, “A full duplex multi-channel MAC protocol for multi-hop cognitive radio networks,” in *Proc. ICST/IEEE CrownCom’06*, Mykonos Island, Greece, June 8–10, 2006.

[77] T. Shu, S. Cui, and M. Krunz, “Medium access control for multi-channel parallel transmission in cognitive radio networks,” in *Proc. IEEE GLOBECOM’06*, San Francisco, CA, Nov. 27 – Dec. 1, 2006.

[78] G. Auer, H. Haas, and P. Omiyi, “Interference aware medium access for dynamic spectrum sharing,” in *Proc. IEEE DySPAN’07*, Dublin, Ireland, Apr. 17–20, 2007.

[79] B. Hamdaoui and K. G. Shin, “OS-MAC: An efficient MAC protocol for spectrum agile wireless networks,” *IEEE Trans. Mobile Comput.*, vol. 7, no. 8, pp. 915–930, Aug. 2008.

[80] L. Le and E. Hossain, “OSA-MAC: A MAC protocol for opportunistic spectrum access in cognitive radio networks,” in *Proc. IEEE WCNC’08*, Las Vegas, NV, Mar. 31 – Apr. 3, 2008.

[81] Q. Zhao, L. Tong, A. Swami, and Y. Chen, “Decentralized cognitive MAC for opportunistic spectrum access in ad hoc networks: A POMDP framework,” *IEEE J. Select. Areas Commun.*, vol. 25, no. 3, pp. 589–600, Apr. 2007.

[82] L. Ma, C.-C. Shen, and B. Ryu, “Single-radio adaptive channel algorithm for spectrum agile wireless ad hoc networks,” in *Proc. IEEE DySPAN'07*, Dublin, Ireland, Apr. 17–20, 2007.

[83] S. Sengupta, S. Brahma, M. Chatterjee, and S. Shankar, “Enhancements to cognitive radio based IEEE 802.22 air-interface,” in *Proc. IEEE ICC'07*, Glasgow, Scotland, June 24–28, 2007.

[84] D. Raychaudhuri and X. Jing, “A spectrum etiquette protocol for efficient coordination of radio devices in unlicensed bands,” in *Proc. IEEE PIMRC'03*, Beijing, China, Sept. 7–10, 2003.

[85] J. Peréz-Romero, O. Sallent, R. Augustí, and L. Giupponi, “A novel on-demand cognitive pilot channel enabling dynamic spectrum allocation,” in *Proc. IEEE DySPAN'07*, Dublin, Ireland, Apr. 17–20, 2007.

[86] M. M. Buddhikot, P. Kolodzy, S. Miller, K. Ryan, and J. Evans, “DIMSUM-Net: New directions in wireless networking using coordinated dynamic spectrum access,” in *Proc. IEEE WoWMoM'05*, Taormina – Giardini Naxos, Italy, 2005.

[87] Y. Chen, Q. Zhao, and A. Swami, “Distributed cognitive MAC for energy-constrained opportunistic spectrum access,” in *Proc. IEEE MILCOM'06*, Washington, DC, Oct. 23-25, 2006.

[88] H.-S. W. So, J. Walrand, and J. Mo, “McMAC: A multichannel MAC proposal for ad-hoc wireless networks,” in *Proc. IEEE WCNC'07*, Hong Kong, China, Mar. 11–15, 2007.

[89] P. Pawełczak, R. V. Prasad, and R. Hekmat, “Opportunistic spectrum multichannel OFDMA,” in *Proc. IEEE ICC'07*, Glasgow, Scotland, Mar. 24–28, 2007.

[90] P. Pawełczak, S. Pollin, H.-S. W. So, A. Bahai, R. V. Prasad, and R. Hekmat, “Comparison of opportunistic spectrum multichannel medium access control protocols,” in *Proc. IEEE GLOBECOM'08*, New Orleans, LA, Nov. 30 – Dec. 4, 2008.

[91] A. Birman, “Computing approximate blocking probabilities for a class of all-optical networks,” *IEEE J. Select. Areas Commun.*, vol. 14, no. 5, pp. 852–857, June 1996.

[92] S. Kameshwaran and Y. Narahari, “Effcient algorithms for nonconvex piecewise linear knapsack problems,” *European Journal of Operational Research*, vol. 192, no. 1, pp. 56–68, Jan. 2008.

[93] A. Misra and T. Ott, “Jointly coordinating ECN and TCP for rapid adaptation to varying bandwidth,” in *Proc. IEEE MILCOM’01*, Vienna, VA, Oct. 28–31, 2001.

[94] H. Abrahamsson, O. Hagsand, and I. Marsh, “TCP over high speed variable capacity links: A simulation study for bandwidth allocation,” in *Proc. IFIP/IEEE PIHSN’02*, London, UK, Apr. 22–24, 2002.

[95] A. Gurtov and S. Floyd, “Modeling wireless links for transport protocols,” *ACM SIGCOMM Computer Communication Review*, vol. 34, no. 2, pp. 85–96, Apr. 2004.

[96] A. Gurtov and J. Korhonen, “Effect of vertical handovers on performance of TCP-friendly rate control,” *ACM SIGMOBILE Mobile Computing Communications Review*, vol. 8, no. 3, pp. 73–87, July 2004.

[97] K. Xu, Y. Tian, and N. Ansari, “Improving TCP performance in integrated wireless communications networks,” *Computer Networks*, vol. 47, no. 2, pp. 219–237, Feb. 2005.

[98] A. Mahanti, D. L. Eager, and M. K. Vernon, “Improving multirate congestion control using a TCP Vegas throughput model,” *Computer Networks*, vol. 48, no. 2, pp. 113–136, June 2005.

[99] M. Savoric, H. Karl, M. Schläger, T. Poschwatta, and A. Wolisz, “Analysis and performance evaluation of the EFCM common congestion controller for TCP connections,” *Computer Networks*, vol. 49, no. 2, pp. 269–294, Oct. 2005.

[100] S. McCanne and S. Floyd. Network Simulator Version 2. [Online]. Available: http://www.isi.edu/nsnam/ns/

[101] D. X. Wei and P. Cao, “NS-2 TCP-linux: An NS-2 TCP implementation with congestion control algorithms from Linux,” in *Proc. ICST ValueTools’06*, Pisa, Italy, Oct. 11–13, 2006.

[102] S. Jansen and A. McGregor, “Simulation with real world network stacks,” in *Proc. WSC’05*, Orlando, FL, USA, Dec. 4–7, 2005.

[103] B. Sardar and D. Saha, “A survey of TCP enhancements for last-hop wireless networks,” *IEEE Commun. Surv. and Tut.*, vol. 8, no. 3, pp. 20–34, 2006.

[104] K. Fall and S. Floyd, "Simulation-based comparisons of Tahoe, Reno and SACK TCP," *ACM SIGCOMM Computer Communications Review*, vol. 26, no. 3, pp. 5–21, July 1996.

[105] S. Floyd and T. Henderson, "The NewReno modification to TCP's fast recovery algorithm," Internet Engineering Task Force, Request for Comments (Experimental) 2582, Apr. 1999.

[106] L. Brakmo and L. Peterson, "TCP Vegas: end to end congestion avoidance on a global internet," *IEEE J. Select. Areas Commun.*, vol. 13, no. 8, pp. 1465–1480, Oct. 1995.

[107] M. Mathis, J. Mahdavi, S. Floyd, and A. Romanow, "TCP selective acknowledgment options," Internet Engineering Task Force, Request for Comments (Proposed Standard) 2018, Oct. 1996.

[108] A. Lo, G. Heijenk, and I. Niemegeers, "On the performance of TCP Vegas over UMTS/WCDMA channels with large round-trip time variations," in *Proc. IFIP PWC'04*, Delft, The Netherlands, Sept. 21–23, 2004, pp. 330–342.

[109] E. Cianca, R. Prasad, M. De Sanctis, A. De Luise, M. Antonini, D. Teotino, and M. Ruggieri, "Integrated satellite-HAP systems," *IEEE Commun. Mag.*, vol. 43, no. 12, pp. S33–S39, Dec. 2005.

[110] M. Mathis, J. Semke, J. Mahdavi, and T. Ott, "The macroscopic behaviour of the TCP congestion avoidance algorithm," *ACM SIGCOMM Computer Communications Review*, vol. 27, no. 3, pp. 67–82, July 1997.

[111] J. Padhye, V. Firoiu, D. F. Towsley, and J. F. Kurose, "Modeling TCP Reno performance: a simple model and its empirical validation," *IEEE/ACM Trans. Networking*, vol. 8, no. 2, pp. 133–145, Apr. 2000.

[112] Z. Chen, T. Bu, M. Ammar, and D. Towsley, "Comments on modeling TCP Reno performance: a simple model and its empirical validation," *IEEE/ACM Trans. Networking*, vol. 14, no. 2, pp. 451–453, Apr. 2006.

[113] A. E. Leu, K. Steadman, M. McHenry, and J. Bates, "Ultra sensitive TV detector measurements," in *Proc. IEEE DySPAN'05*, Baltimore, MA, Nov. 8–11, 2005.

[114] M. McHenry, "The probe spectrum access method," in *Proc. IEEE DySPAN'05*, Baltimore, MA, Nov. 8–11, 2005.

[115] A. Rogers, J. Salah, D. Smythe, P. Pratap, J. Carter, and M. Derome, "Interference temperature measurements from 70 to 1500 MHz in suburban and rural enviroment of the northeast," in *Proc. IEEE DySPAN'05*, Baltimore, MA, Nov. 8–11, 2005.

[116] Dutch national frequency register. Agentschap Telecom. [Online]. Available: http://www.at-ez.nl/nfr/tpl/main_nfr_uk.html

[117] S. Geirhofer, L. Tong, and B. M. Sadler, "Dynamic spectrum access in the time domain: Modeling and exploiting white space," *IEEE Commun. Mag.*, vol. 45, no. 5, pp. 66–72, May 2007.

[118] M. Kovacević and A. Acampora, "Benefits of wavelength translation in all-optical clear channel networks," *IEEE J. Select. Areas Commun.*, vol. 14, no. 5, pp. 868–880, June 1996.

[119] D. S. Mitrinović, *Elementary Inequalities.* Groningen, The Netherlands: Noordhoff, 1964.

List of Abbreviations

ACK	Acknowledgment
AGTS	Air Ground Telephone Service
AP	Access Point
ARQ	Automatic Repeat Request
AWGN	Additive White Gaussian Noise
BDP	Bandwith Delay Product
BS	Base Station
CA	Channel Access
CB	Citizen Band
CH	Cluster Head
CMP	Cluster Management Phase
CN	Cognitive Network
CP	Contention Phase
CR	Cognitive Radio
CRN	Cognitive Radio Network
CT2	Cordless Telephone Second Generation
DB	Database
DE	Detection Entity
EAN	Extended Area Network
ECN	Emergency Communication Network
EGC	Equal Gain Combining
ESM	Exclusive Spectrum Management
ETSI	European Telecommunications Standards Institute

FCC	Federal Communications Commission
FEC	Forward Error Correction
HSM	Hierarchical Spectrum Management
HW	Hardware
IAN	Incidence Area Network
IEEE	Institute of Electrical and Electronics Engineers
iid	independent and identically distributed
IP	Internet Protocol
IPv4	Internet Protocol Version 4
ISM	Industrial, Scientific, Medical
IT	Information Theory
JAN	Jurisdiction Area Network
LBT	Listen Before Talk
LEOS	Large Scale Low-Earth Orbit Satellite System
LRT	Likelihood Ratio Test
LU	Least Used
LUCH	Least Used Channel Hopping
MAC	Medium Access Control
ML	Machine Learning
MS	Mobile Station
NLOS	Non-line of sight
NJL	Newly Joined List
Ofcom	Office of Communications
OFDM	Orthogonal Frequency Division Multiplex
OMNG	OSA Network Manager
OSA	Opportunistic Spectrum Access
OSI	Open Systems Interconnection
PDF	Probability Density Function
PSTN	Public Switched Telephone Network
PT	Primary Transmitter
PU	Primary User
QoD	Quality of Detection
QoS	Quality of Service
RCC	Radio Common Carrier
RFE	Radio Front End
RND	Random
ROC	Receiver Operating Characteristics
S	Scanning
SA	Spectrum Analyzer
SACK	Selective Acknowledgment
SC	Spectrum Commons
SDR	Software Defined Radio
SNR	Signal to Noise Level
SSLL	Scanning Subsystem of the Link layer
SU	Secondary User

SW	Software
TCP	Transport Control Protocol
TDMA	Time Division Multiple Acces
TETRA	TErrestrial Trunked RAdio
TIA	Telecommunications Industry Association
U-NII	Unlicensed-National Information Infrastructure
UPCS	Unlicensed Personal Communications Service
UWB	Ultra Wide Band
WGC	Weighted Gain Combining
WIDENS	Wireless Deployable Network System
WLAN	Wireless Local Area Network

List of Symbols

Text Notations

$\mathrm{E}[x]$	expectancy of x
$\Pr[X]$	probability of event X
$\max \mathbf{x}, \min \mathbf{x}$	maximum and minimum of $\mathbf{x}$
$\lfloor x \rfloor$	nearest integer smaller or equal to x
$\lceil x \rceil$	nearest integer greater or equal to x
$diag(X)$	diagonal entries of the matrix X
$\mathbf{D}_i(x)$	$i \times i$ matrix with element x at the diagonal and 0 elsewhere
$*$	convolution

Lowercase Symbols

b	current time slot	—
$f(t)$	PU detector filter response at time t	—
$f_{\bar{\gamma}}(\gamma)$	PDF of SNR γ due to Rayleigh fading	—
$f_{\bar{x},n}(x)$	gamma PDF of x with param. $n-1$ and $\bar{x}$	—
$f_m(\gamma, r_{n,m})$	log-normal PDF of γ on ch. m distanced $r_{n,m}$ from PT	—
$f_m(\gamma)$	log-normal PDF of γ on ch. m, PT-distance independent	—
$f_{P_{tst}}(x)$	PDF of test packet power x	—
g_m	number of groups scanning individual channel m	—
h	hypothesis value on the received PU signal	—
h_{max}	maximum number of sensing samples	—
j	number of successes in arrangement/termination	—
k	number of communicating pairs	—
k_c	number of SNR values taken for combining	—
k_m	cardinality of $\mathbb{G}_{m,x}$	—

l	slot length	μs
m	individual PU channel and PU itself	—
n	number of users (interferers, Rayleigh distr. phasors)	—
$n(t)$	noise at time t	dBm
n_f	average number of LL frame retransmissions	—
$n_{f,max}$	maximum number of retransmissions of one LL frame	—
p	probability of data packet generation	—
p_α	OSA packet discarding factor	—
$p_{a,m}$	probability of gaining slot access on m	—
$p_{\mathbf{A},i}$	probability of choosing ch. i using alg. $\mathbf{A}$	—
$p_{b,m}$	probability of PU channel m being busy	—
$p_{bl,\{1,2\}}$	probability of type 1 and 2 blocking, respectively	—
$p_{bl,t}$	total blocking probability	—
p_{cf}	probability of correct frame reception after $n_{f,max}$ retr.	—
$p_{c,m,\bar{x}}(\varphi)$	probability of packet capture on channel m	—
$p_{c,m,P_{o,m}}(\varphi)$	capture between OSA users only, channel m	—
$p_{c,m,P_{t,m}}(\varphi)$	capture with PU only, channel m	—
p_{dl}	probability of packet transmission in a cluster	—
p_d	probability of detection	—
$p_{d,m}$	probability of PU detection on channel m	—
$p_{d,m,n}$	probability of PU detection on channel m and n interf.	—
p_{ef}	frame error rate	—
p_{ep}	packet error probability	—
p_f	probability of false alarm	—
$p_{f,m}$	probability of false alarm on channel m	—
$p_{k,z}$	transition probability from state k to z	—
p_{sa}	probability of successful arrangement (sim.)	—
$p_{s,\lfloor\kappa(\cdot)\rfloor}$	probability of success in a cluster arriving at $\kappa(\cdot)$	—
$p_{s,\Sigma}$	sum of $p_{s,i}$	—
p_{ss}	probability of sensing scheduling to non-esistent node	—
$p_{ss,max}$	max probability of scheduling to non-esistent node	—
p_Σ	probability that at least one scanning group is active	—
p_ξ	probability of misdetection	—
$p_{\xi,m}$	probability of misdetection on channel m	—
q^{-1}	OSA average data packet length	slots
r	distance of OSA network from the PU transmitter	m
$r(t)$	received energy detector signal at time t	dBm
r_1	minimum distance from PU within OSA cluster $\mathfrak{R}$	m
r_2	maximum distance from PU within OSA cluster $\mathfrak{R}$	m
r_c	distance between centers of two clusters	m
r_d	$r_2 - r_1$	m
r_{dec}	signal decodability region	m
r_s R	size of an OSA network cluster	m
$r_{n,m}$	distance of the node n from PU m	m
$r_{0,m}$	reference range in the far field of the PU antenna	m
s	scanning length	s

$s(t)$	signal at time t	—
s_p	previous number of successful transmissions in a cluster	—
t_0	initial time	s
t_1, t_2	beginning and end of observation period (TCP)	s
t_c	one scanning cycle of individual OSA node	ms
t_{cct}	size of the CH-to-CH frame	ms
t_{cf}	size of the contention phase	ms
t_{cp}	size of CMP	ms
t_{dc}	size of the data communication phase	ms
t_{gb}	size of the guard band	ms
t_{icf}	size of inter-contention phase	ms
t_{is}	inter-scanning time of one OSA node	ms
t_{nss}	report time of each node to cluster head	ms
t_p	channel switching time	μs
t_{pa}	delay of the ARQ protocol	ms
t_{sf}	size of whole sensing phase for all clusters	ms
t_{sl}	number of available slots during CP	ms
t_{sr}	one-way packet delivery time	ms
t_{tot}	total size of the frame (sensing and data)	ms
t_w	average packet delay under SSLL error	ms
t	time instant	s
Δt	time interval	s
u	time-bandwidth product of the PU energy detector	MHzs
v	speed of a node in a cluster	m/s
w_n	weights of the non-equal gain combiner	—
$\bar{x}$	average transmitted power	—

Uppercase Symbols

${}_1F_1(.,.,.)$	confluent hypergeometric function	—
$\mathfrak{A}$	subspace of $\mathfrak{R}$ (sensing cluster)	m^2
A	overlap area of two clusters	m^2
$A_c(t)$	number of bytes acknowledged at the sender at time t	b
B_{λ_D}	fraction of OSA traffic admitted to PU channel	—
$\mathbf{B}_{b,m}$	steady state probability of $\mathbf{Q}_{P,m}$	—
$B_{\mathbb{G}_{m,i}} = \{0,1\}$	group i scanning and not scanning channel m, resp.	
$B_{\mathbb{G}_m} = \{0,1\}$	group i scanning and not scanning channel, resp.	
C	average channel throughput	b/s
C_{act}	OSA link capacity observed by TCP	Mb/s
C_{tot}	total OSA link capacity	Mb/s
$C_\Sigma(t)$	available OSA link rate at time t	—
$\mathbb{G}_m$	set of groups scanning channel m	—
$\mathcal{G}(\cdot,\cdot)$	gamma PDF	—

$H\{0,1\}$	hypothesis: 0 - signal absent, 1 - signal present	—
I_m	probability of interference on channel m	—
L	number of sensing clusters	—
$L_n(\cdot)$	Laguerre polynomial of degree n	—
M	number of PU channels	—
M_C	number of effective data channels	—
$\mathbb{M}$	pool of PU channels	—
$\mathcal{M}$	decision metric	—
N	number of PU detectors (nodes) in the OSA network	—
N_i	current number of nodes in sensing cluster	—
N_0	noise power	dBm
N_F	number of Link Layer frames per TCP packet	—
N_L	number of nodes per cluster	—
$\mathbb{N}$	pool of PU detectors (nodes) in the network	—
O_r	expected length of observation time for random scheme	ms
O_s	expected length of observation time for scheduled scheme	ms
$P_{n,\bar{x}}$	sum of n interference powers (capt. anal.)	—
P_o	power of SU packet	dBm
$P_{o,m}$	received power of the OSA packet, channel m	dBm
P_t	power of the test packet	dBm
$P_{t,m}$	signal amplitude transmitted by PU on channel m	dBm
$\mathbf{P}$	transition probability matrix	—
Q	event of success	—
Q_D	global probability of detection of cooperative scheme	—
Q_F	global probability of false alarm of cooperation scheme	—
$\mathbf{Q}_m$	transition probability matrix for computing m being busy	—
$\mathbf{Q}_{P,m}$	infinitesimal generation matrix for deriving OSA blocking	—
$\mathbf{Q}_{s,g_m}$	supporting matrix to describe $\mathbf{Q}_{s,g_m}$	—
$\mathbf{Q}_{S,g_m}$	infinitesimal generator matrix for Random scanning	—
$Q_u(.,.)$	generalized Marcum Q-function	—
R	system throughput	b/s
R_{opt}	optimized system throughput	b/s
R_{TCP}	TCP bandwidth	Mb/s
$\mathfrak{R}$	region of the OSA network operation	m^2
S	number of access tries	—
$S_{x,n}(\varphi)$	capture probability	—
$S_j^{(k)}$	probability of successful arrangement	—
R	throughput	Mb/s
$T_j^{(k)}$	probability of successful termination	—
V	event of collision	—
W	bandwidth of the observed PU signal	MHz
W_x	number of nodes that unsuccessfully registered	—
X	sum of n interference powers variable	dBm

Y	decision statistic of the PU energy detector	—
Y_n	energy detector output of SU n	—
$Y_{n,j}$	non-quantized jth measurement of SU n	—
Y_{LLC}	test statistic for the log-likelihood combining	—
Y_{WC}	test statistic for the weighted combining	—
$\mathbf{Y}$	vector of measurement outputs	—
Z	power of OSA test packet variable	dBm
$Z(g_m)$	gain of Random scheme over Scheduled given g_m nodes	—

Greek Symbols

α	TCP Vegas min number of queued segments	—
α_i	interference constraint	—
$\alpha_{i,m}$	interference limiting factor on a channel m	—
β	TCP Vegas max number of queued segments	—
β_p	supporting parameter for ${}_1F_1(.,.,.)$	—
γ	instantaneous SNR	dB
γ_Σ	combined SNR of k_m nodes from one cluster	dB
$\overline{\gamma}$	mean SNR	dB
$\overline{\gamma_n}$	mean SNR measured over k SNR values of user n	dB
$\Gamma(.)$	complete gamma function	—
$\Gamma(.,.)$	upper-incomplete gamma function	—
$\Gamma_{R,m}$	PU detection gain on channel m	—
δ	pathloss exponent	—
ϵ	TCP efficiency	—
ϵ_k	supporting parameter for ${}_1F_1(.,.,.)$	—
θ	threshold of the PU energy detector	dB
θ_m	threshold of the PU energy detector on channel m	dB
θ_f	signal activity threshold (measurements)	dBm
$\kappa(t)$	nodes arrival rate to the cluster	—
λ_D	aggregated OSA arrival stream	—
λ_m	aggregated OSA arrival stream after splitting	—
λ_p	arrival rate of the PU activity	—
$\lambda_{p,m}$	arrival rate of the PU activity on channel m	—
$\lambda_{R,m}$	maximum traffic that can be offered on PU channel m	—
$\lambda_{s,m}$	inter-scanning duration of group i	μs
$\lambda_{s,m,i}$	inter-scanning duration of group i on channel m	μs
$\lambda_{T,m}[b]$	total arrival rate (at slot b) in channel m	—
λ_x	general Poisson traffic parameter (capture analysis)	—
$\mathbf{\Lambda_m}$	vector of arrival rates on all PU channels	—
$\mathbf{\Lambda}_{p,m}$	supporting matrix for $\mathbf{Q}_{P,m}$	—
$\mathbf{\Lambda}_{s,g_m}$	supporting matrix to describe $\mathbf{Q}_{s,g_m}$	—
μ_{dB}	mean od the shadow fading	dB

μ_D	aggregated OSA departure stream	—
μ_p	departure rate of the PU activity	—
$\mu_{p,m}$	departure rate of the PU activity on channel m	—
$\mu_{s,m}$	scanning duration of group i	μs
$\mu_{s,m,i}$	scanning duration of group i on channel m	μs
ρ	channel utilization	—
ρ_m	traffic splitting coefficient m	—
$\tilde{\rho}_m$	traffic splitting coefficient m for **LeU** scheme	—
σ_{dB}	shadowing dB spread	dB
φ	packet capture theshold	dB
φ_n	adaptive capture threshold	dB
χ^2_x	chi-square distribution with x degrees of freedom	—
$\chi^2_x(y)$	non-centr. chi-square distr. with param. x and y	—
$\psi(.)$	slot availability	—
Ω	proportion of nodes moving outside of a cluster	—

Publications by the Author

Journal and Magazine Publications

J.1 P. Pawełczak, S. Pollin, H.-S. W. So, A. Bahai, R. V. Prasad, and R. Hekmat, "Performance analysis of multichannel medium access control algorithms for opportunistic spectrum access," *IEEE Trans. Veh. Technol.*, accepted for publication, 6 Oct. 2008.

J.2 P. Pawełczak, S. Pollin, H.-S. W. So, A. Motamedi, A. Bahai, R. V. Prasad, and R. Hekmat, "Quality of service of opportunistic spectrum access: A medium access control approach," *IEEE Wireless Commun.*, vol. 15, no. 5, pp. 20–29, Oct. 2008.

J.3 R. V. Prasad, P. Pawełczak, J. Hoffmeyer, and S. Berger, "Cognitive functionality in next generation wireless networks: Standardization efforts," *IEEE Commun. Mag.*, vol. 46, no. 4, pp. 72–78, Apr. 2008.

Standards

S.1 J. Hoffmeyer, D. Stewart, S. Berger, B. Eydt, F. Frantz, F. Granelli, K. Kontson, D. Murotake, K. Nolan, P. Pawełczak, R. V. Prasad, R. Roy, M. Scoville, D. Sicker, D. Swain, and P. Tenhula, *IEEE Standard Definitions and Concepts for Dynamic Spectrum Access: Terminology Relating to Emerging Wireless Networks, System Functionality, and Spectrum Management*, IEEE 1900.1-2008 Standard, Oct. 2, 2008.

Book Chapter

B.1 P. Pawełczak, R. V. Prasad, "The Process of Defining Cognitive Radio: IEEE 1900 and IEEE SCC41," invited chapter, in "Cognitive Radio Communications and Networks: Principles and Practice," edited by edited by A. Wyglinski, M. Nekovee, and Y. T. Hou, to be published by Elsevier Inc. in 2010.

Peer-Reviewed Conference Publications (Sorted by Topic)

Opportunistic Spectrum Access

C.1 N. Shetty, S. Pollin, and P. Pawełczak, "Identifying Spectrum Usage by Unknown Systems using Experiments in Machine Learning," in *Proc. IEEE WCNC'09*, Budapest, Hungary, 5–9 Apr. 2009.

C.2 P. Pawełczak, S. Pollin, H.-S. W. So, A. Bahai, R. V. Prasad, and R. Hekmat, "Comparison of opportunistic spectrum multichannel medium access control protocols," in *Proc. IEEE GLOBECOM'08*, New Orleans, LA, USA, 30 Nov. – 4 Dec. 2008.

C.3 P. Pawełczak, S. Pollin, H.-S. W. So, A. Motamedi, A. Bahai, R. V. Prasad, and R. Hekmat, "State of the art in opportunistic spectrum access medium access control design," in *Proc. ICST/IEEE CrownCom'08*, Singapore, May 15–17, 2008, (Invited Paper).

C.4 F. E. Visser, G. J. Janssen, and P. Pawełczak, "Multinode spectrum sensing based on energy detection for dynamic spectrum access," in *Proc. IEEE VTC'08-Spring*, Singapore, May 11–14, 2008.

C.5 P. Pawełczak, R. V. Prasad, and R. Hekmat, "Opportunistic spectrum multichannel OFDMA," in *Proc. IEEE ICC'07*, Glasgow, Scotland, June 24–28, 2007.

C.6 A. M. R. Slingerland, P. Pawełczak, A. Lo, R. V. Prasad, and R. Hekmat, "Performance of transport control protocol over dynamic spectrum access links," in *Proc. IEEE DySPAN'07*, Dublin, Ireland, Apr. 17–20, 2007.

C.7 P. Pawełczak, G. Janssen, and R. V. Prasad, "Performance measures of dynamic spectrum access networks," in *Proc. IEEE GLOBECOM'06*, San Francisco, CA, USA, 27 Nov. – 1 Dec. 2006.

C.8 P. Pawełczak, R. V. Prasad, H. Nikookar, and I. Niemegeers, "Performance analysis of periodical spectrum sensing for dynamic spectrum access networks," in *Proc. AWiN (IEEE GLOBECOM'05 Workshop)*, St. Louis, MO, USA, Nov. 28, 2005.

C.9 P. Pawełczak, R. V. Prasad, L. Xia, and I. Niemegeers, "Cognitive radio emergency networks–requirements and design," in *Proc. IEEE DySPAN'05*, Baltimore, MA, USA, Nov. 8–11, 2005.

Wireless Sensor Networks

C.10 J. Zhou, C. Guo, P. Pawełczak, and I. Nemegeers, "Adaptable Link Quality Estimation for Multi Data Rate Communication Networks," in *Proc. IEEE VTC'09-Spring*, Barcelona, Spain, 26–29 Apr. 2009.

C.11 C. Guo, R. Hekmat, and P. Pawełczak, "Analysis and optimization of energy efficient cluster forming for wireless sensor networks," in *Proc. IEEE VTC'07-Fall*, Baltimore, MA, USA, 30 Sep. – 3 Oct. 2007.

C.12 C. Guo, J. Zhou, P. Pawełczak, R. Hekmat, "Improving Packet Delivery Probability Estimation for Indoor Ad Hoc and Wireless Sensor Networks," in *Proc. IEEE CCNC'09*, Las Vegas, NV, USA, Jan. 10–13, 2009.

60 GHz Communications

C.13 B. L. Dang, P. Pawełczak, R. V. Prasad, and I. Niemegeers, "Performance study of a novel architecture for indoor networks at 60 GHz using extended cells," in *Proc. IEEE CCNC'07*, Las Vegas, NV, USA, Jan. 11–13, 2007.

Voice over IP

C.14 R. V. Prasad, V. S. Rao, R. Muralishankar, P. Pawełczak, H. N. Shankar, and I. Niemegeers, "A holistic study of voip session quality—the knobs that control," in *Proc. IEEE CCNC'08*, Las Vegas, NV, USA, Jan. 10–12, 2008.

C.15 R. V. Prasad, H. N. Shankar, P. Pawełczak, and H. Jamadagni, "Fixing number of floors for virtual voice-only conference–an empirical study," in *Proc. IEEE ISM'05*, Irvine CA, USA, Dec. 12–14, 2005.

C.16 R. V. Prasad, H. Shankar, R. Varchas, H. Jamadagni, and P. Pawełczak, "User-centric architecture for virtual voice-only VoIP conferencing," in *Proc. To-QoS (IFIP Networking'06 Workshop)*, Coimbra, Portugal, May 19, 2006.

C.17 R. V. Prasad, R. Muralishankar, V. S. Rao, H. Shankar, P. Pawełczak, and I. Niemegeers, "Voice activity detection for VoIP—an information theoretic approach," in *Proc. IEEE GLOBECOM'06*, San Francisco, CA, USA, 27 Nov. – 1 Dec. 2006.

Technical Reports

R.1 P. Pawełczak, "Status of the AAF project activities within the IEEE SCC41," AAF D4.54 Report, Jun. 1, 2008.

R.2 A. Slingerland, P. Pawełczak, J. Stemerdink, R. Venkatesha Prasad, A. Lo, and R. Hekmat, "Final Link Layer design for a Cognitive Radio-based Ad-hoc Network," AAF D4.41 Report, Aug. 7, 2007.

R.3 P. Pawełczak, C. Guo, R. V. Prasad, and R. Hekmat, "Cluster-Based Spectrum Sensing Architecture for Opportunistic Spectrum Access Networks," IRCTR-S-004-07 Report, Feb. 12, 2007.

R.4 P. Pawełczak and R.A. Yaiz, "Initial Assessment of Cross Layer Interaction for Cognitive Radio in a Personal Network Context," AAF D4.33 Report, Dec. 1, 2006.

R.5 E. Tromp and P. Pawełczak, "Initial Network Layer design for a Cognitive Radio-based Ad-hoc Network," AAF D4.32 Report, Jul. 28, 2006.

R.6 P. Pawełczak, J. Stemerdink, and R. Hekmat, "Link Layer Design for Cognitive-Radio Based Ad Hoc Network," AAF D4.31 Report, Jul. 28, 2006.

R.7 A. Kokkeler, F. Hoeksema, P. Pawełczak, H. Nikookar, L. Xia, J.Stemerdink, and M. de Graaf, "System Architecture: Data communications in emergency situations through Cognitive Radio," AAF D2.22 Report, Nov. 23, 2005.

R.8 P. Pawełczak, "Resource Discovery in Cognitive Radio-based Ad-hoc Network," AAF D4.21 Report, Nov. 1, 2005.

R.9 P. Pawełczak, "Protocol Requirements for Cognitive Radio Networks," AAF D4.11 Report, Jul. 20, 2005.

Other Publications

O.1 P. Pawełczak, and R. V. Prasad, "Book Review: Bruce A. Fette (editor)—Cognitive Radio Technology," *IEEE Commun. Mag.*, vol. 46, no. 5, p. 32, May 2008.

O.2 S. B. Raghunathan, M. van den Oever, R. Doost-Mohammady, P. Pawełczak, I. Budiarjo, M. Heskamp, Q. Zhang, A. Kokkeler, H. Nikookar, Z. Qin, R. Hekmat, and L. P. Lighart, "Dynamic Spectrum Access AAF Platform," IEEE DySPAN 2008 Demonstration Session, 11–14 Oct. 2008, Chicago, IL, USA.

Seminar Talks

T.1 P. Pawełczak, "Technical Challenges of Cognitive Radio-related Systems," Competition and Regulation in Network Industries, Brussels, Belgium, October 28, 2008.

T.2 P. Pawełczak, "What is Cognitive Radio?," 11th Economics of Infrastructures Conference (Avoiding Harmful Interference and Cognitive Radio Workshop), TU Delft, the Netherlands, May 22, 2008.

T.3 P. Pawełczak, "Squeezing Spectrum to the Limit: Opportunistic Spectrum Access for Wireless Networks," KIVI NIRIA Telecommunicatieprijs 2008 final presentation, TU Delft, the Netherlands, May 16, 2008.

T.4 P. Pawełczak, "Cognitive Radio: From Utopia to Reality," Freeband Ambient Communication Event (FACE 2006), Enschede, the Netherlands, July 4, 2006.

Relations to this Thesis

This thesis is based on the previously published publications. Table B.1 provides a relation between publications and chapters of this thesis. Only the publications that are strictly related to the topic of this thesis are listed in the table and only the contributory chapters are listed.

Table B.1: *Relation between chapters of the thesis and the list of publications by the author; ●: major relation, ○: minor relation*

Publication	Ch. 1	Ch. 2	Ch. 3	Ch. 4	Ch. 5
J.1	○	○	○	●	
J.2	○			●	
J.3	●				
S.1	●				
B.1	●				
C.2				●	
C.3	○			●	
C.4		●			
C.5			●		
C.6					●
C.7			●		
C.8		●			
C.9		●	○		
R.1	●				
R.2					●
R.3		●			
R.4	○				
R.5					○
R.6					○
R.7	○	○			
R.8			○		
R.9				●	
O.2		●			

Curriculum Vitae

Przemysław Pawełczak was born in Tomaszów Lubelski, Poland on December 30, 1980. After graduating, with honors, in October 2004 from Wrocław University of Technology, Poland, with a M.Sc. degree (mgr. inż) in Electronics and Telecommunications, he joined Siemens Software Development Center in Wrocław. As a member of the technical staff he was responsible for the development of Hierarchical Cell Structure for the UMTS radio access interface. In February 2005 he became a researcher and a PhD candidate at the Wireless and Mobile Communications Group of Delft University of Technology. His work, which resulted in this thesis, focused on link and transport layer protocol design for Opportunistic Spectrum Access networks. In the meantime, between October 2007 and January 2008, he was a visiting scholar at the Connectivity Lab of the University of California, Berkeley.

He received the annual KIVI NIRIA Telecommunicatieprijs in 2008 for the best PhD student in the field of Telecommunications in the Netherlands. He was also an originator and organizing committee member of IEEE CogNet workshops collocated with the IEEE International Conference on Communications in 2007, 2008 and 2009. As a founder of the Polish Student Association in the Netherlands he tried to have a leading role in promoting Polish student culture among Dutchmen. Mr. Pawełczak is a member of the IEEE Communications Society, IEEE Technical Committee on Cognitive Networks and IEEE Standards Coordinating Committee 41.

List of publications (with copyright acknowledgments) on which the thesis was based on:

- Journal and Magazine Publications

[J1] © [2009] IEEE. Reprinted, with permission, from P. Pawełczak, S. Pollin, H.-S. W. So, A. Bahai, R. V. Prasad, and R. Hekmat, "Performance analysis of multichannel medium access control algorithms for opportunistic spectrum access," IEEE Trans. Veh. Technol., vol. 58, no. 6, pp. 3014-3031, Jul. 2009
DOI http://dx.doi.org/10.1109/TVT.2008.2009350
Note: Parts of [C1], [C2], [J2] reused here with permissions

[J2] © [2008] IEEE. Reprinted, with permission, from P. Pawełczak, S. Pollin, H.-S. W. So, A. Motamedi, A. Bahai, R. V. Prasad, and R. Hekmat, "Quality of service of opportunistic spectrum access: A medium access control approach," IEEE Wireless Commun., vol. 15, no. 5, pp. 20–29, Oct. 2008.
DOI: http://dx.doi.org/10.1109/MWC.2008.4653128
Note: Parts of [C1], [C2] reused here with permissions

[J3] © [2008] IEEE. Reprinted, with permission, from R. V. Prasad, P. Pawełczak, J. Hoffmeyer, and S. Berger, "Cognitive functionality in next generation wireless networks: Standardization efforts," IEEE Commun. Mag., vol. 46, no. 4, pp. 72–78, Apr. 2008.
DOI: http://dx.doi.org/10.1109/MCOM.2008.4481343

- Standards

[S1] © [2008] IEEE. Reprinted, with permission, from J. Hoffmeyer, D. Stewart, S. Berger, B. Eydt, F. Frantz, F. Granelli, K. Kontson, D. Murotake, K. Nolan, P. Pawełczak, R. V. Prasad, R. Roy, M. Scoville, D. Sicker, D. Swain, and P. Tenhula, "IEEE Standard Definitions and Concepts for Dynamic Spectrum Access: Terminology Relating to Emerging Wireless Networks, System Functionality, and Spectrum Management", IEEE 1900.1-2008 Standard, Oct. 2, 2008.
DOI: http://dx.doi.org/10.1109/IEEESTD.2008.4633734

- Book Chapter

[B1] Copyright Elsevier (2009), P. Pawełczak, R. V. Prasad, "Defining cognitive radio," invited chapter, in Ch. 13 "Cognitive Radio Communications and Networks: Principles and Practice," edited by A. Wyglinski, M. Nekovee, and Y. T. Hou, Elsevier Inc. pp. 367-387, 2009.
Link: http://www.elsevier.com/books/cognitive-radio-communications-and-networks/wyglinski/978-0-12-374715-0#
Note: reprint in part from [J3], with permission

- Peer-Reviewed Conference Publications (Sorted by Topic)

Opportunistic Spectrum Access

[C1] © [2008] IEEE. Reprinted, with permission, P. Pawełczak, S. Pollin, H.-S. W. So, A. Bahai, R. V. Prasad, and R. Hekmat, "Comparison of opportunistic spectrum multichannel medium access control protocols," in Proc. IEEE GLOBECOM'08, New Orleans, LA, USA, 30 Nov. – 4 Dec. 2008.
DOI: http://dx.doi.org/10.1109/GLOCOM.2008.ECP.591

[C2] © [2008] IEEE. Reprinted, with permission, P. Pawełczak, S. Pollin, H.-S. W. So, A. Motamedi, A. Bahai, R. V. Prasad, and R. Hekmat, "State of the art in opportunistic spectrum access medium access control design," in Proc. ICST/IEEE CrownCom'08, Singapore, May 15–17, 2008, (Invited Paper).
DOI: http://dx.doi.org/10.1109/CROWNCOM.2008.4562475

[C3] © [2008] IEEE. Reprinted, with permission, F. E. Visser, G. J. Janssen, and P. Pawełczak, "Multinode spectrum sensing based on energy detection for dynamic spectrum access," in Proc. IEEE VTC'08-Spring, Singapore, May 11–14, 2008.
DOI: http://dx.doi.org/10.1109/VETECS.2008.293

[C4] © [2007] IEEE. Reprinted, with permission, P. Pawełczak, R. V. Prasad, and R. Hekmat, "Opportunistic spectrum multichannel OFDMA," in Proc. IEEE ICC'07, Glasgow, Scotland, June 24–28, 2007.
DOI: http://dx.doi.org/10.1109/GLOCOM.2010.5683356

[C5] © [2007] IEEE. Reprinted, with permission, A. M. R. Slingerland, P. Pawełczak, A. Lo, R. V. Prasad, and R. Hekmat, "Performance of transport control protocol over dynamic spectrum access links," in Proc. IEEE DySPAN'07, Dublin, Ireland, Apr. 17–20, 2007.
DOI: http://dx.doi.org/10.1109/DYSPAN.2007.71

[C6] © [2006] IEEE. Reprinted, with permission, P. Pawełczak, G. Janssen, and R. V. Prasad, "Performance measures of dynamic spectrum access networks," in Proc. IEEE GLOBECOM'06, San Francisco, CA, USA, 27 Nov. – 1 Dec. 2006.
DOI: http://dx.doi.org/10.1109/GLOCOM.2006.671

[C7] P. Pawełczak, R. V. Prasad, H. Nikookar, and I. Niemegeers, "Performance analysis of periodical spectrum sensing for dynamic spectrum access networks," in Proc. AWiN (IEEE GLOBECOM'05 Workshop), St. Louis, MO, USA, Nov. 28, 2005.
DOI: Not available

[C8] © [2005] IEEE. Reprinted, with permission, P. Pawełczak, R. V. Prasad, L. Xia, and I. Niemegeers, "Cognitive radio emergency networks–requirements and design," in Proc. IEEE DySPAN'05, Baltimore, MA, USA, Nov. 8–11, 2005.

DOI: http://dx.doi.org/10.1109/DYSPAN.2005.1542678

Other Publications

[O1] S. B. Raghunathan, M. van den Oever, R. Doost-Mohammady, P. Pawełczak, I. Budiarjo, M. Heskamp, Q. Zhang, A. Kokkeler, H. Nikookar, Z. Qin, R. Hekmat, and L. P. Lighart, "Dynamic Spectrum Access AAF Platform," IEEE DySPAN 2008 Demonstration Session, 11–14 Oct. 2008, Chicago, IL, USA.

Technical Reports (Note: except for [T4]: internal project reports, which contain information from previously published material from [J1-J3], [B1], [S1], [C1-C8])

[T1] P. Pawełczak, "Status of the AAF project activities within the IEEE SCC41," AAF D4.54 Report, Jun. 1, 2008.

[T2] A. Slingerland, P. Pawełczak, J. Stemerdink, R. Venkatesha Prasad, A. Lo, and R. Hekmat, "Final Link Layer design for a Cognitive Radio-based Ad- hoc Network," AAF D4.41 Report, Aug. 7, 2007.

[T3] P. Pawełczak, C. Guo, R. V. Prasad, and R. Hekmat, "Cluster-Based Spec- trum Sensing Architecture for Opportunistic Spectrum Access Networks," IRCTR-S-004-07 Report, Feb. 12, 2007.

[T4] P. Pawełczak and R.A. Yaiz, "Initial Assessment of Cross Layer Interaction for Cognitive Radio in a Personal Network Context," AAF D4.33 Report, Dec. 1, 2006.

[T5] E. Tromp and P. Pawełczak, "Initial Network Layer design for a Cognitive Radio-based Ad-hoc Network," AAF D4.32 Report, Jul. 28, 2006.

[T6] P. Pawełczak, J. Stemerdink, and R. Hekmat, "Link Layer Design for Cognitive Radio Based Ad Hoc Network," AAF D4.31 Report, Jul. 28, 2006.

[T7] A. Kokkeler, F. Hoeksema, P. Pawełczak, H. Nikookar, L. Xia, J.Stemerdink, and M. de Graaf, "System Architecture: Data communications in emergency situations through Cognitive Radio," AAF D2.22 Report, Nov. 23, 2005.

[T8] P. Pawełczak, "Resource Discovery in Cognitive Radio-based Ad-hoc Network," AAF D4.21 Report, Nov. 1, 2005.

[T9] P. Pawełczak, "Protocol Requirements for Cognitive Radio Networks," AAF D4.11 Report, Jul. 20, 2005.

Seminar Talks

[M1] P. Pawełczak, "Technical Challenges of Cognitive Radio-related Systems," Competition and Regulation in Network Industries, Brussels, Belgium, October 28, 2008.
Note: lecture note publication based on [B1]

[M2] P. Pawełczak, "What is Cognitive Radio?," 11th Economics of Infrastructures Conference (Avoiding Harmful Interference and Cognitive Radio Work- shop), TU Delft, the Netherlands, May 22, 2008.

[M3] P. Pawełczak, "Squeezing Spectrum to the Limit: Opportunistic Spectrum Access for Wireless Networks," KIVI NIRIA Telecommunicatieprijs 2008 final presentation, TU Delft, the Netherlands, May 16, 2008.

[M4] P. Pawełczak, "Cognitive Radio: From Utopia to Reality," Freeband Ambient Communication Event (FACE 2006), Enschede, the Netherlands, July 4, 2006.

Publications of the author (as of dissertation defense date), not used in the thesis

Peer-Reviewed Conference Publications (Sorted by Topic)

Opportunistic Spectrum Access

N. Shetty, S. Pollin, and P. Pawełczak, "Identifying Spectrum Usage by Unknown Systems using Experiments in Machine Learning," in Proc. IEEE WCNC'09, Budapest, Hungary, 5–9 Apr. 2009.
DOI: http://dx.doi.org/10.1109/WCNC.2009.4917741

Wireless Sensor Networks

J. Zhou, C. Guo, P. Pawełczak, and I. Nemegeers, "Adaptable Link Quality Estimation for Multi Data Rate Communication Networks," in Proc. IEEE VTC'09-Spring, Barcelona, Spain, 26–29 Apr. 2009.
DOI: http://dx.doi.org/10.1109/VETECS.2009.5073358

C. Guo, R. Hekmat, and P. Pawełczak, "Analysis and optimization of energy efficient cluster forming for wireless sensor networks," in Proc. IEEE VTC'07-Fall, Baltimore, MA, USA, 30 Sep. – 3 Oct. 2007.
DOI: http://dx.doi.org/10.1109/VETECF.2007.42

C. Guo, J. Zhou, P. Pawełczak, R. Hekmat, "Improving Packet Delivery Probability Estimation for Indoor Ad Hoc and Wireless Sensor Networks," in Proc. IEEE CCNC'09, Las Vegas, NV, USA, Jan. 10–13, 2009.

DOI: http://dx.doi.org/10.1109/CCNC.2009.4784749

60 GHz Communications

B. L. Dang, P. Pawełczak, R. V. Prasad, and I. Niemegeers, "Performance study of a novel architecture for indoor networks at 60 GHz using extended cells," in Proc. IEEE CCNC'07, Las Vegas, NV, USA, Jan. 11–13, 2007.
DOI: http://dx.doi.org/10.1109/CCNC.2007.11

Voice over IP

R. V. Prasad, V. S. Rao, R. Muralishankar, P. Pawełczak, H. N. Shankar, and I. Niemegeers, "A holistic study of voip session quality—the knobs that control," in Proc. IEEE CCNC'08, Las Vegas, NV, USA, Jan. 10–12, 2008.
DOI: http://dx.doi.org/10.1109/ccnc08.2007.191

R. V. Prasad, H. N. Shankar, P. Pawełczak, and H. Jamadagni, "Fixing number of floors for virtual voice-only conference–an empirical study," in Proc. IEEE ISM'05, Irvine CA, USA, Dec. 12–14, 2005.
DOI: http://dx.doi.org/10.1109/ISM.2005.59

R. V. Prasad, H. Shankar, R. Varchas, H. Jamadagni, and P. Pawełczak, "User-centric architecture for virtual voice-only VoIP conferencing," in Proc. To-QoS (IFIP Networking'06 Workshop), Coimbra, Portugal, May 19, 2006.

R. V. Prasad, R. Muralishankar, V. S. Rao, H. Shankar, P. Pawełczak, and I. Niemegeers, "Voice activity detection for VoIP—an information theoretic approach," in Proc. IEEE GLOBECOM'06, San Francisco, CA, USA, 27 Nov. – 1 Dec. 2006.
DOI: http://dx.doi.org/10.1109/GLOCOM.2006.603

Other Publications

P. Pawełczak, and R. V. Prasad, "Book Review: Bruce A. Fette (editor)— Cognitive Radio Technology," IEEE Commun. Mag., vol. 46, no. 5, p. 32, May 2008.